

Synoptic reconstruction of a major ancient lake system: Eocene Green River Formation, western United States

M. Elliot Smith*

Alan R. Carroll

Brad S. Singer

Department of Geology and Geophysics, University of Wisconsin, 1215 West Dayton Street, Madison, Wisconsin 53706, USA

ABSTRACT

Numerous $^{40}\text{Ar}/^{39}\text{Ar}$ experiments on sanidine and biotite from 22 ash beds and 3 volcanoclastic sand beds from the Greater Green River, Piceance Creek, and Uinta Basins of Wyoming, Colorado, and Utah constrain ~8 m.y. of the Eocene Epoch. Multiple analyses were conducted per sample using laser fusion and incremental heating techniques to differentiate inheritance, ^{40}Ar loss, and ^{39}Ar recoil. When considered in conjunction with existing radioisotopic ages and lithostratigraphy, biostratigraphy, and magnetostratigraphy, these new age determinations facilitate temporal correlation of linked Eocene lake basins in the Laramide Rocky Mountain region at a significantly increased level of precision. To compare our results to the geomagnetic polarity time scale and the regional volcanic record, the ages of Eocene magnetic anomalies C24 through C20 were recalibrated using seven $^{40}\text{Ar}/^{39}\text{Ar}$ ages. Overall, the ages obtained for this study are consistent with the isochroneity of North American land-mammal ages throughout the study area, and provide precise radioisotopic constraints on several important biostratigraphic boundaries.

Applying these new ages, average sediment accumulation rates in the Greater Green River Basin, Wyoming, were approximately three times faster at the center of the basin versus its ramp-like northern margin during deposition of the underfilled Wilkins Peak Member. In contrast, sediment accumulation occurred faster at the edge of the basin during deposition of the balanced filled to overfilled Tipton and Laney

Members. Sediment accumulation patterns thus reflect basin-center-focused accumulation rates when the basin was underfilled, and supply-limited accumulation when the basin was balanced filled to overfilled. Sediment accumulation in the Uinta Basin, at Indian Canyon, Utah, was relatively constant at ~150 mm/k.y. during deposition of over 5 m.y. of both evaporative and fluctuating profundal facies, which likely reflects the basin-margin position of the measured section. The most rapid sediment accumulation for the entire system (>1 m/k.y.) occurred between 49.0 and 47.5 Ma, when volcanoclastic materials from the Absaroka and/or Challis volcanic fields entered the Green River Formation lakes from the north.

Our new ages combined with existing paleomagnetic and biostratigraphic control permit the first detailed synoptic comparison of lacustrine depositional environments in all the Green River Formation basins. Coupled with previously published paleocurrent observations, our detailed correlations show that relatively freshwater lakes commonly drained into more saline downstream lakes. The overall character of Eocene lake deposits was therefore governed in part by the geomorphic evolution of drainage patterns in the surrounding Laramide landscape. Freshwater (overfilled) lakes were initially dominant (53.5–52.0 Ma), possibly related to high erosion rates of remnant Cretaceous strata on adjacent uplifts. Expansion of balanced-fill lakes first occurred in all Green River Formation basins at 52.0–51.3 Ma and again between 49.6 and 48.5 Ma. Evaporative (underfilled) lakes occurred in various basins between 51.3 and 45.1 Ma, coincident with the end of the early Eocene climatic optima and subsequent onset of global cooling defined from marine record. However, evaporite intervals in the different depocenters were deposited at different times rather

than being confined to a single episode of arid climate. Evaporative terminal sinks were initially located in the Greater Green River and Piceance Creek Basins (51.3–48.9 Ma), then gradually migrated southward to the Uinta Basin (47.1–45.2 Ma). This history is likely related to progressive southward construction of the Absaroka Volcanic Province, which constituted a major topographic and thermal anomaly that contributed to a regional north to south hydrologic gradient. The Greater Green River and Piceance Creek Basins were eventually filled from north to south with Absaroka-derived detritus at sedimentation rates 1–2 orders of magnitude greater than the underlying lake deposits.

Keywords: Ar-Ar, Absaroka, Uinta Basin, Piceance Creek Basin, land-mammal ages, lake type, Laramide, Eocene, Green River Formation

INTRODUCTION

Large lakes are widely recognized for their importance as economic resources and as archives of faunal, floral, and climatic evolution (e.g., Bradley, 1929; Franczyk et al., 1989; Wilf, 2000) but are less well understood with regard to the geomorphic evolution of the landscapes surrounding them (cf. Surdam and Stanley, 1980; Pietras et al., 2003a; Carroll et al., 2006). The Eocene Green River Formation (Hayden, 1869) of Wyoming, Colorado, and Utah represents one of the best-documented ancient lake systems and has long been a type example for understanding lacustrine depositional systems (Bradley, 1929; Eugster and Surdam, 1973; Carroll and Bohacs, 1999). Since Marsh (1871) speculated that the Green River Formation lakes were hydrologically connected, numerous authors have proposed temporal correlations of its strata across the Uinta uplift (e.g., Bradley, 1931; Roehler, 1974; Surdam and Stanley, 1980). However, due to the absence of intervening strata between

*Present address: Department of Geology, Sonoma State University, 1801 East Cotati Avenue, Rohnert Park, California 94928, USA, e-mail: michael.smith@sonoma.edu

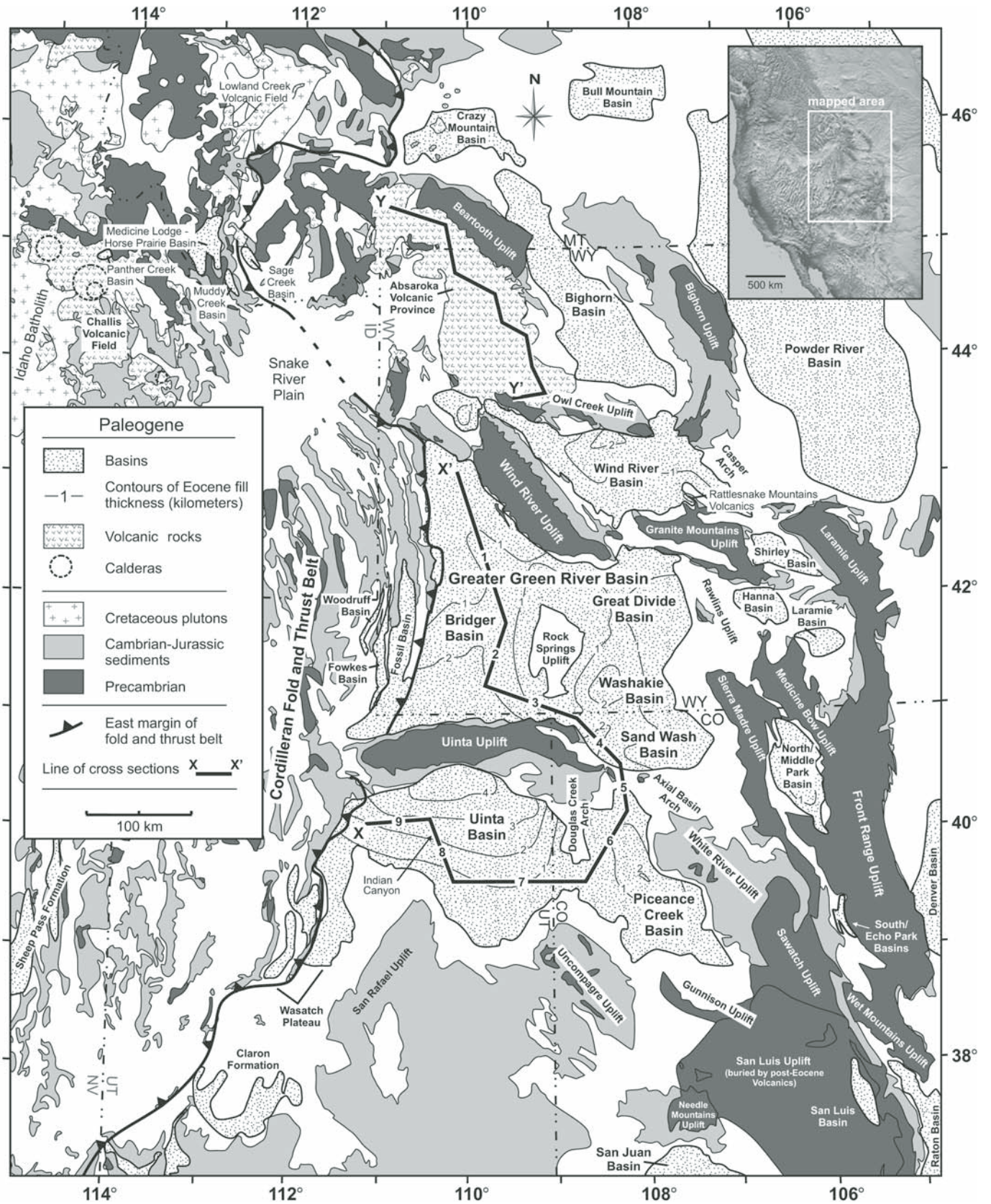


Figure 1. Map showing the locations of Eocene basins and basin-bounding uplifts. Compiled from Ross et al. (1955), Grose (1972), Witkind and Grose (1972), Bond and Wood (1978), Stewart and Carlson (1978), Tweto (1979), Love and Christiansen (1985), Constenius (1996), and Mitchell (1998). Eocene stratal thicknesses are from Robinson (1972).

decenters (Fig. 1), lateral facies changes, and limited radioisotopic age control, temporal correlation has been insufficiently precise to address more specific questions concerning basin evolution. This paper provides an $^{40}\text{Ar}/^{39}\text{Ar}$ -based age framework that allows for the first detailed delineation on upstream-downstream relationships between the sequences of lakes that occupied the Green River Formation basins and provides a fundamental measurement of lacustrine sediment accumulation rates over ~8 m.y. of the Eocene Epoch.

Until recently, mammalian biostratigraphy was the only available method for determining the relative age of strata in the terrestrial basins that contain the Green River Formation (Wood et al., 1941; Lillegraven, 1993; Robinson et al., 2004). However, mammalian fossils are typically preserved in adjacent alluvial deposits that can be difficult to correlate with lake deposits using the physical characteristics of the strata (cf. Clyde et al., 2004; Smith et al., 2004). The temporal resolution of mammalian biostratigraphy is also fundamentally limited by the richness of collections at particular sites. Moreover, phenomena such as diachronous first and last occurrences of taxa caused by taphonomic biases (Smith and Holroyd, 2003) and geographic or climatic heterogeneity (Gunnell and Bartels, 2001) can only be assessed using geochronology that is independent of mammalian biostratigraphy.

Paleomagnetic polarity records have also been used to establish the timing of Eocene terrestrial strata and have the potential to provide precise relative age control (e.g., Tauxe et al., 1994; Clyde et al., 2001). However, paleomagnetic records are inherently binary and can be hampered by changing sedimentation rates, lacuna, poor remanence acquisition, and magnetic overprinting. Comparisons between magnetic polarity records from continental strata and the geomagnetic polarity time scale (Cande and Kent, 1992, 1995; Ogg and Smith, 2004) have proven problematic because higher numbers of polarity reversals are often preserved in terrestrial sediments than are recorded by ocean-floor magnetic anomalies (Elston et al., 1994). Nevertheless, paleomagnetic stratigraphy provides a vital component of terrestrial geochronology but also requires adequate independent calibration.

Several K-Ar and early $^{40}\text{Ar}/^{39}\text{Ar}$ geochronology efforts were undertaken in the Green River Formation and related Eocene continental strata prior to ca. 1990 using phenocrysts from ash beds (Evernden et al., 1964; Mauger, 1977; O'Neill, 1980). However, due to the lower sensitivity of older instruments and difficulty in acquiring sufficient quantities of sanidine, these studies focused on large aliquots of biotite,

which tend to be more susceptible to chemical weathering than sanidine (Renne, 2000; Smith et al., 2006). Age determinations were further limited in accuracy by the unavoidable inclusion of inherited or altered biotite grains in the large samples analyzed (cf. Smith et al., 2006), and limited in their precision by lower resolution mass spectrometry. Recently, $^{40}\text{Ar}/^{39}\text{Ar}$ geochronologic studies of tuff beds using smaller samples and more sensitive mass spectrometry have begun to significantly refine the timing of the Green River Formation and related alluvial strata (Wing et al., 1991; Smith et al., 2003, 2004, 2006). This study integrates 25 new age determinations with detailed facies and geochemical analyses to construct the most comprehensive and highly resolved chronostratigraphic model available for any major pre-Quaternary lake system.

GEOLOGIC SETTING

The Green River Formation of Wyoming, Colorado, and Utah was deposited in a series of continental basins that occupy a broken foreland province to the east of the Cordilleran fold and thrust belt. These basins are separated from one another by chains of anticlinal basement-cored uplifts that collectively comprise the Laramide orogeny, and were variably active from the Cretaceous through Eocene (Fig. 1; Beck et al., 1988; Dickinson et al., 1988). The formation has a maximum thickness of nearly 2 km and spans much of the early and middle Eocene Epoch (Figs. 2 and 3). The Green River Formation basins are part of a suite of basins that have been differentiated based on their structural setting and strata into four principle types: ponded, perimeter, axial, and extensional (Dickinson et al., 1988; Constenius, 1996; Fig. 4; see GSA Data Repository Table DR1¹). Ponded basins, for which the Green River Formation basins are the type example, are bounded by basement-involved uplifts and contain evidence for internal drainage during at least portion of their history. They typically contain thick packages (3–5 km) of alluvial and lacustrine strata (Dickinson et al., 1988; Baars et al., 1988). Perimeter basins occur on the east edge of the broken foreland province and contain alluvial strata with east-directed paleocurrent indicators that indicate external drainage (Dickinson et al., 1988). Axial basins are small, elongate, intermontane basins that formed amid the main

series of basement uplifts of central Colorado and southeastern Wyoming (Fig. 1). These basins typically contain 1–2 km packages of coarse-grained alluvial strata (Dickinson et al., 1988). Extensional basins are strike-elongate grabens and half grabens that overlie the former Cordilleran fold and thrust belt, are commonly bounded by normal faults that reactivate Cordilleran thrust faults, and often contain thick (2–5 km) but areally restricted packages of alluvial and lacustrine strata (Constenius, 1996).

Volcanism occurred over broad areas of the northwestern United States during the Eocene and provided both fallout tuffs and volcanoclastic sediment to the Green River Formation lake basins (Fig. 1; Surdam and Stanley, 1980; Fritz and Harrison, 1985; Armstrong and Ward, 1991). Major volcanic centers include the Absaroka Volcanic Province, Challis volcanic field, and Lowland Creek Volcanics; minor fields are scattered throughout the region (Fig. 1). The stratigraphic and time-stratigraphic constraints for Eocene volcanic fields in Wyoming, Montana, and Idaho are summarized in Figure 5.

NONMARINE SEDIMENTARY FACIES

Lake Types

Representing a broad range of lacustrine facies, several thick lenses of the Green River Formation occupy two principle basins: the Greater Green River Basin and the Uinta-Piceance Creek Basin, which are separated from one another by the east-west-trending, anticlinal Uinta uplift (Fig. 1; Bradley, 1964; Johnson, 1985; Roehler, 1992a). The names Lake Gosiute (King, 1878, p. 446) and Lake Uinta (Bradley, 1931) were assigned to the lakes that existed in the northern (Greater Green River) and southern (Uinta-Piceance Creek) basins, respectively. Each of these lakes varied greatly in their chemistries and areal extents during the course of Green River Formation deposition (Fig. 2A).

Distinctive assemblages of lithologies and fossils within the Green River Formation allow for its subdivision into three principle lacustrine facies associations: fluvial lacustrine, fluctuating profundal, and evaporative (Carroll and Bohacs, 1999). These associations are the basis for interpreting lake type, which reflects the long-term balance between potential accommodation and water plus sediment fill (Carroll and Bohacs, 1999; Bohacs et al., 2000; Carroll and Bohacs, 2001). Carroll and Bohacs (1999) defined the facies associations and lake type interpretations for the Green River Formation in the Greater Green River Basin. In this study we have extended these interpretations to Green River Formation strata in the Uinta, Piceance Creek,

¹GSA Data Repository Item 2007211, containing full documentation of $^{40}\text{Ar}/^{39}\text{Ar}$ geochronology and supporting references for stratigraphic synthesis, is available at www.geosociety.org/pubs/ft2007.htm. Requests may also be sent to editing@geosociety.org.

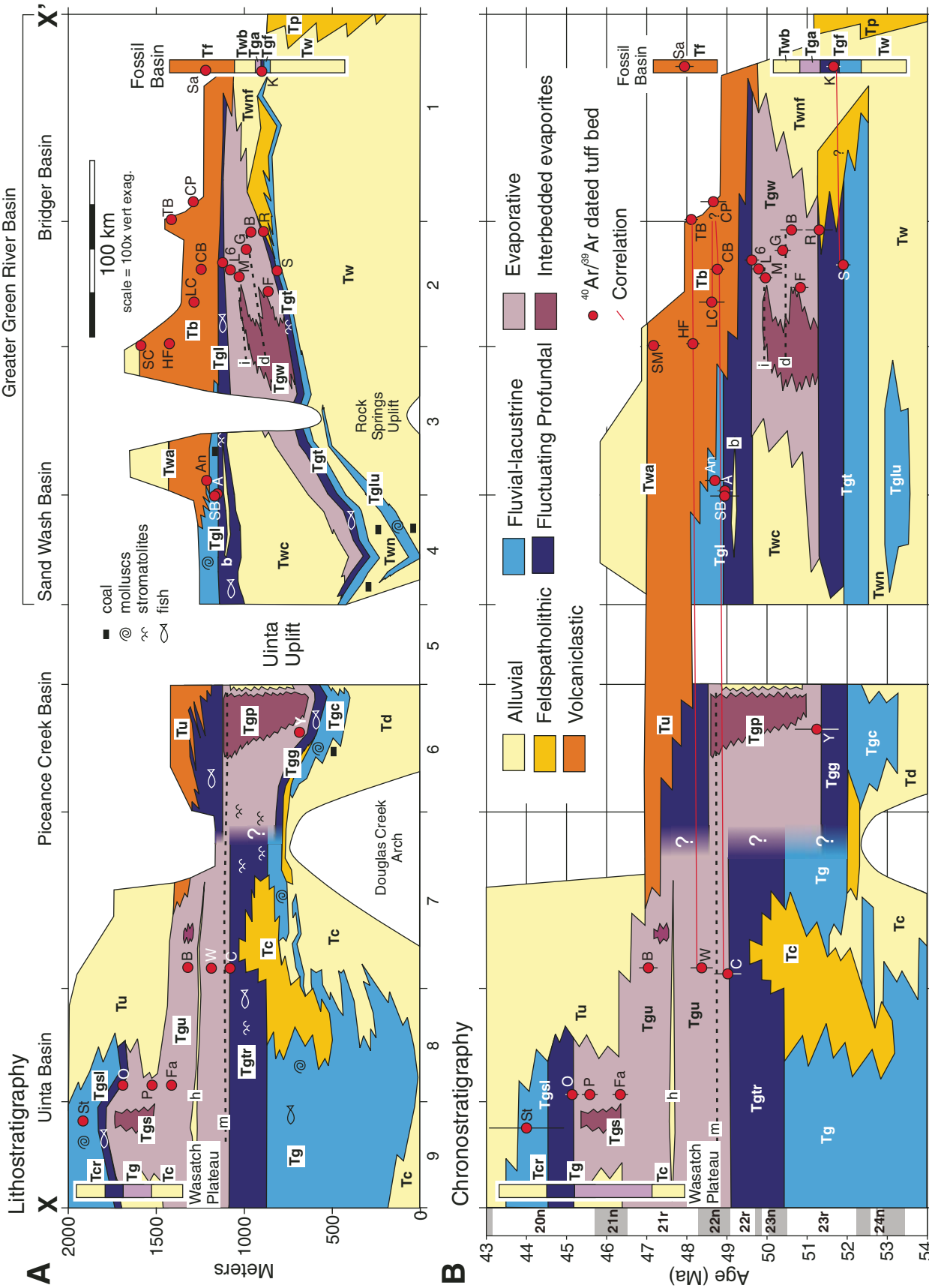


Figure 2. Lithostratigraphic and time stratigraphic cross sections of Eocene strata in the Greater Green River, Piceance Creek, and Uinta Basins along cross-section X-X' (see Fig. 1) showing the stratigraphic position of facies associations, structural features, and dated tuff beds. Cross-section line was chosen in order to intersect area of thickest sediment accumulation, sites of bedded evaporites, and principle sills. Inset columns with white background depict stratigraphy and chronostratigraphy of the Green River Formation in the Fossil Basin and Wasatch Plateau region. The stratigraphic references for numbered segments used to construct the cross section are in Table DR7 (see footnote 1). (Continued on following page).

Formations and Members**Tg _Green River Formation:**

Tgl _Laney Member
 b _Buff Marker bed
 Tgw _Wilkins Peak Member
 i _"I" clastic marker bed
 d _"D" clastic marker bed
 Tgt _Tipton Member
 Tglu _Luman Tongue
 Tga _Angelo Member
 Tgf _Fossil Butte Member
 Tgp _Parachute Creek Member
 h _Horse Bench sandstone
 m _Mahogany zone
 Tga _Anvil Points Member
 Tgg _Garden Gulch Member
 Tgc _Cow Ridge Member
 Tgsl _sandstone & limestone facies
 Tgs _saline facies
 Tgu _upper member
 Tgtr _transitional interval

Tb _Bridger Formation

Tbtb _Turtle Bluff Member
 Tbt _Twin Buttes Member
 Tbb _Blacks Fork Member

Twa _Washakie Formation

Twka _Adobe Town Member
 Twkk _Kinney Rim Member

Tw _Wasatch Formation

Twc _Cathedral Bluffs Tongue
 Twnf _New Fork Tongue
 Twn _Niland Tongue
 Twm _Main Body
 Twb _Bullpen Member

Tf _Fowkes Formation**Tp _Pass Peak Formation****Tcr _Crazy Hollow Formation****Tu _Uinta Formation****Tc _Colton Formation****Td _Debeque Formation****Tuff beds****Greater Green River Basin**

SC _Sage Creek Mtn. pumice
 Sa _Sage tuff
 TB _Tabernacle Butte tuff
 HF _Henrys Fork tuff
 LC _Leavitt Creek tuff
 Co _Continental tuff
 CB _Church Buttes tuff
 An _Antelope sand bed
 SB _Sand Butte tuff
 A _Analcite tuff
 6 _Sixth tuff
 L _Layered tuff
 M _Main tuff
 G _Grey tuff
 B _Boar tuff
 F _Firehole tuff
 R _Rife tuff
 K _K-spar tuff
 S _Scheggs tuff

Uinta-Piceance Creek Basin

St _Strawberry tuff
 O _Oily tuff
 P _Portly tuff
 Fa _Fat tuff
 Bl _Blind Canyon tuff
 W _Wavy tuff
 C _Curly tuff
 Y _Yellow tuff

and Fossil Basins (Fig. 1). Although a wide variety of characteristics has been utilized to define lacustrine facies associations (Horsfield et al., 1994; Bohacs et al., 2000), several key features outlined here and in Table 1 provide the strongest evidence for these associations. Evaporative facies are best recognized via the presence of bedded evaporites and absence of fish fossils, and are interpreted to represent the deposits of hypersaline lakes within underfilled basins in which water rarely rose above the level of the downstream sill. Fluvial-lacustrine facies preserve abundant mollusc fossils and occasional fish fossils, and are interpreted to have been deposited from freshwater lakes in overfilled basins where water consistently spilled over the downstream sill. Fluctuating profundal facies are typically composed of laminated, organic-rich carbonate mudstones intercalated with thin desiccation horizons, and are interpreted to represent the deposits of brackish to saline lakes that occupied balanced-filled basins where water oscillated near the sill level. Assignments of facies association and lake type in most cases correspond to previously identified stratal units and are primarily employed to help standardize terminology between the basins.

Alluvial Facies

Alluvial strata surround and interfinger with the Green River Formation (Fig. 2A; Roehler, 1992a). For this study, alluvial deposits have been subdivided into three broad facies associations according to their mode of deposition: deltaic, alluvial plain, and alluvial fan. Deltaic deposits signify influxes of water and sediment from rivers and typically consist of well-sorted, coarsening- and shallowing-upward packages of sandstone and siltstone that exhibit progradational stratal geometries (Fig. 2A). Alluvial plain facies are typically composed of mud, silt, and sand deposits that are often channelized and pedogenically altered, reflecting the avulsion of streams over broad, exposed plains (Braunage and Stanley, 1977; Roehler, 1993). Alluvial fan deposits typically consist of moderately to poorly sorted sand- to boulder-sized clasts derived from and deposited adjacent to basin-bounding uplifts. They signify the downstream termini of short, steep drainage networks and record the denudation of the uplifts from which the sediments were eroded (Crews and Ethridge, 1993; Carroll et al., 2006). Alluvial deposits as a whole have also been differentiated into two petrographic types: (1) locally derived feldspathic, sublithic, and quartz arenite sandstones; and (2) volcanic-lithic deposits delivered from contemporaneous volcanic fields (Fig. 2A; Surdam and Stanley, 1980; Dickinson et al., 1986).

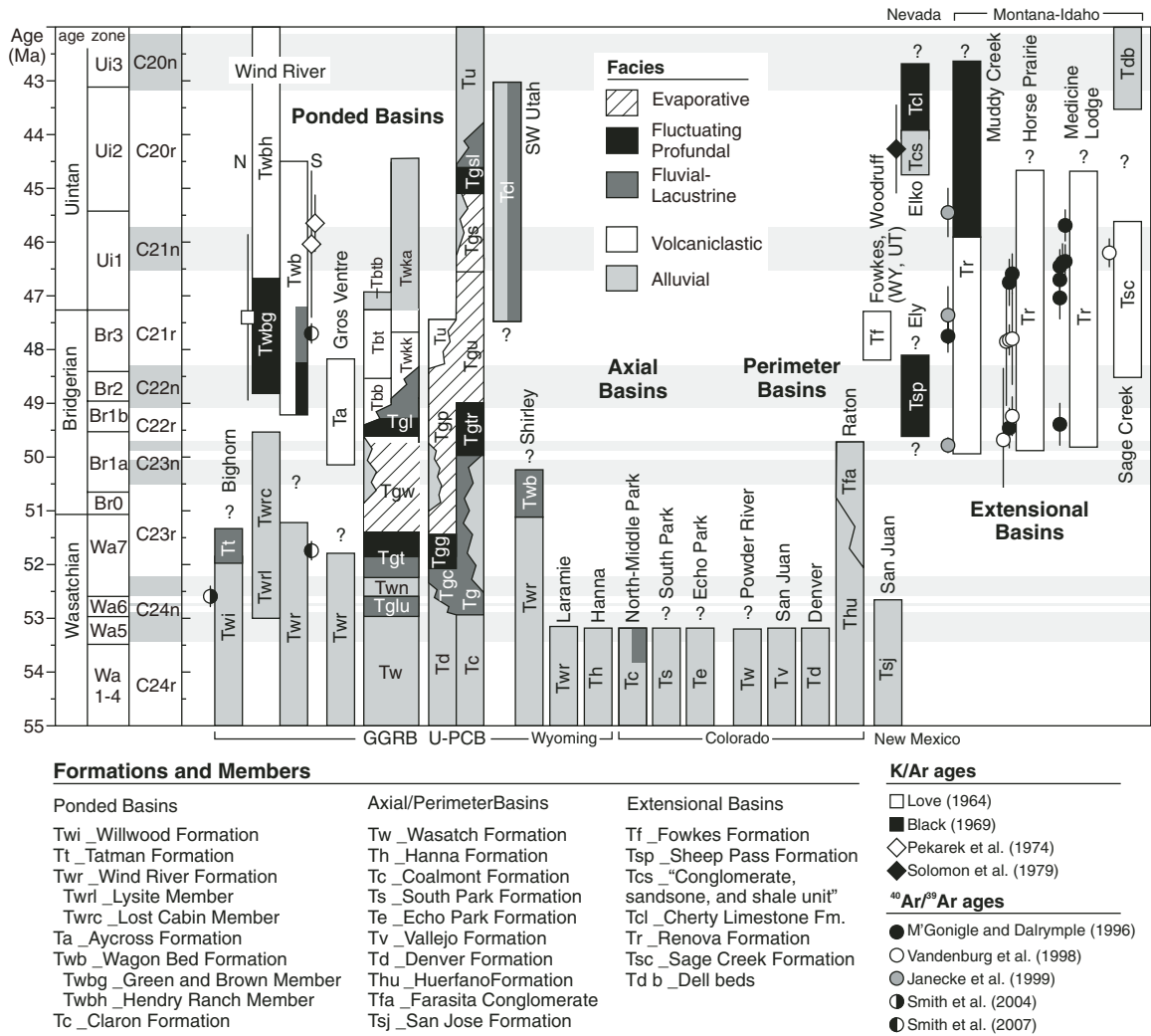
REGIONAL LITHOSTRATIGRAPHY**Greater Green River Basin**

The Greater Green River Basin consists of four subbasins (Bridger, Great Divide, Washakie, and Sand Wash) that are partitioned from one another by the north-south-trending Rock Springs uplift and several smaller east-west-trending structures (Fig. 1; Love et al., 1961). Each subbasin contains a unique succession of strata, but all record a long-term evolution from open to closed and return to open hydrologic conditions during deposition of the Green River Formation (Fig. 2A; Roehler, 1993; Carroll and Bohacs, 1999). The Luman, Tipton, and Wilkins Peak Members record a progression from fluvial-lacustrine to fluctuating profundal through evaporative facies. The evaporative Wilkins Peak Member is primarily restricted to the Bridger subbasin and contains bedded evaporites, predominantly trona, shortite, and halite (Fahey, 1962; Pietras et al., 2003a), and is laterally equivalent to alluvial deposits of the Cathedral Bluffs Member of the Wasatch Formation in adjacent subbasins (Sullivan, 1985; Roehler, 1992a). The fluctuating profundal to fluvial-lacustrine LaClede bed of the Laney Member overlies the Wilkins Peak Member and records an expansion of lake facies into all of the subbasins of the Greater Green River Basin (Fig. 2A; Surdam and Stanley, 1979; Roehler, 1992a). Volcaniclastic alluvium of the Sand Butte bed of the Laney Member, Bridger Formation, and lower Washakie Formation replace lacustrine strata from north to south in a time-transgressive fashion (Stanley and Surdam, 1978; McCarroll et al., 1996a; Evanoff et al., 1998).

Fossil Basin

The smaller, wedge-top Fossil Basin occupies the fold and thrust belt to the west of the Greater Green River Basin (Fig. 1; Oriel and Tracey, 1970; Lamerson, 1982; DeCelles and Currie, 1996; Chandler, 2006). The fluvial-lacustrine to fluctuating profundal Fossil Butte Member overlies the alluvial Wasatch Formation and is overlain by the evaporative Angelo Member (Fig. 2A). The alluvial Bullpen Member of the Wasatch Formation overlies the Angelo Member (Fig. 2A; Oriel and Tracey, 1970; Buchheim, 1994; Buchheim and Eugster, 1998). In the Fowkes and Woodruff Basins to the west of the Fossil Basin, the Bullpen Member is unconformably overlain by volcaniclastic alluvial strata of the Fowkes Formation (Figs. 1 and 2A; Oriel and Tracey, 1970; Nelson, 1973).

Figure 2. (continued)



Absaroka Volcanic Province units in NW Wind River Basin and western Bighorn Basin are shown in Fig. 5. Formations and Members in Greater Green River, Piceance Creek, and Uinta Basins as in Fig. 2.

Figure 4. Age model for the Green River Formation and strata in adjacent Eocene basins. Ages for biostratigraphic and magnetostratigraphic boundaries as in Figure 2. References for individual basins are included in Table DR1 (see footnote 1). We use (and cite) the terminology of Dickinson et al. (1988) and Constenius (1996). All ⁴⁰Ar/³⁹Ar ages are shown with 2σ intercalibration uncertainties relative to the standard values of Renne et al. (1998). GGRB—Greater Green River Basin; U-PCB—Uinta–Piceance Creek Basin.

Piceance Creek Basin

As in the Greater Green River Basin, lacustrine strata in the Piceance Creek Basin record a progression from open to closed and return to open hydrologic conditions (Fig. 2A). Alluvial deposits in the Piceance Creek and Uinta Basins are physically separated by the Douglas Creek arch, and from strata in the Greater Green River Basin by the Uinta uplift and Axial Basin arch (Figs. 1 and 2). To more clearly differentiate between these strata, we have adopted the names DeBeque Formation (Piceance Creek Basin) and Colton Formation (Uinta Basin) in place of Wasatch Formation

for alluvial deposits underlying and interfingering with the Green River Formation in these basins (cf. Powell, 1876; Bradley, 1964; Robinson et al., 2004).

In the center of the Piceance Creek Basin, the mollusc-bearing Cow Ridge Member of the Green River Formation (Johnson, 1984) overlies the alluvial DeBeque Formation (Donnell, 1961b; Kihm, 1984) and is overlain by the Garden Gulch Member of the Green River Formation, which lacks molluscs (Bradley, 1931; Johnson, 1985). Above the Garden Gulch Member, the evaporative lower Parachute Creek Member (Donnell, 1961a; Trudell et al., 1974) is intercalated with both bedded and disseminated

evaporites, predominantly nacholite and halite (Bradley, 1931; Dyni, 1981).

Lacustrine strata overlying the eastern flank of the Douglas Creek arch have been collectively referred to the Douglas Creek Member (Bradley, 1931; Donnell, 1961a). However, several features of these deposits suggest genetic ties with their lateral equivalents in the basin center. At Douglas Pass, which overlies the Douglas Creek arch, lacustrine strata equivalent to the Cow Ridge and Garden Gulch Members contain gastropods at their base but none above, mirroring the shift to fluctuating profundal facies observed in the basin center (Moncure and Surdam, 1980; Johnson et al., 1988). Strata equivalent to the

TABLE 1. CRITERIA FOR CLASSIFICATION OF GREEN RIVER FORMATION LAKE TYPE

Basin type	Facies association	Typical facies	Stratigraphy	Fauna	Hydrologic interpretation
Overfilled	Fluvial-lacustrine	Sandstone, coal, massive to laminated mudstone, coquina limestone	Dominantly progradational	Molluscs common; occasional fish	Freshwater open lake
Balanced filled	Fluctuating profundal	Organic-rich laminated mudstone, stromatolites, oolites	Mixed aggradational and progradational	Fish, ostracodes	Fluctuating salinity, intermittently open and closed lake
Underfilled	Evaporative	Na-rich evaporites, mudcracked mudstone and siltstone, thin organic-rich laminated mudstone beds	Aggradational	Fauna absent	Hypersaline closed lake

lower Parachute Creek Member on the Douglas Creek arch contain evaporite casts and abundant exposure horizons, consistent with the evaporative facies in the basin center (Moncure and Surdam, 1980; Cole, 1985).

The upper part of the Parachute Creek Member contains the Mahogany zone (Bradley, 1931; Cashion, 1967), a 20–60 m interval predominantly composed of laminated organic-rich micrite that extends across the Douglas Creek arch into both the Uinta and Piceance Creek Basins (Fig. 2A; Cashion and Donnell, 1972; Remy, 1992). Although it represents the broadest expansion of Lake Uinta, the Mahogany zone in the Piceance Creek Basin contains evaporites (Trudell et al., 1973; Dyni, 1981) and largely lacks fish fossils in the Uinta Basin (Cashion, 1967; Remy, 1992). In addition, a tuff bed within the Mahogany zone in the Piceance Creek Basin exhibits K-spar alteration of its formerly glassy ash matrix, denoting deposition in alkaline lake water with an elevated solute concentration (Surdam and Parker, 1972; Mason, 1983). We have therefore categorized the facies of the Mahogany zone as evaporative rather than fluctuating profundal. Above the Mahogany zone in the Piceance Creek Basin, the Parachute Creek Member is composed of fluctuating profundal facies and interfingers with the volcanoclastic deltaic and alluvial Uinta Formation (Trudell et al., 1970; Hail, 1987).

Uinta Basin

The Green River Formation achieves its greatest thickness in the Uinta Basin and records an open to closed to open hydrologic trajectory similar to that observed in the other two major basins (Fig. 2A). Unfortunately, stratigraphic terminology in the Uinta Basin is beset by informal and overlapping designations, due in part to limited surface exposure (cf. Remy, 1992). In the interest of consistency, we have adopted the informal stratigraphic designations of Weiss

et al. (1990) and Remy (1992) but recommend future adoption of nongenetic formal stratal designations for these units. At the base of the Eocene succession, nearly 1000 m of lacustrine deposits occupy the subsurface depocenter of the basin (Ryder et al., 1976; Fouch, 1981) and are equivalent to mollusc-bearing fluvial-lacustrine facies exposed at the basin margins (Bradley, 1931; Cashion, 1967; Remy, 1992). This interval is also correlative to the upper part of the alluvial Colton Formation (Spieker, 1946; Cashion, 1967; Pusca, 2003). These basal fluvial-lacustrine strata are overlain by ~200 m of fluctuating profundal strata assigned to the transitional interval (Remy, 1992; Pusca, 2003). The evaporative upper member overlies the transitional interval and contains the Mahogany zone at its base (Bradley, 1931; Cashion, 1967; Remy, 1992). In the eastern Uinta Basin, the upper member interfingers with and is overlain by the alluvial Uinta Formation (Douglass, 1914; Cashion, 1967). However, in the western Uinta Basin, the Green River Formation above the upper member thickens to >500 m. Two additional units are preserved as a result: the evaporative, evaporite-bearing saline facies, and the overlying fluctuating profundal to fluvial-lacustrine sandstone and limestone facies above (Dane, 1955; Dyni et al., 1985; Weiss et al., 1990). These units are equivalent to the lower part of the alluvial Uinta Formation in the eastern Uinta Basin, and are overlain by the upper Uinta Formation (Fig. 2A; Dane, 1955; Prothero, 1996).

High Plateaus of Utah

Extending southward from the Uinta Basin into central Utah along the margin of the Sevier fold and thrust belt are isolated exposures of Green River Formation (Figs. 1 and 2; Spieker, 1949; Doelling, 1972). These strata overlie the alluvial Colton Formation and consist of evaporative to fluvial-lacustrine strata that are loosely correlated to the saline facies and sandstone and

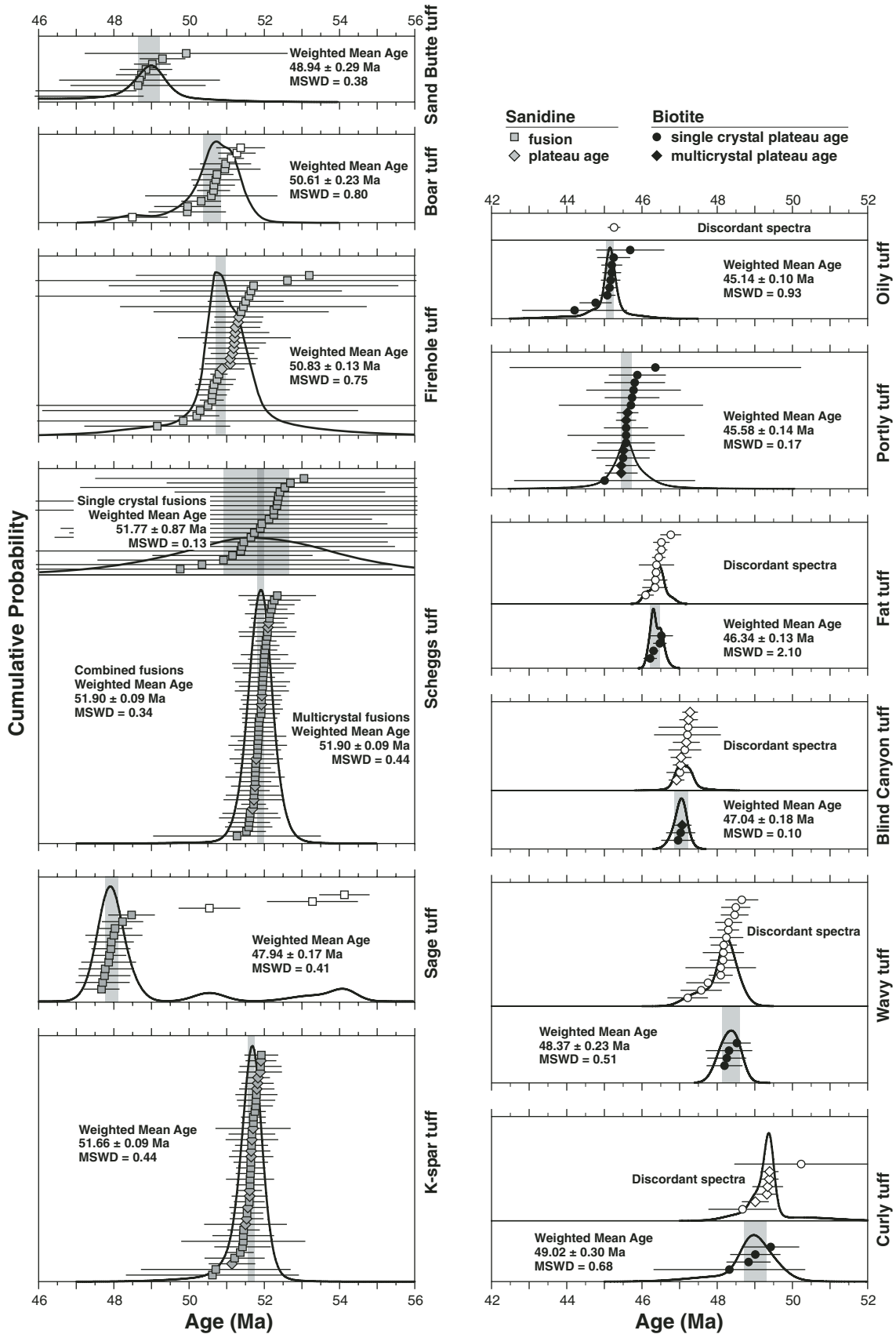
limestone facies (McGookey, 1960; Sheliga, 1980). Overlying the Green River Formation in the eastern half of the region is the alluvial Crazy Hollow Formation (Weiss and Warner, 2001), whereas the volcanoclastic alluvial Golden's Ranch Formation (Muessig, 1951; Doelling, 1972) is the uppermost Eocene unit in the western half. Farther to the southwest along the fold and thrust belt, Eocene alluvial and lacustrine strata are referred to as the Claron Formation (Figs. 1 and 4; Goldstrand, 1994).

GEOCHRONOLOGY

⁴⁰Ar/³⁹Ar Methodology

The geochronology of Green River Formation and associated strata was accomplished via ⁴⁰Ar/³⁹Ar dating of volcanic phenocrysts preserved in ash beds and volcanoclastic sandstone beds (cf. Smith, 2007). The majority of dated units are preserved within laminated to finely bedded lacustrine facies (Table DR2 [see footnote 1]; cf. Smith et al., 2003). The origins of the names of sampled units are explained in Table DR2. Samples were collected from the base of tuff beds, which are often subtly graded, in order to maximize phenocryst grain size and limit contamination by admixed detrital grains. Minerals for dating were obtained using the separation techniques outlined in Smith et al. (2003, 2006) and were irradiated together with flux monitors at the Oregon State University Triga reactor (details of *J* value calculations are found in Data Repository Fig. DR1). Ar isotopic compositions were determined using a CO₂ laser to fuse or incrementally heat sanidine or biotite crystals following the procedures detailed in Smith et al. (2003, 2006).

Ages were determined on the basis of 2234 analyses of phenocrysts from 25 tuffaceous samples (Figs. 6–8; Tables 2 and DR3). Age plateaus are here defined as three or more contiguous, concordant steps containing at least 50% of the total ³⁹Ar released. Heating steps were considered concordant if the mean squared weighted deviation (MSWD) resulting from their inclusion was less than the Students-T distribution limit for the number of included steps (Koppers, 2002). When MSWD exceeded 1, analytical errors were multiplied by the square root of the MSWD (cf. York, 1969; Koppers, 2002). Plateau ages are the weighted mean of included steps, whereas integrated (total fusion) ages combine the Ar released during all heating steps. Inverse-variance weighted mean ages and uncertainties were calculated from both fusion and plateau ages according to Taylor (1982) using Isoplot 3.00 (Ludwig, 2003). An arbitrary outlier exclusion criteria adapted from



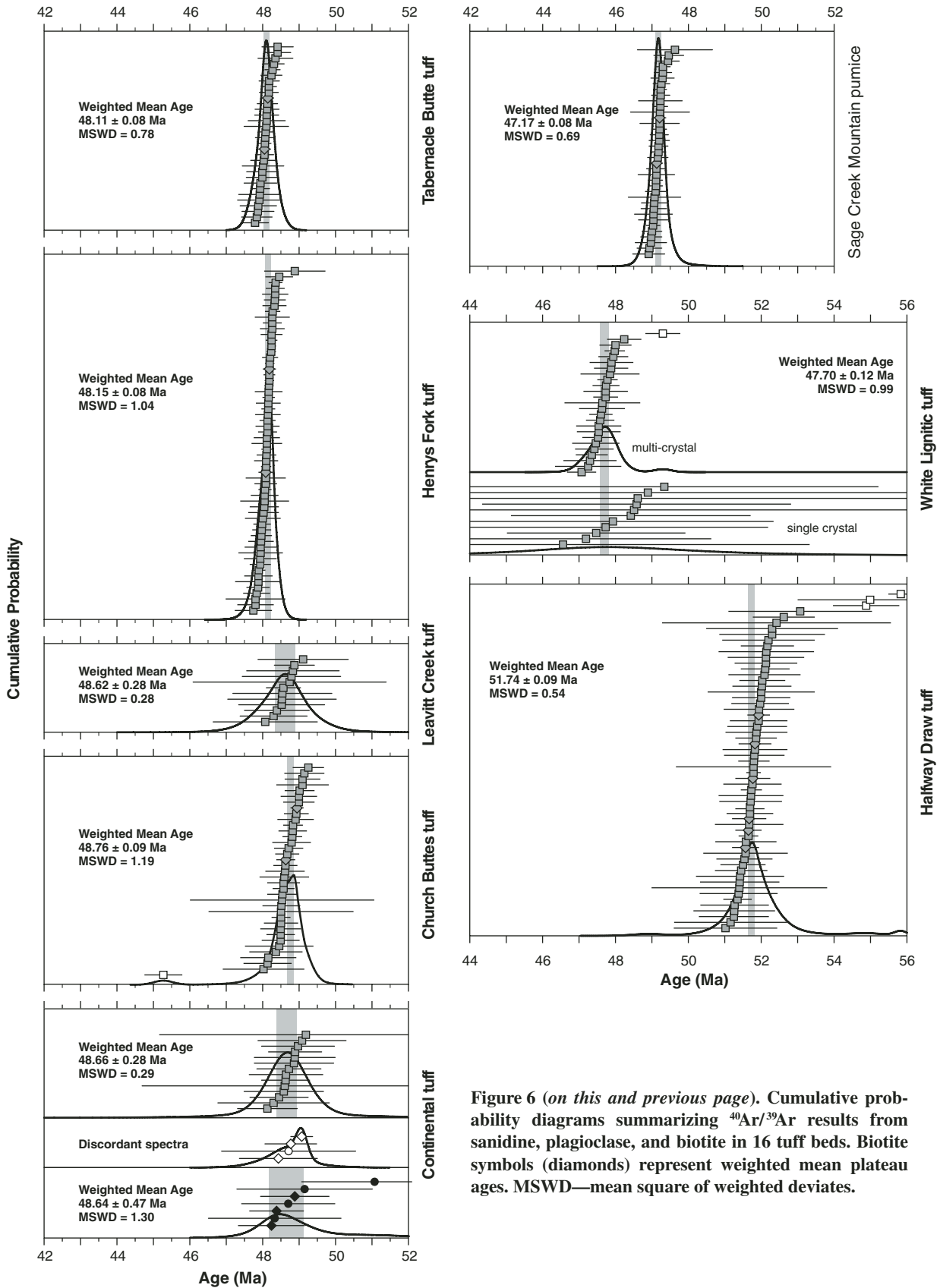


Figure 6 (on this and previous page). Cumulative probability diagrams summarizing $^{40}\text{Ar}/^{39}\text{Ar}$ results from sanidine, plagioclase, and biotite in 16 tuff beds. Biotite symbols (diamonds) represent weighted mean plateau ages. MSWD—mean square of weighted deviates.

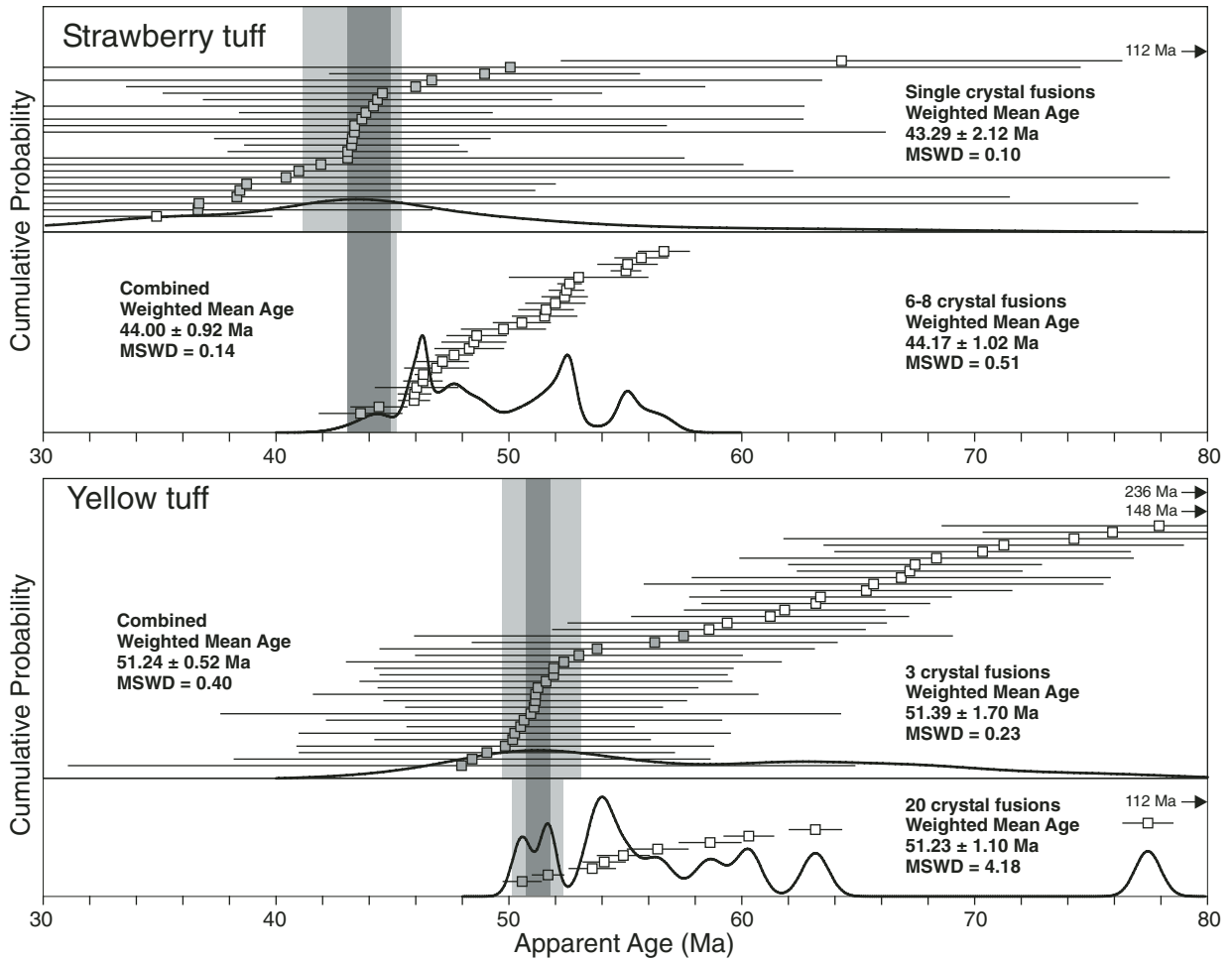


Figure 7. Cumulative probability diagrams showing sanidine and biotite ages obtained from the Yellow and Strawberry tuff beds. Feldspars from these beds exhibit marked contamination by older grains. Note that multiple single-crystal analyses isolate a young, presumably juvenile magmatic population from both ash beds when older xenocrysts are excluded from the age calculation. MSWD—mean square of weighted deviates.

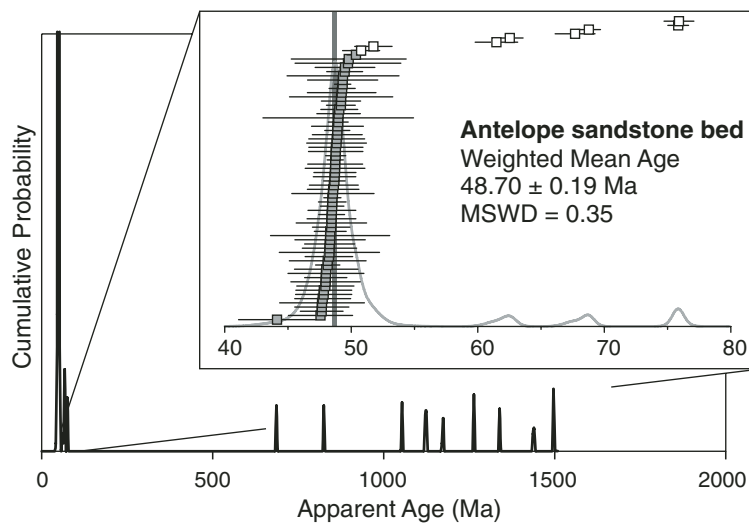


Figure 8. Cumulative probability diagram showing analyses of detrital orthoclase and sanidine from a sandstone bed near the base of the Sand Butte bed of the Laney Member. MSWD—mean square of weighted deviates.

TABLE 2. SUMMARY OF $^{40}\text{Ar}/^{39}\text{Ar}$ EXPERIMENTAL RESULTS FOR 29 ASH BEDS

Basin		Location	Isochron analysis ¹			Average K/Ca $\pm 2\sigma$	Apparent ages [†]				
Name (Sample) Formation, Symbol	Mineral		Analysis type	n	SUMS (N-2)		$^{40}\text{Ar}/^{39}\text{Ar}_i$ $\pm 2\sigma$	Isochron age (Ma) $\pm 2\sigma^g$	MSWD	Weighted mean age (Ma) $\pm 2\sigma^g$	$\pm 2\sigma$
Greater Green River Basin											
Sage Creek Mt. pumice (SCM)		N41°7'56.5" W110°8'11.7"									
Tb, SC											
Sanidine	SF	35 of 35	0.74	312.3 \pm 89.8	47.16 \pm 0.11	74 \pm 4	0.72	47.17 \pm 0.08			
	MI (2 of 2)	10 of 10	0.22	444.2 \pm 292.1	47.10 \pm 0.19	59 \pm 18	0.47	47.17 \pm 0.13			
	SF + MI	45 of 45	0.63	336.9 \pm 84.9	47.14 \pm 0.10	72 \pm 4	0.69	47.17 \pm 0.08 [†]	± 0.16	± 0.81	
Tabernacle Butte tuff (TaB)		N42°26'0.6" W109°22'31.4"									
Tb, TB											
Sanidine	SF	30 of 30	0.76	302.8 \pm 33.6	48.10 \pm 0.10	63 \pm 3	0.81	48.11 \pm 0.08			
	MI (2 of 2)	10 of 10	0.34	735.8 \pm 1064	47.91 \pm 0.36	55 \pm 11	0.59	48.10 \pm 0.12			
	SF + MI	40 of 40	0.76	306.7 \pm 32.8	48.09 \pm 0.09	61 \pm 4	0.78	48.11 \pm 0.08 [†]	± 0.16	± 0.83	
Henry's Fork tuff (HeF)		N41°7'25.3" W110°9'27.7"									
Tb, HF											
Sanidine	SF	56 of 56	1.10	302 \pm 60	48.14 \pm 0.09	60 \pm 2	1.08	48.15 \pm 0.08			
	MI (3 of 3)	15 of 15	1.08	451 \pm 207	48.02 \pm 0.18	51 \pm 7	1.39	48.16 \pm 0.11			
	SF + MF	71 of 71	1.12	331 \pm 60	48.13 \pm 0.33	58 \pm 2	1.04	48.15 \pm 0.08 [†]	± 0.18	± 0.83	
Leavitt Creek tuff (LeC)		N41°14'13.1" W110°12'41.8"									
Tb, LC											
Sanidine	SF	12 of 14	0.30	312.6 \pm 38.3	48.55 \pm 0.60	54 \pm 14	0.28	48.62 \pm 0.28 [†]	± 0.31	± 0.88	
Church Buttes tuff (ChB)		N41°28'34.5" W110°8'04.3"									
Tb, CB											
Sanidine	SF	34 of 38	1.17	266 \pm 40	48.74 \pm 0.12	51 \pm 9	1.17	48.72 \pm 0.09			
	MI (2 of 2)	8 of 8	0.24	631 \pm 474	48.47 \pm 0.51	47 \pm 4	0.73	48.88 \pm 0.15			
	SF + MI	42 of 46	1.19	279 \pm 43	48.77 \pm 0.11	50 \pm 7	1.30	48.76 \pm 0.09 [†]	± 0.16	± 0.84	
Continental Peak tuff (CP-1)		N42°16'06.2" W108°43'7.5"									
Tb, CP											
Biotite	SI (4 of 5)	20 of 26	0.53	312.6 \pm 38.3	48.80 \pm 1.12	35 \pm 9	1.70	49.12 \pm 1.08			
	MI (3 of 6)	15 of 30	0.73	274.0 \pm 19.3	48.76 \pm 0.49	40 \pm 16	0.69	48.54 \pm 0.54			
	SI + MI	35 of 56	0.75	287.0 \pm 17.4	48.77 \pm 0.46	36 \pm 8	1.30	48.64 \pm 0.47			
Sanidine	MF	12 of 16	0.27	359.5 \pm 276.2	48.51 \pm 0.64	37 \pm 8	0.29	48.66 \pm 0.28 [†]	± 0.31	± 0.88	
Antelope sand bed (AC-3)		N41°23'45.9" W108°30'54.2"									
Tgt, An											
K-feldspar	SF	62 of 82	0.35	292.8 \pm 32.7	48.70 \pm 0.21	1188 \pm 260	0.35	48.70 \pm 0.19 [†]	± 0.23	± 0.86	
Sand Butte tuff (SB-3)		N41°20'43.7" W108°40'13.7"									
Tgt, SB											
Feldspar	MF	9 of 9	0.42	290.3 \pm 18.5	49.05 \pm 0.45	0.1 \pm 0.1	0.38	48.94 \pm 0.29 [†]	± 0.32	± 0.89	
Analcite tuff (SB-1)		N41°21'1.4" W108°40'4.7"									
Tgt, A											
Sanidine	SF	21 of 21	0.82	331.5 \pm 87.9	48.61 \pm 0.84	27 \pm 3	0.82	48.57 \pm 0.73			
	MF ^{††}	19 of 19	0.79	281.9 \pm 52.3	49.00 \pm 0.22	23 \pm 2	0.71	48.95 \pm 0.12			
	SF + MF	40 of 40	0.79	297.5 \pm 42.7	48.95 \pm 0.19	25 \pm 2	0.75	48.95 \pm 0.12 [†]	± 0.18	± 0.85	
Sixth tuff (TR-5)		N41°32'31.1" W109°28'52.9"									
Tgw, 6											
Sanidine	SF	37 of 40	0.09	450 \pm 614	49.21 \pm 1.48	108 \pm 15	0.10	49.68 \pm 0.59			
	MF	11 of 30	0.51	292.8 \pm 14.6	49.71 \pm 0.61	2360 \pm 1300	0.47	49.68 \pm 0.59			
	SF + MF	48 of 70	0.18	293.1 \pm 14.4	48.69 \pm 0.43	109 \pm 14	0.18	49.68 \pm 0.42			
Biotite	SI + MI (21 of 26) ^{§§}	119 of 142	0.53	299.9 \pm 6.5	49.61 \pm 0.11	274 \pm 46	1.00	49.62 \pm 0.10 [†]	± 0.17	± 0.86	
Layered tuff (TR-6)		N41°32'33.6" W109°28'55.6"									
Tgw, L											
Sanidine	MF ^{§§}	64 of 73	0.32	315 \pm 31	49.75 \pm 0.12	79 \pm 2	0.42	49.79 \pm 0.09 [†]	± 0.17	± 0.86	
Main tuff (TR-1)		N41°32'28.1" W109°28'52.0"									
Tgw, M											
Sanidine	MF ^{††}	30 of 31	0.77	293.4 \pm 6.4	49.98 \pm 0.09	98 \pm 11	0.65	49.96 \pm 0.08 [†]	± 0.16	± 0.86	
Boar tuff (BT-14)		N41°57'48.6" W109°15'9.8"									
Tgw, B											
Sanidine	MF	10 of 14	0.66	179 \pm 105	51.09 \pm 0.41	3007 \pm 1400	0.80	50.61 \pm 0.23 [†]	± 0.27	± 0.90	
Grey tuff (WN-1)		N41°39'24.3" W109°17'18.8"									
Tgw, G											
Sanidine	MF ^{††}	18 of 18	0.73	285.7 \pm 11.3	50.55 \pm 0.21	190 \pm 130	0.67	50.39 \pm 0.13 [†]	± 0.19	± 0.87	
Firehole tuff (FC-2)		N41°21'0.7" W109°22'59.9"									
Tgw, F											
Sanidine	MF	41 of 41	0.77	295.3 \pm 2.3	50.83 \pm 0.13	71 \pm 3	0.94	50.83 \pm 0.13 [†]	± 0.19	± 0.88	
Rife tuff (BT-18)		N41°57'47.2" W109°15'8.7"									
Tgt, R											
Biotite	MF + SF ^{††}	15 of 38	0.71	290.1 \pm 10.7	51.58 \pm 0.62	867 \pm 240	0.68	51.30 \pm 0.30 [†]	± 0.33	± 0.93	
	MI (4 of 8)	16 of 29	0.61	285.5 \pm 14.9	53.35 \pm 0.58	20 \pm 8	0.92	53.15 \pm 0.53			
Scheggs tuff (WP-3)		N41°31'9.9" W109°19'29.8"									
Tgt, S											
Sanidine	SF	21 of 21	0.13	356 \pm 585	51.52 \pm 1.80	109 \pm 19	0.13	51.77 \pm 0.87			
	MF	62 of 62	0.30	562 \pm 319	51.57 \pm 0.29	81 \pm 7	0.42	51.90 \pm 0.09			
	SF + MF	83 of 83	0.27	508 \pm 248	51.63 \pm 0.24	86 \pm 7	0.34	51.90 \pm 0.09 [†]	± 0.17	± 0.89	

(Continued)

Synoptic reconstruction of the Eocene Green River Formation

TABLE 2. SUMMARY OF ⁴⁰Ar/³⁹Ar EXPERIMENTAL RESULTS FOR 29 ASH BEDS

Basin Name (Sample) Formation, Symbol	Location	Isochron analysis [†]				Apparent ages [†]				
		SUMS (N-2)	⁴⁰ Ar/ ³⁹ Ar _i ± 2σ	Isochron age (Ma) ± 2σ [§]	Average K/Ca ± 2σ	MSWD	Weighted mean age (Ma) ± 2σ [§]	±2σ	±2σ ^{††}	
Mineral	Analysis type	n								
Fossil-Fowkes Basin										
K-spar tuff (FQ-1)										
N41°47'32.2" W110°42'39.6"										
Tgf, K										
Sanidine	MF	55 of 56	0.39	389 ± 133	51.51 ± 0.20	76 ± 5	0.44	51.66 ± 0.09[‡]	±0.17	±0.89
Sage tuff (FF)										
N41°46'26.8" W110°57'48.4"										
Tf, Fo										
Sanidine	MF	19 of 25	0.26	1041 ± 2845	47.18 ± 1.09	50 ± 6	0.41	47.94 ± 0.17[‡]	±0.22	±0.84
Piceance Creek Basin										
Yellow tuff (WR-1)										
N40°1'1.9" W108°6'53.2"										
Tgp, Y										
Sanidine	MF	23 of 53	0.37	331.8 ± 82.5	50.03 ± 0.74	73 ± 12	0.40	51.24 ± 0.52[‡]	±0.54	±1.02
Uinta Basin										
Strawberry tuff (SR-1)										
N40°9'54.0" W110°33'5.6"										
Tgsl, St										
Sanidine	MF	2 of 43				85 ± 10	0.51	44.17 ± 1.02		
	SF	20 of 25	0.09	-775 ± 9887	50.44 ± 10.87	63 ± 47	0.10	43.29 ± 2.12		
	SF + MF	22 of 68	0.15	383 ± 1248	43.77 ± 1.61	64 ± 40	0.14	44.00 ± 0.92[‡]	±0.93	±1.19
Biotite	MI (IA; 5 of 12)	26 of 61				13 ± 3	1.80	41.30 ± 1.20		
Oily tuff (IC-6)										
N40°2'56.8" W110°31'42.1"										
Tgs, O										
Biotite	SI (9 of 10)	43 of 49	0.91	280.4 ± 11.9	45.18 ± 0.11	100 ± 29	0.93	45.14 ± 0.10[‡]	±0.16	±0.78
Portly tuff (IC-5)										
N39°58'47.6" W110°37'16.3"										
Tgs, P										
Biotite	SI (11 of 11)	55 of 55	0.19	259.9 ± 29.5	45.81 ± 0.26	168 ± 45	0.13	45.67 ± 0.26		
	MI (5 of 5)	29 of 29	0.92	280.9 ± 19.9	45.61 ± 0.17	76 ± 31	0.19	45.55 ± 0.16		
	SI + MI	84 of 84	0.45	275.4 ± 16.5	45.66 ± 0.14	141 ± 33	0.17	45.58 ± 0.14[‡]	±0.19	±0.79
Fat tuff (IC-2)										
N39°58'46.5" W110°37'6.9"										
Tgs, Fa										
Biotite	SI (4 of 13)	19 of 65	1.13	300.1 ± 12.9	46.34 ± 0.10	90 ± 36	2.10	46.34 ± 0.13[‡]	±0.18	±0.80
Blind Canyon tuff (SW-1)										
N39°50'41.4" W110°11'11.8"										
Tgu, Bl										
Biotite	SI + MI (3 of 13)	13 of 73	0.95	256.7 ± 32.1	47.18 ± 0.20	418 ± 1100	0.10	47.04 ± 0.18[‡]	±0.22	±0.83
Wavy tuff (GC-2b)										
N39°50'59.3" W110°15'17.5"										
Tgu, W										
Biotite	MF	7 of 9	1.44	281.6 ± 26.6	48.83 ± 0.71	27 ± 5	1.45	48.47 ± 0.18		
	SF	50 of 54	1.33	293.4 ± 14.9	48.56 ± 0.24	65 ± 15	1.31	48.53 ± 0.17		
	SI (4 of 18)	23 of 107	0.73	281.1 ± 16.8	48.49 ± 0.27	31 ± 12	0.51	48.37 ± 0.23[‡]	±0.27	±0.86
Curly tuff (GC-5b)										
N39°50'33.8" W110°15'3.1"										
Tgu, C										
Biotite	SI (4 of 10)	11 of 26	0.89	194.5 ± 59.4	49.51 ± 0.37	548 ± 200	0.68	49.02 ± 0.30[‡]	±0.33	±0.89
Wind River Basin										
White Lignitic tuff (WB-1)										
N42° 42' 54.3" W108° 11' 11.8"										
Twb										
Sanidine	SF	11 of 11	0.09	500 ± 255	46.70 ± 5.13	30 ± 4	0.10	47.97 ± 1.31		
	MF	24 of 25	1.24	510 ± 305	47.33 ± 0.37	3.9 ± 0.4	1.42	47.70 ± 0.13		
	SF + MF	35 of 36	0.85	507 ± 264	47.33 ± 0.33	3.9 ± 0.4	0.99	47.70 ± 0.12[‡]	±0.18	±0.83
Halfway Draw tuff (HD-1)										
N42° 51' 52.9" W108° 17' 57.1"										
Twr										
Sanidine	SF	51 of 54	0.54	300 ± 7	51.73 ± 0.11	113 ± 7	0.57	51.75 ± 0.10		
	MI (6 of 6)	19 of 19	0.36	530 ± 411	51.32 ± 0.61	97 ± 13	0.38	51.72 ± 0.16		
	SF + MI	70 of 73	0.53	301 ± 7	51.73 ± 0.10	109 ± 6	0.54	51.74 ± 0.09[‡]	±0.17	±0.89

Note: Summary of 2234 individual analyses. Twi—Willwood Formation; Twr—Wind River Formation; Twb—Wagon Bed Formation; Tb—Bridger Formation; Tgl—Laney Member—Green River Formation; Tgw—Wilkins Peak Member—Green River Formation; Tgt—Tipton Member—Green River Formation; Tgf—Fossil Butte Member—Green River Formation; Tf—Fowkes Formation; Tgsl—sandstone and limestone member—Green River Formation; Tgs—saline member—Green River Formation; Tgp—Parachute Creek Member—Green River Formation. Only experiments yielding 100% concordant age spectra are included in calculation of weighted means of plateau ages. MI—multicrystal laser incremental heating experiments; SI—single crystal laser incremental heating experiments; MF—multicrystal laser fusion experiments; SF—single crystal laser fusion experiments; IA—integrated ages. Concordant experiments include all incremental heating steps. MSWD—mean square weighted deviate. Corrections for undesirable nucleogenic reactions on ⁴⁰K and ⁴⁰Ca are as follows: [⁴⁰Ar/³⁹Ar]_K = 0.00086; [³⁶Ar/³⁷Ar]_{Ca} = 0.000264; [³⁹Ar/³⁷Ar]_{Ca} = 0.000673. More than 1000 measurements of sanidine from the Taylor Creek rhyolite (TCs) were used to monitor the experiments. Its age is 28.34 ± 0.28 Ma relative to the GA-1550 biotite primary standard (98.79 ± 0.96 Ma; Renne et al., 1998). Mass discrimination was monitored using an on-line air pipette and varied between 1.0020 ± 0.0010 and 1.0065 ± 0.0010 per amu, during the analytical periods. K/Ca reflects measured ³⁷Ar and ³⁹Ar, and is a derived atomic ratio. The large uncertainty in K/Ca for some samples is an artifact of the imprecision of the ³⁷Ar measurement for samples analyzed after a significant proportion of the nucleogenically derived ³⁷Ar had decayed away. Latitude and longitude referenced to NAD27 datum.

[†]Ages relative to 28.34 Ma for TCs (Renne et al., 1998).

[‡]Preferred age.

[§]Analytical uncertainty.

[¶]Analytical and intercalibration uncertainty for preferred age.

^{††}Fully propagated uncertainty for preferred age.

^{‡‡}From Smith et al. (2003).

^{§§}From Smith et al. (2006).

Deino and Potts (1990) was applied, in which apparent plateau and fusion ages were excluded if they contributed to a MSWD >1.5, thereby eliminating only obvious outliers from the age calculation (Smith et al., 2006). Isochrons were regressed using the method of York (1969) in order to test for excess argon, and in virtually all cases exhibit atmospheric intercepts (Fig. DR2; see footnote 1).

⁴⁰Ar/³⁹Ar Results

Sanidine

Fusions and incremental heatings were performed on single crystals and small multicrystal aliquots of sanidine from 18 of the dated samples (Figs. 6 and DR3). Single-crystal fusions of sanidine from six samples yielded precise results due to their large size (>250 μm), showed no distinct outliers, and gave weighted mean ages of 51.74 ± 0.09 Ma (Halfway Draw tuff), 47.70 ± 0.12 Ma (White Lignitic tuff), 48.76 ± 0.09 Ma (Church Buttes tuff), 48.62 ± 0.28 Ma (Leavitt Creek tuff), 48.15 ± 0.08 Ma (Henrys Fork tuff), and 48.11 ± 0.08 Ma (Tabernacle Butte tuff) (Fig. 6; Table 2). However, sanidine from several ash beds were too small (<180 μm in diameter) to achieve an adequate signal to blank ratio from single crystals, necessitating the use of multicrystal aliquots to achieve usefully high precision (i.e., <5% uncertainty). In most cases, multicrystal analyses yield Gaussian apparent age distributions with few outliers and give stratigraphically consistent weighted mean ages of 51.90 ± 0.09 Ma (Scheggs tuff), 50.61 ± 0.23 Ma (Boar tuff), 48.94 ± 0.29 Ma (Sand Butte tuff), 48.66 ± 0.28 Ma (Continental tuff), and 51.66 ± 0.09 Ma (K-spar tuff) (Fig. 6; Table 2). Note that new analyses of sanidine from the Firehole and Analcite tuff beds have resulted in a slight revision of the preferred ages for these beds (Table 2). Incremental heating experiments performed on multicrystal sanidine aliquots from several tuffs all yield internally concordant plateau ages consistent with fusion ages, suggesting that ⁴⁰Ar* loss due to alteration is insignificant (Table 2; Fig. DR3).

Although concerns have been raised about the ability to distinguish xenocrysts when multiple sanidine crystals are analyzed (cf. Machlus et al., 2004; Smith et al., 2006), single-crystal fusion results suggest that contamination present in Green River Formation ash beds is composed of significantly older grains that can be readily distinguished and excluded even when using small multicrystal aliquots. To assess the distribution and magnitude of potential contamination of multicrystal aliquots, single-crystal fusions of sanidine from the Analcite, Scheggs, and Sixth tuffs were conducted. Although

these measurements are relatively imprecise due to lower signal to blank ratios (i.e., >10% uncertainty), single fusions of Analcite tuff and Scheggs tuff sanidine produced no obvious outliers and yield weighted mean ages that are indistinguishable from those of multicrystal analyses (Figs. 6 and DR4). Sanidine from the Sixth tuff proved to be more problematic (cf. Smith et al., 2003). New single-crystal fusions (n = 37) of Sixth tuff sanidine yield a weighted mean of 48.68 ± 0.59 Ma that is consistent with the more precise age of 49.62 ± 0.10 Ma acquired via the incremental heating of individual biotite, which remains its preferred age (Smith et al., 2006). However, three single-crystal fusions gave apparent ages that are significantly overestimated (>70 Ma; Fig. DR4). Accordingly, when Sixth tuff sanidine were analyzed as 5 crystal aliquots (cf. Smith et al., 2003), only 11 of 30 fusions yielded stratigraphically reasonable apparent ages, whereas 19 gave distinctly older ages (Fig. DR4). We interpret these older outliers to reflect the admixture of a small proportion (<10%) of xenocrystic or detrital grains with a larger number of juvenile magmatic sanidine.

Sanidine from the Strawberry and Yellow tuff beds exhibited the largest amount of age scatter, which limits the precision of the age determinations for these beds (Fig. 7). More than 10% of single-crystal fusions of Strawberry tuff sanidine yielded distinctly older ages, and accordingly, >90% of 6- to 8-crystal analyses gave anomalously old apparent ages. Similarly, only 50% of 3-crystal fusions of sanidine from the Yellow tuff gave stratigraphically reasonable apparent ages, and only 20% of fusions of 20-crystal aliquots could be included in the weighted mean calculation. We infer that the age scatter observed for both samples can be attributed to the inclusion of 10%–20% inherited grains.

Excluding the Strawberry and Yellow tuffs, only 11 of 296 (3.7%) of sanidine analyses were excluded from age calculations (Table 2; Fig. 6). Based on the apparent absence of fluvial reworking of most sampled tuffs (Table DR2; see footnote 1) and largely unimodal sanidine age distributions (Fig. 6; Table DR2), we interpret their weighted mean ages to represent the best estimate of their age of eruption and deposition.

Detrital Feldspar

Laser fusion measurements were performed on single detrital feldspar grains from three volcanoclastic sand beds and yielded apparent ages indicative of rapid transport and deposition of erupted materials with little admixture of detrital grains. Of 82 analyses of K-feldspar from the Antelope sand bed near the base of the Sand Butte bed of the Laney Member, 20 gave apparent ages that range from Paleocene

to Proterozoic (Fig. 8). However, 62 analyses yield Eocene apparent ages that have a Gaussian distribution (Fig. 8), suggesting derivation from a common eruption or set of similarly timed eruptions. We take the weighted mean age of this younger component (48.70 ± 0.19 Ma) to indicate the age of this volcanism and the maximum age of sand deposition (cf. Deino and Potts, 1990). Similarly, 19 of 25 analyses of sanidine from the Sage tuff, a volcanoclastic sand bed in the Bulldog Hollow Member of the Fowkes Formation, gave internally consistent apparent ages with a weighted mean of 47.94 ± 0.17 Ma (Fig. 6). All 35 analyses of >0.5-mm-diameter sanidine from the Sage Creek Mountain pumice within a sand bed near the base of the Turtle Bluff Member of the Bridger Formation gave precise, consistent apparent ages that have a weighted mean of 47.17 ± 0.08 Ma (Fig. 6), suggesting their derivation from a single eruption or closely timed set of eruptions.

Biotite

Several of the tuff beds sampled from the Uinta Basin lack sanidine, which necessitated the use of biotite. Multiple laser incremental heatings of hand-picked euhedral biotite crystals were conducted to assess the potential for alteration-derived discordance and inaccuracy. In addition, electron probe microanalysis was performed on biotite crystals to gauge the presence or absence of alteration phases. (Table DR4 and Figs. DR5 and DR6; see footnote 1) (cf. Smith et al., 2006). Age spectra produced from biotite from Green River Formation tuff beds are of two distinct types: (1) concordant and reproducible, and (2) discordant and indicative of alteration-related ⁴⁰Ar loss and ³⁹Ar recoil during irradiation. Discordant age spectra were observed from biotite from several tuffs (Fig. DR5), and correlate to the presence of intergrown alteration phases (Table DR4; Fig. DR6) and integrated age scatter toward both older and younger apparent ages (Fig. DR7). We consequently take the weighted mean of concordant biotite experiments as the best estimate for the eruptive age of the ash beds from which sanidine was unavailable (Fig. 6; Table 2), but caution that biotite populations yielding predominantly discordant spectra (i.e., the Curly, Wavy, Blind Canyon, and Fat tuffs) are less reliable than those yielding predominantly concordant plateaus, such as the Portly and Oily tuffs.

Analytical Results and Uncertainties

Because our initial emphasis is on delimiting the timing of lacustrine deposition in the

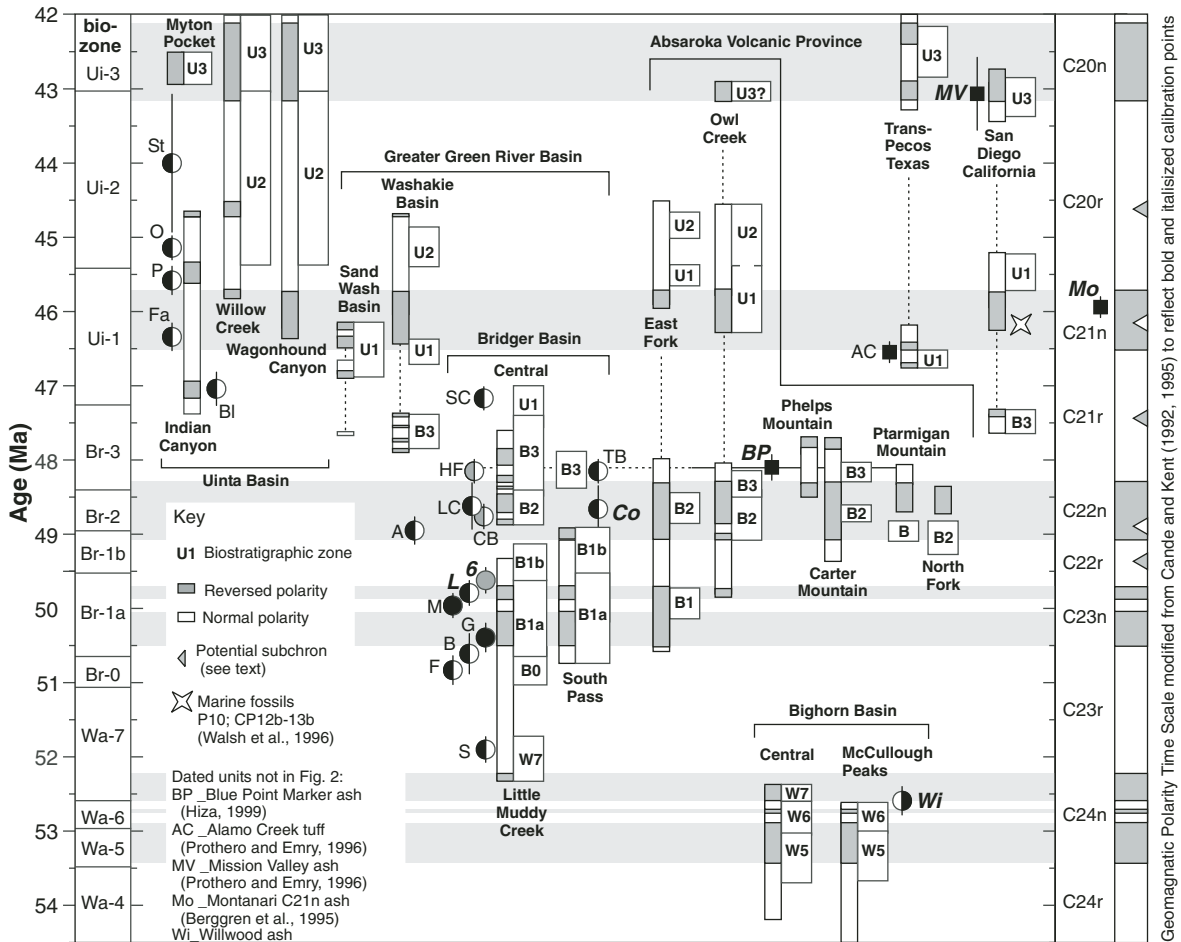


Figure 9. Integrated early and middle Eocene paleomagnetic chronostratigraphy for western North America. All $^{40}\text{Ar}/^{39}\text{Ar}$ ages are shown with 2σ intercalibration uncertainties relative to the standard values of Renne et al. (1998).

Greater Green River Basin and Uinta–Piceance Creek Basin, $^{40}\text{Ar}/^{39}\text{Ar}$ ages are reported with 2σ analytical uncertainties relative to the standard ages of Renne et al. (1998). Table 2 also reports intercalibration and fully propagated uncertainties for each unit (Karner and Renne, 1998; Renne et al., 1998). Intercalibration uncertainties should be considered when making comparisons to $^{40}\text{Ar}/^{39}\text{Ar}$ ages obtained using other standard minerals or to the geomagnetic polarity time scale (Fig. 9; Cande and Kent, 1992, 1995; Ogg and Smith, 2004). Fully propagated uncertainties reflect uncertainty in the ^{40}K decay constant and K/Ar age of the GA-1550 primary biotite standard, and are required for comparisons with isotopic chronometers other than ^{40}K decay, such as U-Pb (Karner and Renne, 1998; Min et al., 2000).

ASH BED CORRELATIONS

Several possible correlations between ash beds are suggested by $^{40}\text{Ar}/^{39}\text{Ar}$ ages (Fig. 2B).

Biotite phenocryst compositions provide an additional test of ash bed correlations (Desborough et al., 1973; Yen and Goodwin, 1976; Mauger, 1977). One potential correlation connects the Henrys Fork, Tabernacle Butte, and Wavy tuffs, all of which have overlapping $^{40}\text{Ar}/^{39}\text{Ar}$ ages (Table 2). The FeO/MgO and TiO_2 compositions of biotite from the Henrys Fork and Wavy tuffs are similar (Fig. 10; Table DR4); however, biotite from the Tabernacle Butte tuff was not analyzed. At a broader spatial scale, these three ashes may correlate to the more proximal Blue Point Marker tuff in the southern Absaroka Volcanic Province, which was $^{40}\text{Ar}/^{39}\text{Ar}$ dated by Hiza (1999) as 48.10 ± 0.17 Ma (Fig. 5). Another potential correlation connects the Continental, Church Buttes, and Curly tuffs, which have overlapping $^{40}\text{Ar}/^{39}\text{Ar}$ ages and biotite with similar FeO/MgO and TiO_2 compositions. However, the ages of the Continental and Curly tuffs also overlap with the age of the Leavitt Creek tuff, which is ~100 m above the Church Buttes tuff

but has not been analyzed for biotite composition (Fig. 10; Table 2).

AGE MODEL FOR THE GREEN RIVER FORMATION

Calibration of North American Land-Mammal Ages

The $^{40}\text{Ar}/^{39}\text{Ar}$ ages presented here add to a radioisotopic data set (Wing et al., 1991; Smith et al., 2003, 2004, 2006) that provides temporal calibration for a large suite of existing lithostratigraphy, biostratigraphy, and magnetostratigraphy (Fig. 3). Overall, the ages determined for this study are entirely consistent with isochroneity of the North American land-mammal ages throughout the study area (Wood et al., 1941; Robinson et al., 2004). The direct temporal implications of these ages for the late Wasatchian, Bridgerian, and Uintan land-mammal ages are summarized in Figure 3 and detailed in Table 3.

Implications for Paleomagnetic Records and the Geomagnetic Polarity Time Scale

New $^{40}\text{Ar}/^{39}\text{Ar}$ ages allow for the calibration of early and middle Eocene paleomagnetic polarity records, which have been obtained at seven sites in basins containing the Green River Formation (Fig. 9; Jerskey, 1981; Flynn, 1986; Prothero and Swisher, 1992; McCarroll et al., 1996a; Stucky et al., 1996; Clyde et al., 1997, 2001). These studies have typically focused on alluvial strata where mammalian fossils are preserved, but in several cases have reported the polarity of lacustrine strata. Previous efforts to correlate magnetic polarity records to the geomagnetic polarity time scale have been hampered by a lack of common $^{40}\text{Ar}/^{39}\text{Ar}$ standard values (cf. Renne et al., 1998; Smith et al., 2003) and uncertain time-stratigraphic relationships between basins (cf. Wing et al., 2000; Smith et al., 2003; Machlus et al., 2004). However, when viewed in total (Fig. 9; Table 4), the current data set resolves many previous uncertainties and permits the recalibration, consistent with the standard ages of Renne et al. (1998), of the ages of chrons C24r through C20n. Our provisional calibration (Table 5) was calculated using seven $^{40}\text{Ar}/^{39}\text{Ar}$ ages for ash beds found within paleomagnetically characterized strata or their correlative equivalents (Fig. 9; Table 4). The new magnetic reversal ages (Table 5) are consistent with magnetostratigraphy at 19 locations, and with the presence of marine index taxa (P10, CP12b-13b) associated with C21n within the Ardath Shale; the shale underlies alluvial strata near San Diego, California, that contain Ui-1 faunas (Berggren et al., 1995; Walsh et al., 1996). The most significant resulting change involves a shift in the age of chron C22, which becomes ~1 m.y. younger than indicated by either Cande and Kent (1992, 1995) or Ogg and Smith (2004). Another interesting feature is the presence of several brief polarity intervals that do not appear in seafloor magnetic anomaly records (Cande and Kent, 1992). If not the result of overprinting, such features may reflect short-term weakenings or reversals of the Earth's magnetic field similar to those observed in the Pliocene–Pleistocene record (Langereis et al., 1997; Singer et al., 2004).

Extrapolation of Age Model to Strata Not Directly Constrained by Tuff Beds

Ash beds have not been identified in the lowest portions of the Green River Formation below the Sheggs and Yellow tuffs (Fig. 2), and therefore mammalian biostratigraphy remains the most useful age constraint. For example, the alluvial DeBeque Formation, which is

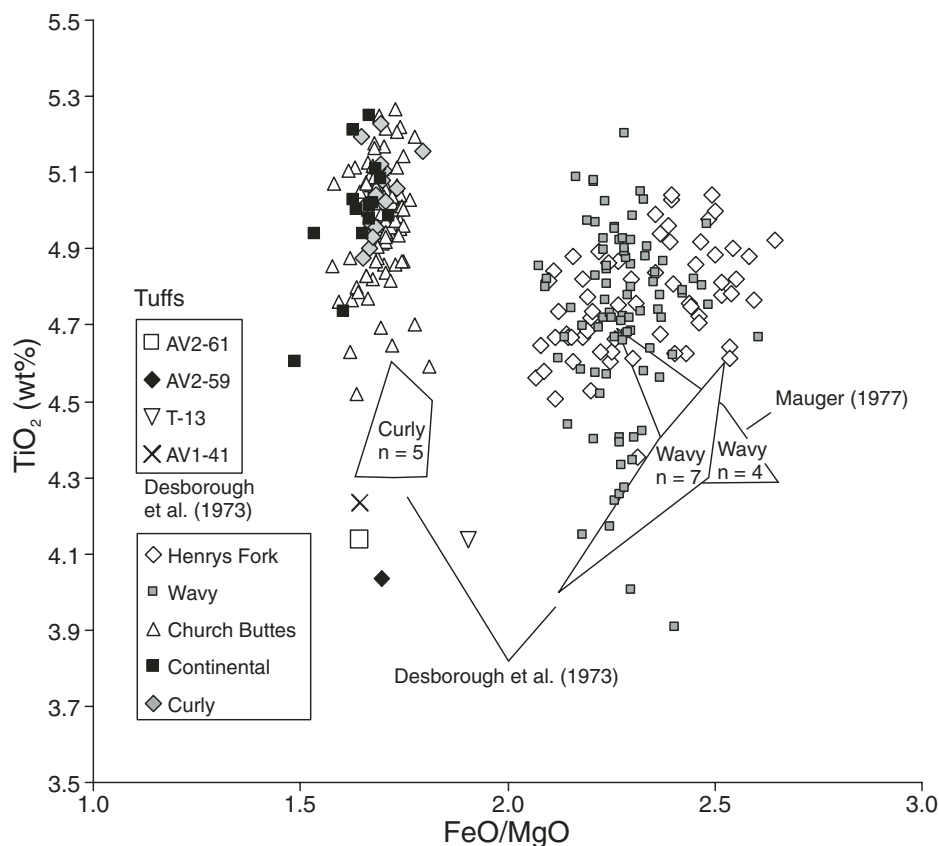


Figure 10. FeO/MgO versus TiO_2 plot of electron microprobe point analyses on biotite from select ash beds illustrating several likely correlations. Values are shown as weight percent. Biotite compositions for Henrys Fork and Church Buttes tuff beds are from Smith (2007). Lower TiO_2 values of Desborough et al. (1973) and Mauger (1977) for biotite from the Wavy and Curly tuff beds may reflect the improved detection and interference correction capabilities of the Cameca SX51 electron microprobe and software used versus those utilized in the 1970s.

equivalent to the lower half of the Green River Formation in the Piceance Creek Basin, has yielded Graybullian (Wa-5) through Gardnerbuttean (Br-0–Br-1a) faunas (Kihm, 1984; Froehlich and Froehlich, 2002). Strata equivalent to the lower part of the Green River Formation in the Greater Green River Basin have produced a similar faunal succession (Fig. 3; Holroyd and Smith, 2000; Zonneveld et al., 2000). In strata where fossil collections are absent, such as the Battle Spring Formation and Colton Formation (Spieker, 1946; Love, 1970), temporal assignments are typically based on bulk lithologic correlations (i.e., the deposits overlie Paleocene deposits and are therefore probably early Eocene in age).

Radioisotopic ages, mammalian fossils, and magnetostratigraphy also provide varying levels of temporal resolution for Eocene strata in the basins and volcanic fields that surround the Green River Formation basins (Figs. 4 and 5). Table DR5 (see footnote 1) provides a comprehensive list of currently available $^{40}\text{Ar}/^{39}\text{Ar}$ age

determinations from the Eocene of the northern Rocky Mountains, all recalibrated to the standard ages of Renne et al. (1998). For a more thorough discussion of the biochronology of Laramide basins, see Table DR1 and excellent reviews by Krishtalka et al. (1987), Lillegraven (1993), and Robinson et al. (2004).

RATES OF DEPOSITION

Radioisotopic ages permit a direct numerical calibration of average sediment accumulation rates for Eocene strata in several Laramide basins. Due to the presence of exposure horizons throughout Green River Formation and its distinctly heterolithic character at the meter scale, a high potential exists for differential sedimentation rates for different facies. Therefore, rates cited here represent long-term averages rather than instantaneous sedimentation rates. Additional uncertainties arise due to the effects of differential compaction and the uncertainties inherent to the $^{40}\text{Ar}/^{39}\text{Ar}$ method. Geochronology

TABLE 3. RADIOISOTOPIC CONSTRAINTS ON NORTH AMERICAN LAND-MAMMAL AGES

Basin	Formation or Member	Dated unit	Age ($\pm 2\sigma$) [†]	Radioisotopic references	Biostratigraphy (zone)	Biostratigraphy references
Bighorn	Willwood Formation	Willwood ash	52.59 \pm 0.19	Smith et al. (2004)	transition: Wa-6 to Wa-7	Rohrer and Gazin (1965); Wing et al. (1991); Gingerich and Clyde (2001)
Wind River	Wind River Formation	Halfway Draw tuff	51.74 \pm 0.17	this study	Wa-7	Sinclair and Granger (1911); Love (1970)
Piceance Creek	Basal Parachute Creek Member	Yellow tuff	51.24 \pm 0.54	this study	overlies Wa-7 strata	Kihm (1984); Krishtalka and Stucky (1986)
Fossil	Fossil Butte Member	K-spar tuff	51.66 \pm 0.17	this study	Wa-7	Ambrose et al. (1997); Froehlich and Breithaupt (1998)
Greater Green River	Tipton Member	Scheggs tuff	51.90 \pm 0.17	this study	overlies and underlies Wa-7 strata	Morris (1954); McGrew and Roehler (1960); Gazin (1962, 1965); Savage et al. (1972); West (1973); Stucky (1984); Honey (1988); Anemone et al. (2000); Holroyd and Smith (2000); Zonneveld et al. (2000, 2003); Smith and Holroyd (2003); Gunnell et al. (2004)
Greater Green River	Wilkins Peak Member	Firehole, Boar, Grey, Main, Layered, and Sixth tuffs	oldest 50.83 \pm 0.19 youngest 49.62 \pm 0.17	this study, Smith et al. (2003, 2006)	laterally equivalent to Wa-7, Br-0, and Br-1a strata	McGrew and Roehler (1960); Gazin (1962, 1965); Simnacher (1970); West (1970, 1973); West and Dawson (1973); Stucky (1984); Honey (1988); Gunnell and Bartels (1994); Gunnell and Yarborough (2000); Zonneveld et al. (2000, 2003); Clyde et al. (2001)
Greater Green River	Bridger Formation	Continental tuff	48.66 \pm 0.31	this study	overlies Br-1b strata	Clyde et al. (2001); Gunnell and Bartels (2001)
Greater Green River	Bridger Formation (Bridger B)	Church Buttes & Leavitt Creek tuffs	48.62 \pm 0.31 48.74 \pm 0.16	this study	Br-2	Mathew (1909); Gazin (1976); West (1976); Evanoff et al. (1998); Murphey (2001)
Greater Green River	Laney Member	Analcite tuff	48.94 \pm 0.18	this study, Smith et al. (2003)	underlies Br-3	Roehler (1973b); West and Dawson (1975); Turnbull (1978); McCarroll et al. (1996a, 1996b); Stucky et al. (1996)
Greater Green River	Bridger Formation (top of Bridger C)	Henrys Fork tuff	48.15 \pm 0.16	this study	Br-3	Mathew (1909); Gazin (1976); West (1976); Covert et al. (1998); Evanoff et al. (1998); Murphey (2001)
Greater Green River	Bridger Formation	Tabernacle Butte tuff	48.11 \pm 0.16	this study	Br-3	McGrew (1959); West and Atkins (1970)
Greater Green River	Turtle Bluffs Member (Bridger E)	Sage Creek Mountain pumice bed	47.17 \pm 0.16	this study	Ui-1	West and Huchison (1981); Evanoff et al. (1994); Murphey (2001)
Uinta-Piceance Creek	Basal Upper Member (UB) and Parachute Creek Member (PCB)	Curly tuff	49.02 \pm 0.33	this study	overlies Br-2	Kay (1957); Gazin (1959); MacGinitie (1969); Izett et al. (1985); Krishtalka and Stucky (1986); Doi (1990); Honey (1990); Gunnell and Bartels (1999); Froehlich and Froehlich (2002)
Fowkes	Bulldog Hollow Member-Fowkes Formation	Sage ash	47.94 \pm 0.22	this study	Br-3	Oriel and Tracey (1970); Nelson (1973)
Wind River	Wagon Bed Formation-Unit 3	White Lignitic tuff	47.70 \pm 0.18	this study	underlies Ui-2	Sinclair and Granger (1911); Van Houten (1964); Emry (1975)
Uinta	Upper Member	Blind Canyon tuff	47.04 \pm 0.22	this study	underlies Ui-2	Osborn (1895); Kay (1934, 1957); Prothero (1996); Rasmussen et al. (1999)
Trans-Pecos, Texas	Devils Graveyard Formation	Tuff below Alamo Creek basalt	46.55 \pm 0.15	Prothero and Emry (1996)	Ui-1	Walton (1992); Prothero and Emry (1996)
San Diego, California	Mission Valley Formation	Ash bed	43.07 \pm 0.49	Prothero and Emry (1996)	Ui-3	Prothero and Emry (1996); Walsh et al. (1996)
Absaroka Volcanic Province	Trout Peak Trachyandesite	Groundmass from lava flows	oldest 48.76 \pm 0.19 youngest 48.37 \pm 0.15	Feeley and Cosca (2003)	overlies Br-2	Bown (1982); Torres and Gingerich (1983); Torres (1985); Gunnell et al. (1992)
Absaroka Volcanic Province	Blue Point Marker	Blue Point ash	48.10 \pm 0.17	Hiza (1999)	Br-3, underlies Ui-1	Eaton (1980, 1982, 1985); Bown (1982); Sundell et al. (1984)

[†]Analytical and intercalibration uncertainties relative to 28.34 Ma for TCs (Renne et al., 1998).

TABLE 4. RADIOISOTOPIC CONSTRAINTS ON THE EARLY AND MIDDLE EOCENE GEOMAGNETIC POLARITY TIME SCALE

Dated unit	Formation or Member	Age $\pm 2\sigma^{\dagger}$ (Ma)	Radioisotopic references	Magnetostratigraphy	Magnetostratigraphy references
Willwood ash	Willwood Formation	52.59 \pm 0.19	Wing et al. (1991); Smith et al. (2004)	C24n (base of lowest subchron)	Clyde et al. (1994); Tauxe et al. (1994)
Layered tuff	Wilkins Peak Member	49.79 \pm 0.17	Smith et al. (2006)	C23n-C22r transition	Clyde et al. (1997, 2001)
Sixth tuff	Wilkins Peak Member	49.62 \pm 0.17	this study; Machlus et al. (2004); Smith et al. (2006)	C23n-C22r transition	Clyde et al. (1997, 2001)
Continental tuff	Bridger Formation	48.66 \pm 0.31	this study	C22n	Clyde et al., (2001)
Blue Point Marker ash	overlies Aycross Formation and Trout Peak Trachyandesite	48.10 \pm 0.22	Hiza (1999)	base of C21r	Eaton (1982); Lee and Shive (1983); Sundell et al. (1984); Flynn (1986)
Montenari ash	?	45.94 \pm 0.14	Berggren et al. (1995)	C21n	Berggren et al. (1995)
Mission Valley ash	Mission Valley Formation	43.07 \pm 0.49	Prothero and Emry (1996)	C20n	Walsh et al. (1996)

[†]Analytical and intercalibration uncertainties relative to 28.34 Ma for TCs (Renne et al., 1998).

derived accumulation rate uncertainty for strata between tuff beds (expressed at the 2σ level) ranges from 9% to >40% and is highest when short time intervals are considered.

Greater Green River Basin

During deposition of the evaporative Wilkins Peak Member, net average sediment accumulation rates in the Greater Green River Basin were approximately three times faster at the basin center (200 mm/k.y.) versus the basin margin (60 mm/k.y.). In contrast, higher rates occurred at the basin margin (180 mm/k.y.) versus the basin center (110 mm/k.y.) during deposition of the fluctuating profundal Rife bed of the Tipton Member (Fig. 11). The most rapid sediment accumulation (>1000 mm/k.y.) occurred when volcanoclastic materials entered the basin from the north and propagated out over fine-grained Laney Member lake strata, which had accumulated an order of magnitude more slowly (120 mm/k.y., Fig. 11).

Uinta Basin

Sediment accumulation at Indian Canyon, Utah, which occupies a basin-margin position within the Uinta Basin (Dane, 1955; Dyni et al., 1985), was relatively constant at ~150 mm/k.y. over a 7 m.y. interval during which both evaporative and fluctuating profundal facies were deposited. The lowest average accumulation rate for the section (100 mm/k.y.) occurred during the deposition of the evaporative saline facies, which is consistent with low accumulation rates observed at the basin margin of the Greater Green River Basin during Wilkins Peak Member deposition. A lack of subsurface stratigraphic information disallows a precise calculation of sediment accumulation rates in the depocenter for the saline facies interval, but a

doubling of stratal thickness and accumulation rate is likely.

Absaroka Volcanic Province

Average accumulation rates in the Absaroka Volcanic Province were in several cases an order of magnitude faster than temporally equivalent portions of the Green River Formation (Fig. 5). At Trout Peak, Wyoming, for example, paleomagnetic polarity stratigraphy (Shive and Pruss, 1977) and several ⁴⁰Ar/³⁹Ar ages ranging from 48.8 to 48.4 Ma (Feeley and Cosca, 2003) indicate that >1 km of volcanoclastic sediment and lava flows were deposited during C22, which is <1 m.y. in duration (Table 5). The resulting average accumulation rate of >1000 mm/k.y. for this section is an order of magnitude faster than the average sedimentation rate for the temporally equivalent Laney Member in the Washakie sub-basin of the Greater Green River Basin. Notably, the bulk of materials preserved in the Absaroka Volcanic Province are volcanoclastic rather than primary volcanic deposits, and volcanic centers are typically identified based on the presence of intrusive rocks (Fig. 5; Smedes and Prostka, 1972; Sundell, 1993). Consequently, the accumulation rates cited above reflect the accumulation of strata in the areas between volcanic centers, whereas individual stratocones may have accumulated at significantly faster rates.

DISCUSSION

Synoptic Lake Type Evolution

An examination of modern lakes reveals that regional drainage relationships can lead to significant differences in the hydrologic budgets for adjacent lakes occupying similar climates. Examples include freshwater Utah Lake, which overflows into the hypersaline Great Salt Lake,

TABLE 5. AGES FOR PALEOMAGNETIC CHRONS 24N THROUGH 19R

Chron (base)	Age (Ma)	Age (Ma)	Age (Ma)
	Cande and Kent (1995)	Ogg and Smith (2004)	This study
C24n.3n	53.35	53.81	53.44
C24n.2r	52.90	53.29	52.89
C24n.2n	52.80	53.17	52.75
C24n.1r	52.76	53.12	52.71
C24n.1n	52.66	53.00	52.59
C23r	52.36	52.65	52.23
C23n.2n	51.74	51.90	50.50
C23n.1r	51.05	51.06	50.04
C23n.1n	50.95	50.93	49.88
C22r	50.78	50.73	49.71
C22n	49.71	49.43	49.07
C21r	49.04	48.60	48.30
C21n	47.91	47.24	46.52
C20r	46.26	45.35	45.71
C20n	43.79	42.77	43.16
C19r	42.54	41.59	42.12

Note: The intercalibration uncertainties for the ⁴⁰Ar/³⁹Ar ages used as calibration points for the geomagnetic polarity timescale range from ± 0.2 to ± 0.5 m.y. Due to additional uncertainty resulting from interpolation between these calibration points, these uncertainties represent the *minimum* age uncertainty for magnetic chron boundaries ages that are interpolated between them. Comparisons of these ages to other chronometers (such as U-Pb) would require the use of fully propagated uncertainties (Renne et al., 1998), which range from ± 0.8 to ± 1.0 m.y.

and freshwater Lake Kinneret, which overflows into the hypersaline Dead Sea (Eugster and Hardie, 1978). A few studies have documented similar upstream and downstream hydrologic relationships in Pleistocene lake systems (Benson et al., 1990), but interbasin relationships for pre-Quaternary lake systems are difficult to evaluate due to the limitations of nonmarine geochronology (Surdam and Stanley, 1980).

The age model presented here allows for the highest resolution reconstruction yet available for the Green River Formation lake system and permits for the first time direct upstream and

downstream comparisons of strata in separate basins at the member scale and even bed scale (Figs. 2B). Lake type observations (Table 1) have been combined with paleocurrent indicators and provenance data (cf. Table DR6) in order to reconstruct the paleohydrologic configuration of the Laramide landscape for eight discrete time slices (Fig. 12). The resulting maps are intended to be synoptic views of the Green River Formation lakes and the hydrologic links between them and were selected to illustrate the principle lake type configurations. As with any such reconstruction, uncertainties incurred from stratigraphic correlation and geochronology inevitably introduce some time averaging of facies and paleoenvironments. However, time averaging in this case is limited to $\sim\pm 100$ k.y., which represents an order of magnitude improvement in resolution relative to previous reconstructions (Surdam and Stanley, 1980; Grande, 1984; Dickinson et al., 1988; Lillegraven and Ostresh, 1988).

53.0 Ma

At the onset of lacustrine deposition, two major extrabasin catchments drained into the Green River Formation basins and fed several small freshwater lakes (Cow Ridge and Luman Members; Fig. 12A). One stream entered into the northwest Greater Green River Basin and the other flowed into the southern Uinta Basin. Pinyon type quartzite clasts likely derived from southwest Montana (Krause, 1985; Janecke et al., 2000) in the Pass Peak Formation (Dorr et al., 1977) attest to a significant catchment area ($\sim 100,000$ km²) for the northern stream (Fig. 1). Arkosic sandstone derived from uplifts in southern Colorado in the Colton Formation and outward-directed paleocurrent directions in the South and Echo Park, Denver, Raton, and San Juan Basins (Fig. 1; Table DR1) constrain the potential catchment area of the stream feeding the southern Uinta Basin to $\sim 50,000$ km² (Dickinson et al., 1986). Fluvial-lacustrine facies in all of the major basins imply the existence of an outlet stream somewhere, but its location remains unknown. Alluvial fan deposits limit possible outlet locations to the northeast margin of the Greater Green River Basin and southwest margin of the Uinta Basin (Fig. 12A; Sklenar and Anderson, 1985). Any stream exiting to the northeast would likely have joined with north-directed streams that flowed from the Bighorn, Wind River, and Shirley Basins into the Powder River Basin (Fig. 1; Seeland, 1978, 1992, 1998). Any south-directed outlet streams would have likely drained into the Claron Formation basins of southwest Utah (Fig. 1), which contain poorly dated alluvial and lacustrine Eocene strata (Fig. 4; Goldstrand, 1994). Volcanism at the time appears to have been confined to the

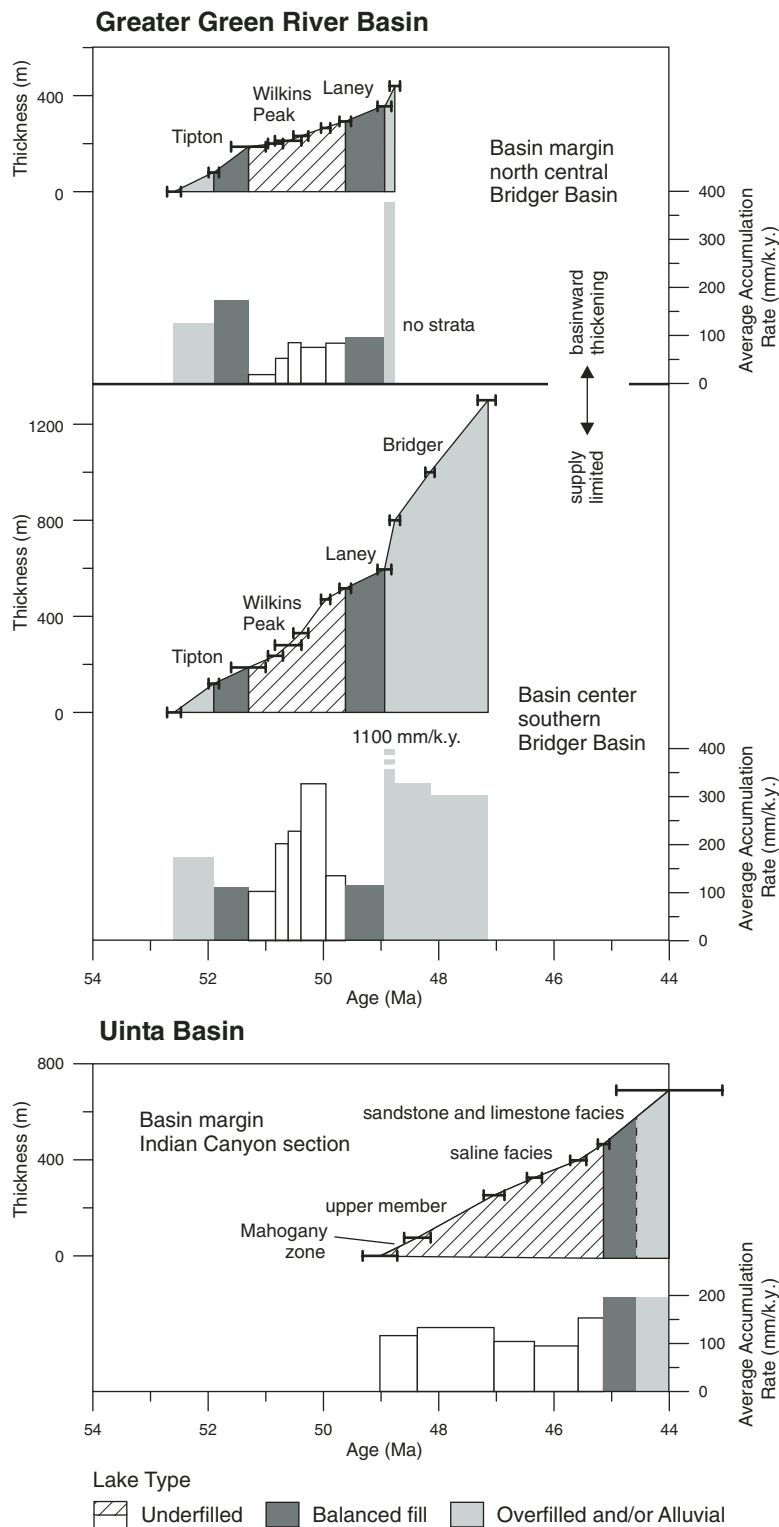


Figure 11. Cumulative thicknesses and average accumulation rates for Eocene strata between ⁴⁰Ar/³⁹Ar dated units at basin-margin and basin-center sites in the Greater Green River Basin and at a basin-margin site in the Uinta Basin. Thicknesses for Bridger Basin are from Roehler (1992b) and Evanoff et al. (1998); thicknesses for Indian Canyon section were provided by J.R. Dyni (2005, personal commun.).

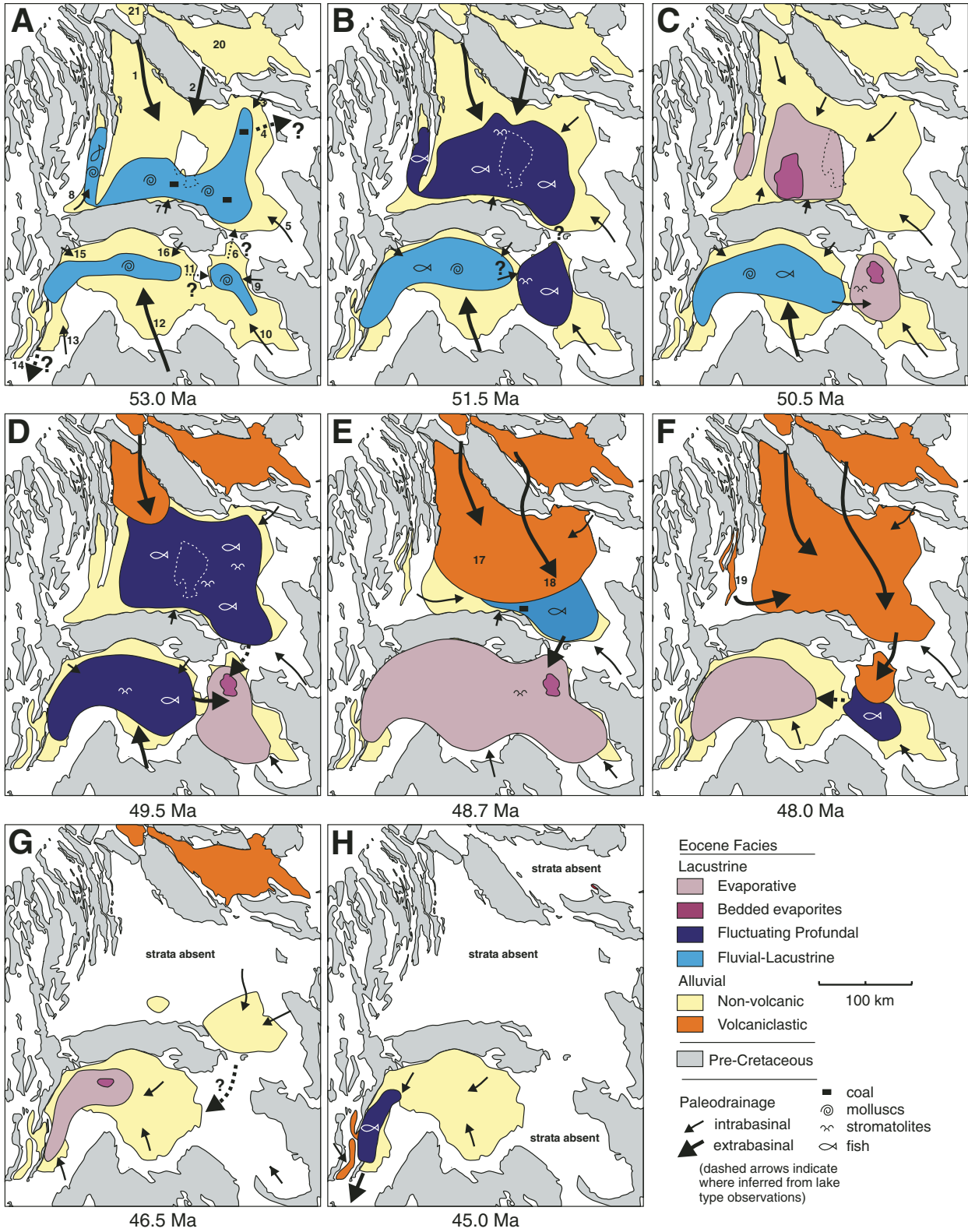


Figure 12. Annotated synoptic maps showing paleohydrologic configuration of the Green River Formation lakes at eight discrete times between 53 and 45 Ma. Locations of bedded evaporites are from Bradley and Eugster (1969), Dyni (1974), and Dyni et al. (1985). Time slices were selected to highlight major hydrologic configurations of the Green River Formation lake system. Paleocurrent and provenance information are summarized from a large number of sources, referenced in Table DR6 (see footnote 1) to the numbers shown. Note that knowledge of the continuity of lacustrine deposition in the central Greater Green River Basin is limited by the absence of Eocene strata atop the Rock Springs uplift. See Figure 1 for detailed geographic reference.

Lowland Creek Field and several centers in the northwest Absaroka Volcanic Province (Fig. 5; Chadwick, 1969; Ispolatov, 1997; Hiza, 1999; Feeley et al., 2002).

51.5 Ma

Two broad, moderately saline lakes occupied the Greater Green River and Piceance Creek Basins at this time and continued to be fed by the two aforementioned paleodrainages (Fig. 12B). Deposition in the Uinta Basin continued to be fluvial lacustrine, whereas fluctuating profundal facies were deposited in the Greater Green River Basin and Piceance Creek Basin (Tipton and Garden Gulch Members), implying a lack of consistent outflow (Fig. 12B). A freshwater lake also occupied the Bighorn Basin at this time (Fig. 4, Tatman Formation; Rohrer and Smith, 1969), but it is uncertain whether it drained to the north or south. Regional expansion of lake facies was postulated by Carroll et al. (2006) to reflect a decrease in sediment delivery from basin-bounding uplifts subsequent to the removal of easily eroded Cretaceous cover from their crests. Volcanism continued at this time to be confined to the northwest Absaroka and Lowland Creek fields (Fig. 5), either of which may have contributed distal ash beds to the Green River Formation lake basins.

50.5 Ma

The Bridger subbasin of the Greater Green River Basin and the Piceance Creek Basin had both become terminal sinks in which evaporites were deposited by this time (Wilkins Peak and Parachute Creek Members; Fig. 12C). Concurrent thrusting along the southern margins of the

Gros Ventre, Wind River, and Granite Mountains uplifts (Love, 1970; Lageson, 1987; Steidtmann and Middleton, 1991) likely diverted the northern catchment away from the Greater Green River Basin, causing it to become underfilled (Pietras et al., 2003a). Pinyon type quartzite gravels characteristic of the northern catchment were diverted into the Bighorn and Wind River Basins, where deposition of fluvial-lacustrine to alluvial facies prevailed (Krause, 1985; Seeland, 1998). Coarse alluvial fan deposits, crosscutting fault relations, and pronounced differential subsidence all imply concurrent uplift of the Uinta Mountains and Axial Basin arch (Fig. 1; Trudell et al., 1970; Ryder et al., 1976; Roehler, 1993), which became hydrologic barriers between Lake Gosiute and Lake Uinta. As a consequence, smaller interbasin sills such as the Rock Springs uplift and Douglas Creek arch became important controls on local deposition. Alluvial and fluvial-lacustrine facies in the Washakie, Sand Wash, Great Divide, and Uinta Basins reflect overflow of water and dissolved solutes into the evaporative sinks that occupied Bridger subbasin and Piceance Creek Basin (Fig. 12C). The amount of evaporation responsible for solute concentrations high enough for evaporite deposition in these downstream basins was therefore not only the consequence of evaporation at the depositional site, but also the integrated evaporation from all upstream subbasins. When lake level in downstream subbasins rose above the interbasin sills, solutes from neighboring subbasins could no longer be flushed downstream, causing solute concentrations in upstream basins to rise (Fig. 13). Integrations of the collective solute loads for all of the upstream and

downstream basins during such expansions may explain, for example, the dolomitic stromatolite horizons in the otherwise alluvial Cathedral Bluffs Member of the Wasatch Formation in the Washakie subbasin (Roehler, 1992b), and short-term salinity increases interpreted by Keighley et al. (2003) in the otherwise overfilled transitional interval in the Uinta Basin.

Regionally, all of the perimeter and axial basins east of long $\sim 107^\circ\text{W}$ stopped accumulating sediments at this time and lack further middle and late Eocene accumulations (Fig. 4). This widespread regional unconformity may reflect the formation of a regional drainage divide (Love, 1960), which encouraged the continuation of internal drainage in the ponded basins to the west. Volcanoes continued to erupt in the Lowland Creek and northwestern Absaroka Volcanic Province (Ispolatov, 1997; Hiza, 1999), and several volcanic centers in the north-central Absaroka Mountains (Crandall, Independence, Sunlight) erupted for the first time (Fig. 5; Harlan et al., 1996; Hiza, 1999; Feeley and Cosca, 2003).

49.5 Ma

The Green River Formation lakes were increasingly influenced by northern volcanism at this time. In the northern Absarokas, the Sunlight, Crandall, and Independence volcanoes grew into large edifices, represented by the proximal Wapiti Formation and Trout Peak Trachyandesite and distal Aycross Formation to the south (Fig. 5; Nelson and Pierce, 1968; Feeley and Cosca, 2003). In addition, the Slough Creek tuff, the first of several large ash-flow deposits, was erupted from the northern Absaroka Volcanic Province (Fig. 5; Hickenlooper and Gutmann, 1982; Hiza, 1999). At roughly the same time, volcanism commenced in the Challis volcanic field, with several major caldera-forming eruptions of thick ash-flow tuffs (Moye et al., 1988). Several southeast-directed paleovalleys and extensional basins within the fold and thrust belt to the east of the Idaho Batholith in southwest Montana and eastern Idaho were actively being filled by extrusive Challis volcanic rocks (Janecke and Snee, 1993; M'Gonigle and Dalrymple, 1996). Nonvolcanic strata of the Sheep Pass Formation fill similar basins to the south in Nevada (Figs. 1 and 4; Winfrey, 1960; Solomon et al., 1979). The Bighorn, Wind River, Gros Ventre, and Greater Green River Basins were all receiving a significant influx of volcanic detritus from the Absaroka and potentially Challis volcanic fields at this time (Fig. 5; MacGinitie, 1974; Stucky, 1982; Torres, 1985). Volcaniclastic sediment initially entered into the northwest corner of the Greater Green River Basin and rapidly propagated southward to the central Bridger subbasin (Fig. 12D; West,

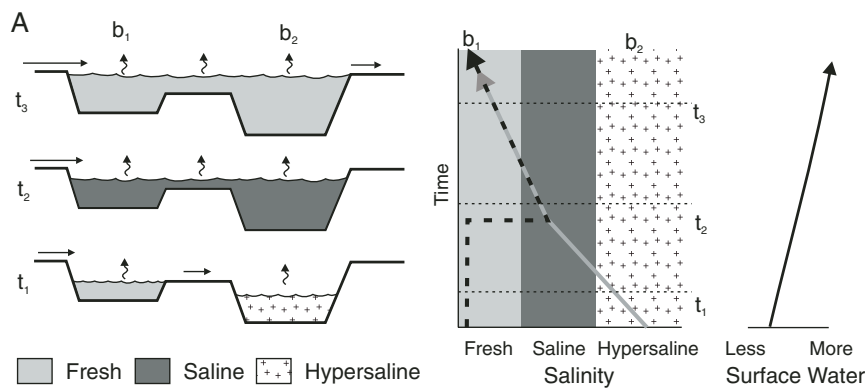


Figure 13. Conceptual model illustrating the effects of an increase in available surface water on the salinity and distribution of lake waters in upstream and downstream basins (modified from Kelts, 1988). During t_1 , available surface water is low, and basins b_1 and b_2 are occupied by freshwater and hypersaline lakes, respectively. An increase in available surface water (t_2) causes the lake in basin b_2 to rise and amalgamate with the lake in basin b_2 , resulting in one broad saline lake. Further increases in available surface water during t_3 result in a rise and freshening of the combined lake in b_1 and b_2 .

1973; Surdam and Stanley, 1980). High rates of sediment accumulation (Fig. 11), the 48.70 Ma mean age for detrital feldspar in the Sand Butte bed (Fig. 8), and andesite cobbles in the lower Bridger Formation (Kistner, 1973) point to a major input of freshly erupted volcanics.

Increased influx of water and volcanoclastic sediment caused Lake Gosiute to expand in areal extent and overflow occasionally into the Piceance Creek Basin (cf. Surdam and Stanley, 1980), which is indicated by the change from evaporative to fluctuating profundal facies (lower LaClède bed of the Laney Member) in the former. This new input may have caused the Piceance Creek Basin lake to expand and merge with the lake in the Uinta Basin, thereby causing balanced-fill conditions (transitional interval) to be propagated upstream (i.e., Fig. 13). However, the continued deposition of evaporites in the Piceance Creek Basin at the time (Fig. 2) attests to the existence of a west to east hydrologic gradient across the Douglas Creek arch, at least during intervals of evaporite deposition.

48.7 Ma

Major volcanism in the Absaroka and Challis fields continued with the growth of volcanic centers and several eruptions of ash-flow tuff (Moye et al., 1988; Hiza, 1999) and had an increasing influence on deposition in the Green River Formation basins (Fig. 12E). The locus of volcanism in the Absarokas had migrated southward, resulting in shorter transport distances for detritus delivered to the basins to the south (Fig. 5). Southwest-directed paleocurrent indicators adjacent to the Wind River uplift in alluvial deposits in the northwest Greater Green River Basin (upper Bridger Formation) indicate that volcanoclastic detritus was transported directly across its crest (Groll and Steidtmann, 1987). Deposition of volcanoclastic sediment had propagated from north to south across the Greater Green River Basin, replacing lacustrine facies (Laney Member) with alluvial facies (Bridger Formation and Washakie Formation) and leaving Lake Gosiute restricted to its southeast corner (Roehler, 1993). To the west of the Fossil Basin, the Fowkes and Woodruff extensional grabens (Fig. 1) became active and may have acted as conduits funneling volcanoclastic sediment (Fowkes Formation) from the north into the southwest Greater Green River Basin (Figs. 2 and 12E; Oriol and Tracey, 1970; Nelson, 1973). Although coarse sediment was deposited in these basins, their lack of lacustrine strata implies that an unknown fraction of that sediment was transported through them. Molluscan faunas and other fluvial-lacustrine indicators in the upper LaClède bed of the Laney Member indicate

that the Greater Green River Basin likely overflowed into the Piceance Creek Basin (Roehler, 1992b). Lake Uinta expanded greatly in extent (the Mahogany zone of the upper Parachute Creek Member and upper member), becoming one vast saline lake that covered both the Uinta and Piceance Creek Basins and overlapped the Douglas Creek arch (Fig. 12E). The organic-rich Mahogany zone marks a shift from evaporative to fluctuating profundal facies in the Piceance Creek Basin, whereas in the Uinta Basin it records a shift from fluctuating profundal to evaporative facies (Fig. 2B).

48.0 Ma

By this time, volcanoclastic input from the north had filled much of the accommodation in the Greater Green River Basin with volcanoclastic alluvial plain strata (Bridger and Washakie Formations) and displaced lacustrine deposition downstream toward the Uinta Basin (Fig. 12F; Stucky et al., 1996; Evanoff et al., 1998; Buchheim et al., 2000). Sediment not deposited in the Greater Green River Basin spilled into the Piceance Creek Basin, building a thick deltaic package on its northern margin (Uinta Formation; Hail, 1992). Volcanoclastic material continued to fill extensional basins to the west of the Greater Green River Basin and in southwest Montana. Evaporite deposition occurred for the first time in the Uinta Basin (upper member), marking a reversal of the hydrologic gradient across the Douglas Creek arch (Fig. 12F). Volcanoes in the Absaroka Volcanic Province continued to propagate southward, abandoning northern centers and filling nearby basins with proximal volcanoclastic sediment (Fig. 5). At the same time, Challis volcanism was nearing its peak of activity and buried significant local paleotopography in east-central Idaho and southwest Montana.

46.5 Ma

A lack of preserved strata from this time in much of the study area limits paleogeographic certainty, but a few remnant deposits yield important clues (Fig. 12G). An evaporative lake occupied the western Uinta Basin and extended into the plateau province (saline facies; Shelliga, 1980; Dyni et al., 1985), whereas alluvial sedimentation was predominant in the eastern Uinta Basin (Uinta Formation; Dane, 1955; Prothero, 1996) and southwest (Turtle Bluffs Member of the Bridger Formation; Evanoff et al., 1998; Murphey, 2001) and southeast Greater Green River Basin (Adobe Town Member of the Washakie Formation; McCarroll et al., 1996a; Stucky et al., 1996). Although volcanism continued in the Absaroka and Challis fields (Snider and Moye, 1989;

Hiza, 1999), and became active in the Rattlesnake Hills area (Fig. 5; Van Houten, 1964), volcanoclastic input to the Greater Green River and Piceance Creek Basins appears to have ceased ca. 47.1 Ma (Hail, 1992; Stucky et al., 1996; Murphey, 2001) and was replaced by deposition of locally derived arkosic alluvium. This change indicates that volcanic areas to the north were no longer part of the catchment of the Green River Formation basins. We speculate that doming caused by a thermal anomaly associated with the southern Absaroka Volcanic Province and Rattlesnake Hills Volcanics (e.g., Pierce and Morgan, 1992) may have uplifted the northern Greater Green River Basin and promoted the rerouting of Absarokan detritus and water away from the area.

45.0 Ma

The last stages of Green River Formation deposition are the most sparsely documented. Surviving strata indicate that a lake occupying the Uinta Basin had become freshwater by this time (sandstone and limestone facies; Fig. 12H). South-directed paleocurrents in the overlying Uinta Formation (Anderson and Picard, 1974) indicate that overflow was probably directed into basins toward the southwest. These basins contain the alluvial and lacustrine Claron Formation, which also exhibits south-directed paleocurrent indicators (Goldstrand, 1994). The volcanoclastic Golden's Ranch Formation on the east side of the Plateau Province (Muessig, 1951) attests to a proximal but unidentified volcanic field that may have been an important source for the thick, coarse tuff beds in saline facies and sandstone and limestone facies of the western Uinta Basin.

SEDIMENT ACCUMULATION RATES

All of the main lacustrine depocenters of the Green River Formation occupy sites of high differential subsidence (Figs. 1 and 2; Dyni, 1969; Roehler, 1993). In detail, however, average sedimentation rate patterns differ significantly for closed versus open intervals, with rapid accumulation occurring in the basin center during underfilled intervals and near the basin margin during overfilled intervals (Fig. 11). This pattern reflects several fundamental differences between open versus closed basins in terms of production, delivery, and preservation of sediment.

High accumulation rates in the basin center during evaporite deposition are consistent with a closed basin in which all solutes are retained and lake level fluctuated significantly below sill level. Although solute delivery rates may be relatively low due to low levels of inflow, very rapid net accumulation rates have been

obtained in modern and Quaternary arid closed basins (Ku et al., 1998; Bobst et al., 2001). Sedimentation in underfilled basins tends to be focused into the basin center during periods of low lake level when solutes are the most concentrated and evaporite beds are deposited. In both the Wilkins Peak Member and saline facies of the Green River Formation, for example, both alluvial and evaporite beds thicken basinward (Culbertson, 1966; Smoot, 1983; Dyni et al., 1985).

In contrast, solutes are periodically to continuously flushed out of overfilled and balanced-filled basins and may never reach concentrations required to precipitate evaporites. Although the absolute rate of solute delivery is likely greater during periods of lake expansion due to a corresponding increase in the hydrologic inflow, these solutes bypass the basin and are carried downstream. As a result, the most rapid sedimentation rates occur at basin margins due to their proximity to sediment sources, whereas basin-center areas are sediment starved and characterized by deposition of condensed intervals. Examples of basinward thinning of strata include the Farson and Sand Butte beds of the Tipton and Laney Members in the Greater Green River Basin (Fig. 2; Stanley and Surdam, 1978; Roehler, 1992a) and the Garden Gulch Member in the Piceance Creek Member (Johnson, 1985).

Yearly accumulation rates in most balanced-fill facies (~100 mm/k.y.) are comparable to the average lamination thicknesses observed in these units (Bradley, 1929; Crowley et al., 1986; Ripepe et al., 1991) and therefore permissive of an annual origin for laminae. However, this coincidence does not necessarily imply that all laminae are annual. Laminae between two correlated ash beds in the Fossil Basin have been observed to increase in number by 134% from the basin center to the basin margin (Church and Buchheim, 2002), making the assumption of an annual origin for laminae (Bradley, 1929; Ripepe et al., 1991) strongly suspect. Buchheim and Eugster (1998) proposed that inflow of calcium-rich stream waters into calcium-undersaturated but carbonate-rich lake waters may explain higher nearshore carbonate sedimentation rates and lamination counts.

ROLE OF INTERBASIN AND INTRABASIN SILLS

Upstream Sills

Initial closure of the Greater Green River Basin occurred at the inception of Wilkins Peak Member deposition in response to diversion of major inlet stream due to uplift of an upstream drainage barrier. The northward diversion of this

stream into the Bighorn Basin, which previously fed into the northwest Greater Green River Basin (Krause, 1985; Seeland, 1998), closely coincided with southwest-vergent thrusting along the south edge of the Gros Ventre, Wind River, and Granite Mountains uplift trend (Love, 1970; Lageson, 1987; Steidtmann and Middleton, 1991). This diversion rerouted rivers draining the east slopes of the Idaho Batholith and portions of southwest Montana (Janecke et al., 2000), shut off delivery of Pinyon type quartzite conglomerates into the northwest Bridger subbasin (Dorr et al., 1977), and hydrologically isolated the Greater Green River Basin, leading to an underfilled Lake Gosiute (Pietras et al., 2003a). The subsequent reintroduction of this or a similar northern drainage ~1.5 m.y. later, ca. 49.5 Ma, was an important factor in shifting the Greater Green River Basin from an underfilled to balanced-fill state via overflow into the Piceance Creek Basin (Fig. 12; Surdam and Stanley, 1980). Although evidence is incomplete due to poor preservation of younger strata, this northern drainage and its volcanoclastic sediments appear again to have been diverted away from the Green River Formation lake system ca. 47 Ma (Fig. 12G), and possibly contributed to a concurrent pulse of evaporite deposition in the downstream Uinta Basin (saline facies). Evidence includes the upsection replacement of volcanoclastic detritus by locally derived arkosic alluvium in the Bridger, Washakie, and Uinta Formations (Fig. 2) and geochronologic support for ongoing volcanism in the Absaroka Volcanic Province (Fig. 5).

Downstream Sills

For any given lake basin, the elevation of its downstream sill is a fundamental control on effective accommodation and can directly determine whether a basin is open or closed (Carroll and Bohacs, 1999). Because uplifts surrounded most margins of the ponded basins (Dickinson et al., 1988), the elevation of low-lying areas connecting the major basins played a key role in determining the hydrologic configuration of the Green River Formation lake system. Low points in the Owl Creek, Granite Mountains, Wind River, and Uinta uplifts functioned at varying times as sills and barriers between lake basins and interbasin drainage networks (Fig. 12). During periods of lower lake level, intrabasin arches such as the Douglas Creek arch and Rock Springs uplift played similar roles (Fig. 12), making the differentiation of intrabasin versus interbasin structures somewhat subjective.

Interbasin sills promote the partitioning of clastic sediments in overfilled upstream basins from chemical sediments in underfilled

downstream subbasins (Bradley and Eugster, 1969). This phenomenon has been observed in the modern Great Salt Lake following construction of a causeway (Eugster and Hardie, 1978), and in Holocene deposits of Lake Bogoria in Kenya (Renaut and Tiercelin, 1994). Expansion of underfilled downstream lakes above their upstream sills can lead to more saline conditions in upstream basins (Fig. 13; Kelts, 1988), as occurred in the Washakie Basin during the initiation of Laney Member deposition (Fig. 12D), and in the Uinta Basin during deposition of the Mahogany zone (Fig. 12E). Counterintuitively, a shift toward more saline conditions in an upstream basin may reflect an increase rather than decrease in climatic humidity (cf. Kelts, 1988).

Upstream subbasins (e.g., the Sand Wash subbasin during Wilkins Peak time) that have high rates of clastic influx may undergo alluvial rather than lacustrine deposition, even if subsidence is rapid. In a long-term sense, such basins served as upstream sediment traps that prevented clastic material from inundating downstream basins but allowed dissolved solutes to pass through. Thus, while absolute subsidence in particular subbasins may play an important role in determining the location of evaporative sinks, the paleogeography of sediment distribution is an equally important factor.

The Douglas Creek arch, which formed the main sill between the Uinta and Piceance Creek Basins, preserves the most complete record available of an interbasin sill (Fig. 2; Bradley, 1931; Cole, 1985). For ~4 m.y. (ca. 53–49 Ma), the dominant hydrologic polarity over the Douglas Creek arch was from west to east into the downstream Piceance Creek Basin, but was reversed following deposition of the Mahogany zone (ca. 49.0–48.5 Ma). This east to west polarity was subsequently retained until the demise of Green River Formation deposition ca. 44 Ma. In detail, however, we suspect that the lake type status of the Eocene deposits overlying the Douglas Creek arch is more complex than can be represented at the scale of Figure 2, and may have changed state repeatedly during different phases of individual lacustrine expansion-contraction cycles in the Piceance Creek Basin (e.g., Fig. 13). Expanded phases of the Piceance Creek Basin lake may have transformed the Douglas Creek arch from a sill to an underwater saddle (Keighley et al., 2003). Nevertheless, below the Mahogany zone, evaporites are restricted to the Piceance Creek Basin (Fig. 2), indicating that it was consistently downstream during periods of low lake level. More detailed stratigraphic work is needed in order to understand the detailed history of the arch.

REGIONAL MAGMATIC INFLUENCE

A marked increase in volcanic activity in the northwest U.S. beginning ca. 50 Ma had a fundamental effect on the character of deposition in Laramide basins (Fig. 12). Construction of major volcanic edifices in the Absaroka, Challis, and other volcanic fields likely affected the Green River Formation lakes in several ways: (1) increased rainfall in upstream catchments due to volcanic topography, (2) regional doming (Pierce and Morgan, 1992), (3) an increase in sediment supply, and (4) short-term interruption of drainages by avalanches, volcanic collapse, and lava flows (Grant et al., 2003).

The addition of volcanoclastic detritus and water derived from the Absaroka and perhaps the Challis volcanic fields overwhelmed previously closed basins, causing them to progressively fill with water, then sediment (Fig. 12; Surdam and Stanley, 1980). Volcanoclastic detritus had propagated downstream to the eastern Uinta Basin prior to shutting off abruptly throughout the Green River Formation basins ca. 47.2 Ma. Subsequently, the region reverted back to a similar configuration of areally restricted evaporative lakes, as existed previously (Fig. 12F). At a finer temporal scale, it remains unclear what the effect, if any, that individual eruptions had on sedimentation, but it can be imagined that short-term pulses of sediment delivery to the Green River Formation lakes may have occurred following explosive eruptions, as easily eroded fallout ash was flushed from the landscape. The unimodal detrital sanidine age distribution in the Sage Creek pumice bed and Sage tuff (Fig. 6) suggests a lack of mixing of recently erupted material with sediment from older eruptions.

It is also uncertain whether an increase in the average altitude of upstream volcanic areas may have caused an increase in the annual precipitation in these areas (e.g., Wotling et al., 2000), and thereby caused downstream basins to shift toward more overfilled states.

A potentially important factor that remains relatively unexplored is the influence of short-term barriers to upstream catchments created by extrusion of lava flows (Hamblin, 1994) and the effects of volcanic sector collapses on upstream catchments in volcanic fields (Malone, 1995). Studies of modern and ancient landslide dams in both volcanic and nonvolcanic catchments have concentrated on the downstream effect of their failure (e.g., flooding and debris flows; Saula et al., 2002; Schneider et al., 2004), but virtually no information exists concerning post-landslide but pre-failure effects on downstream sediment and water budgets. Because lakes can be highly sensitive to changes in water and sediment input, we suspect that ancient landslides in upstream drainage basins may be a highly underappreciated influence on the fine-scale character of their deposits.

PALEOCLIMATIC SIGNIFICANCE OF GREEN RIVER FORMATION EVAPORITES

Evaporite minerals contained within the Green River Formation have long been interpreted as evidence for periods of relatively arid climate (Bradley, 1929; Bradley and Eugster, 1969; Roehler, 1993). This interpretation is consistent with the restricted occurrence of most large, modern hypersaline lakes in areas with mean annual precipitation of <40 cm/yr (Herdendorf, 1984; Fig. 14). However, the presence of evaporites in a

specific basin is not necessarily a direct recorder of increased evaporation or decreased precipitation, but is actually a complex function of the precipitation-to-evaporation ratio and the geometry of surface flow over the entire catchment of a closed basin (Fig. 13; Eugster and Hardie, 1978). During the period ca. 51–45 Ma, regional deposition of evaporative facies in various Green River Formation basins occurred nearly continuously (Figs. 2 and 12), at the limits of our temporal resolution. This period corresponds broadly to the end of the early Eocene climatic optima (ca. 53–49 Ma) and onset of subsequent global cooling, based on $\delta^{18}\text{O}$ in marine benthic foraminifera (Fig. 2; Zachos et al., 2001).

In contrast to the relatively dry conditions implied by long-term evaporite deposition, Eocene flora preserved at Little Mountain in the southern Green River Basin have produced precipitation estimates of ~80 cm/yr and higher. The Little Mountain flora is a composite of several closely spaced collection sites that are ~10 km north of the Uinta Mountain front. Leaf fossils occur only within laminated lacustrine facies in a mixed alluvial and lacustrine interval that is equivalent to the upper Wilkins Peak and Laney Members (P. Wilf, 2006, personal commun.). Comparison of floral composition to living relatives (MacGinitie, 1969; Leopold and MacGinitie, 1972), leaf margin physiognomy (Wolfe et al., 1998), and leaf area physiognomy (Wilf, 2000) of the Little Mountain flora and other Green River Formation floras all indicate that Eocene climates in the region were humid subtropical (Fig. 3; cf. Wilf, 2000).

The apparent conflict between the occurrence of evaporite intervals and paleobotanical evidence for moderately wet conditions cannot be simply resolved by invoking long-term climate

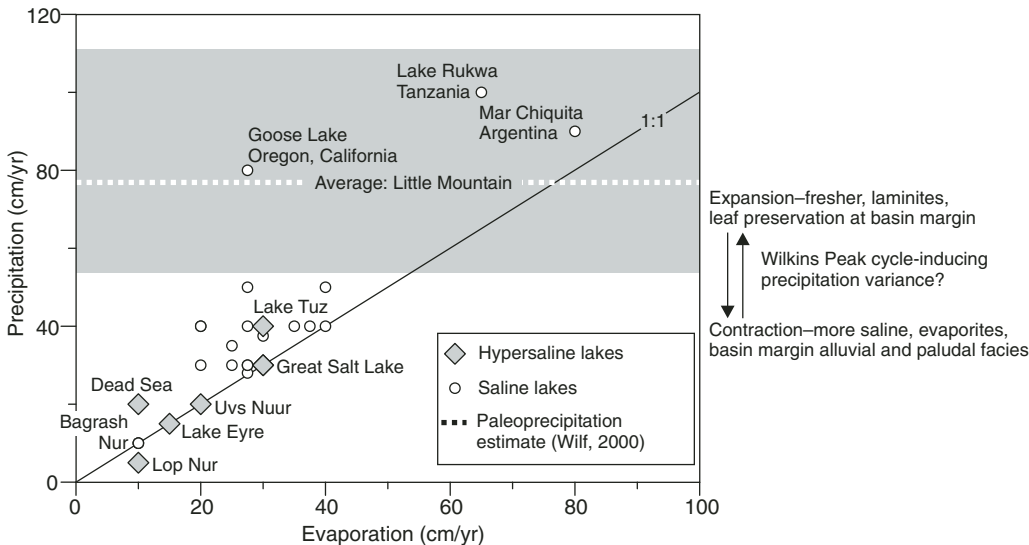


Figure 14. Comparison of mean annual precipitation and evaporation rates for modern lakes (Herdendorf, 1984) with mean annual precipitation estimates from leaf fossils (see Fig. 2) from the interval of evaporite deposition in the Green River Formation (Wilf, 2000). The flora from which this estimate is derived is actually a composite of two sites, one from the upper Wilkins Peak near the Main tuff, and the other from the lower LaCiede Bed of the Laney Member (P. Wilf, 2006, personal commun.). Saline lakes are included to add additional context, based on their implication of higher relative evaporation.

change, because the temporal framework presented in this study shows that deposition of the Little Mountain flora was broadly synchronous with bedded evaporite deposition in the Piceance Creek Basin. One potential explanation for this apparent discordance is that the Little Mountain flora reflects local conditions near the Uinta Mountain front, rather than regional climate. Large location variations in precipitation are well known in modern orogenic landscapes, but this idea is difficult to test based solely on the floral collections. It also may conflict with other studies suggesting that moisture was imported to the Uinta Mountains from the south or southeast (Fricke, 2003; Sewall and Sloan, 2006). Alternatively, the association of leaf fossils with laminated facies may indicate that preservation of flora was limited to relatively short (<100 k.y.), climatically induced phases of lake expansion (Pietras et al., 2003b), whereas evaporite deposition occurred only during intervening dry periods (Burnside and Culbertson, 1979; Roehler, 1992b; Dyni, 1996). Further research is needed to help resolve these issues.

CONCLUSIONS

More than 2000 $^{40}\text{Ar}/^{39}\text{Ar}$ experiments on sanidine and biotite from 22 fallout tuffs and 3 volcanoclastic sandstone beds allow for the paleogeographic reconstruction of the central sector of the Eocene Rocky Mountains. Furthermore, the chronologic framework presented here should serve as the starting point for a broad suite of related tectonic, paleoclimatic, magmatic, biotic, and paleogeomorphic studies. The following conclusions can be made concerning the relative timing and evolution of Lake Gosiute (Greater Green River Basin) and Lake Uinta (Uinta and Piceance Creek Basins).

1. All available chronostratigraphic evidence is consistent with isochronous boundaries between land-mammal ages in the Eocene of the western United States.

2. Evaporite deposition occurred from ca. 51 to ca. 45 Ma and coincided with the early Eocene climatic optima. However, evaporites were not always deposited synchronously from basin to basin, and often coexisted with fluvial-lacustrine deposition in nearby upstream subbasins. Specific evaporite intervals do not necessarily provide evidence for increases in regional aridity.

3. Leaf fossils from the Green River Formation indicate that wetter conditions existed during evaporative intervals than currently occur adjacent to modern evaporite-depositing lakes. This apparent contradiction may be explained by local orographic precipitation gradients or short-term (~10 k.y.) variations in mean annual precipitation from <40 to >60 cm/yr that may also

account for lacustrine expansion-contraction cycles observed in the Green River Formation.

4. Drainage diversions and reintegrations played a key role in determining the hydrologic balance of the Green River Formation lake system, and are attributed to specific episodes of crustal deformation and volcanism.

5. Beginning ca. 49.5 Ma and continuing until ca. 47 Ma, water and volcanoclastic sediment arrived diachronously into the Greater Green River, Piceance Creek, and Uinta Basins, which each progressively freshened then filled with sediment from north to south.

6. Lacustrine sediment accumulation occurred most rapidly in basin centers during underfilled periods, and most rapidly along the basin margins during period of overfilled conditions. Volcanoclastic sandstones that overlie the Laney Member (49.6–48.4 Ma) in the Greater Green River Basin exhibit sediment accumulation rates that are an order of magnitude faster (1000 mm/k.y.) than typical balanced-fill lacustrine deposition (100 mm/k.y.).

ACKNOWLEDGMENTS

This contribution represents a portion of Smith's doctoral dissertation at the University of Wisconsin-Madison. R.N. Smith, J.J. Scott, L.J. Freimund, G. Nelson, and S.A. Hynck assisted with field work and sample collection. J.H. Fouzelle, B.R. Jicha, X. Zhang, K. Min, and L.M. Chetel contributed to data analysis and interpretation. Discussions with H.P. Buchheim, P. Wilf, W.C. Clyde, J.J. Scott, K.M. Bohacs, J.C. Knox, J.A. Simo, B. Tikoff, J.R. Dyni, and P.C. Murphey contributed to the development of this manuscript. We are grateful to W.R. Dickinson for commenting on an early version, and to E.H. Christiansen, P.W. Layer, and M.T. Heizler for their careful reviews. Funding was provided by National Science Foundation grants EAR-0230123, EAR-0114055, and EAR-0516760, the Bailey Distinguished Graduate Fellowship, Conoco-Phillips, Chevron-Texaco, and the Donors to the Petroleum Research Fund of the American Chemical Society.

REFERENCES CITED

- Ambrose, P., Bartels, W.S., Gunnell, G.F., and Williams, E.M., 1997, Stratigraphy and vertebrate paleontology of the Wasatch Formation, Fossil Butte National Monument, Wyoming: *Journal of Vertebrate Paleontology*, v. 17, no. 3, supplement, p. 29.
- Anderson, D.W., and Picard, M.D., 1974, Evolution of synorogenic clastic deposits in the intermontane Uinta Basin of Utah, in Dickinson, W.R., ed., *Tectonics and sedimentation: Society of Economic Paleontologists and Mineralogists Special Publication 22*, p. 167–189.
- Anemone, R.L., Over, D.J., Nachman, B.A., and Harris, J., 2000, A new late Wasatchian mammalian fauna from the Great Basin, Sweetwater County, Wyoming: *Journal of Vertebrate Paleontology*, v. 20, no. 3, supplement, p. 26.
- Armstrong, R.L., and Ward, P., 1991, Evolving geographic patterns of Cenozoic magmatism in the North American Cordillera: The temporal and spatial association of magmatic and metamorphic core complexes: *Journal of Geophysical Research*, v. 96, no. B8, p. 13,201–13,224.
- Baars, D.L., Bartleson, B.L., Chapin, C.E., Curtis, B.F., De Voto, R.H., Everett, J.R., Johnson, R.C., Molenaar, C.M., Peterson, F., Schenk, C.J., Love, J.D., Merin,

- I.S., Rose, P.R., Ryder, R.T., Waechter, N.B., and Woodward, L.A., 1988, Basins of the Rocky Mountain region, in Sloss, L.L., ed., *The geology of North America: Boulder, Colorado, Geological Society of America*, v. D-2, p. 198–220.
- Beck, R.A., Vondra, C.F., Filkins, J.E., and Olander, J.D., 1988, Syntectonic sedimentation and Laramide basement thrusting, Cordilleran foreland; timing of deformation, in Schmidt, C.J., and Perry, W.J., Jr., eds., *Interaction of the Rocky Mountain foreland and the Cordilleran thrust belt: Geological Society of America Memoir 171*, p. 465–487.
- Benson, L.V., Currey, D.R., Dorn, R.I., Lajoie, K.R., Oviatt, C.G., Robinson, S.W., Smith, G.I., and Stine, S., 1990, Chronology of expansion and contraction of four Great Basin lake systems during the past 35,000 years: *Palaeogeography, Palaeoclimatology, Palaeoecology*, v. 78, p. 241–286, doi: 10.1016/0031-0182(90)90217-U.
- Berggren, W.A., Kent, D.V., Swisher, C.C., III, and Aubry, M.-P., 1995, A revised Cenozoic geochronology and chronostratigraphy, in Berggren, W.A., et al., eds., *Geochronology, time scales, and global stratigraphic correlation: SEPM (Society for Sedimentary Geology) Special Publication 54*, p. 129–212.
- Black, C.C., 1969, Fossil vertebrates from the late Eocene and Oligocene, Badwater Creek area, Wyoming, and some regional correlations, in Barlow, J.A., ed., *Symposium on Tertiary rocks of Wyoming: Wyoming Geological Association 21st Annual Field Conference Guidebook*, p. 43–47.
- Bobst, A.L., Lowenstein, T.K., Jordan, J.E., Godfrey, L.V., Ku, T.-L., and Luo, S., 2001, A 106 ka paleoclimate record from drill core of the Salmar de Atacama, northern Chile: *Palaeogeography, Palaeoclimatology, Palaeoecology*, v. 173, p. 21–42, doi: 10.1016/S0031-0182(01)00308-X.
- Bohacs, K.M., Carroll, A.R., Neal, J.E., and Mankiewicz, P.J., 2000, Lake-basin type, source potential, and hydrocarbon character: An integrated sequence-stratigraphic-geochemical framework, in Gierlowski-Kordesch, E.H., and Kelts, K.R., eds., *Lake basins through space and time: American Association of Petroleum Geologists Studies in Geology 46*, p. 3–34.
- Bond, J.G., and Wood, C.H., compilers, 1978, *Geologic map of Idaho: Idaho Department of Lands, Bureau of Mines and Geology, scale 1:500,000*.
- Bown, T.M., 1982, *Geology, paleontology, and correlation of Eocene volcanoclastic rocks, southeast Absaroka range, Hot Springs County, Wyoming: U.S. Geological Survey Professional Paper 1201-A*, 75 p.
- Bradley, W.H., 1929, The varves and climate of the Green River epoch: *U.S. Geological Survey Professional Paper 158-E*, 110 p.
- Bradley, W.H., 1931, Origin and microfossils of the oil shale of the Green River Formation of Colorado and Utah: *U.S. Geological Survey Professional Paper 168*, 58 p.
- Bradley, W.H., 1964, The geology of the Green River Formation and associated Eocene rocks in southwestern Wyoming and adjacent parts of Colorado and Utah: *U.S. Geological Survey Professional Paper 496-A*, 86 p.
- Bradley, W.H., and Eugster, H.P., 1969, Geochemistry and paleolimnology of the trona deposits and associated authigenic minerals of the Green River Formation of Wyoming: *U.S. Geological Survey Professional Paper 496-B*, 71 p.
- Braunagel, L.H., and Stanley, K.O., 1977, Origin of variegated redbeds in the Cathedral Bluffs Tongue of the Wasatch Formation (Eocene), Wyoming: *Journal of Sedimentary Petrology*, v. 47, p. 1201–1219.
- Buchheim, H.P., 1994, Eocene fossil lake, Green River Formation, Wyoming: A history of fluctuating salinity, in Renaut, R.W., and Last, W.M., eds., *Sedimentology and geochemistry of modern and ancient saline lakes: SEPM (Society for Sedimentary Geology) Special Publication 50*, p. 239–247.
- Buchheim, H.P., and Eugster, H.P., 1998, Eocene Fossil Lake: The Green River Formation of Fossil Basin, southwestern Wyoming, in Pitman, J.K., and Carroll, A.R., eds., *Modern and ancient lake systems; new problems and perspectives: Utah Geological Association Publication 26*, p. 191–208.
- Buchheim, H.P., Brand, L.R., and Goodwin, H.T., 2000, Lacustrine to fluvial floodplain deposition in the

- Eocene Bridger Formation: Palaeogeography, Palaeoclimatology, Palaeoecology, v. 162, p. 191–209, doi: 10.1016/S0031-0182(00)00112-7.
- Burnside, M.J., and Culbertson, W.C., 1979, Trona deposits in the Green River Formation, Sweetwater, Uinta, and Lincoln Counties, Wyoming: U.S. Geological Survey Open-File Report 79–737, 10 p.
- Cande, S.C., and Kent, D.V., 1992, A new geomagnetic polarity timescale for the Late Cretaceous and Cenozoic: *Journal of Geophysical Research*, v. 100, p. 13,917–13,951.
- Cande, S.C., and Kent, D.V., 1995, Revised calibration of the geomagnetic polarity timescale for the Late Cretaceous and Cenozoic: *Journal of Geophysical Research*, v. 100, p. 6093–6095, doi: 10.1029/94JB03098.
- Carroll, A.R., and Bohacs, K.M., 1999, Stratigraphic classification of ancient lakes: Balancing tectonic and climatic controls: *Geology*, v. 27, p. 99–102, doi: 10.1130/0091-7613(1999)027<0099:SCOALB>2.3.CO;2.
- Carroll, A.R., and Bohacs, K.M., 2001, Lake-type controls on petroleum source rock potential in nonmarine basins: *American Association of Petroleum Geologists Bulletin*, v. 85, p. 1033–1053.
- Carroll, A.R., Chetel, L.M., and Smith, M.E., 2006, Feast to famine: Sediment supply control on Laramide basin fill: *Geology*, v. 34, p. 197–200, doi: 10.1130/G22148.1.
- Cashion, W.B., 1967, Geology and fuel resources of the Green River Formation Southeastern Uinta Basin, Utah and Colorado: U.S. Geological Survey Professional Paper 548, 48 p.
- Cashion, W.B., and Donnell, J.R., 1972, Chart showing correlation of key units in the organic-rich sequence of the Green River Formation, Piceance Creek basin, Colorado, and Uinta basin, Utah: U.S. Geological Survey Oil and Gas Investigations Chart OC-65, 1 p.
- Chadwick, R.A., 1969, The northern Gallatin Range, Montana: Northwestern part of the Absaroka-Gallatin Volcanic Field: University of Wyoming Contributions to Geology, v. 8, p. 150–166.
- Chandler, M.R., 2006, The provenance of Eocene tuff beds in the Fossil Butte Member of the Green River Formation: Relation to tephra deposits in the Greater Green River basin and the Absaroka and Challis volcanic fields [M.S. thesis]: Provo, Utah, Brigham Young University, 89 p.
- Church, M., and Buchheim, H.P., 2002, Varves and varve-derived climate cycles? Evidence from Eocene Green River Formation: *Geological Society of America Abstracts with Programs*, v. 34, no. 6, p. 555.
- Clyde, W.C., Stamatakos, J., and Gingerich, P.D., 1994, Chronology of the Wasatchian Land-Mammal Age (early Eocene): Magnetostratigraphic results from the McCullough Peaks Section, Northern Bighorn Basin, Wyoming: *Journal of Geology*, v. 102, p. 367–377.
- Clyde, W.C., Zonneveld, J.-P., Stamatakos, J., Gunnell, G.F., and Bartels, W.S., 1997, Magnetostratigraphy across the Wasatchian/Bridgerian NALMA boundary (early to middle Eocene) in the western Green River Basin, Wyoming: *Journal of Geology*, v. 105, p. 657–669.
- Clyde, W.C., Sheldon, N.D., Koch, P.L., Gunnell, G.F., and Bartels, W.S., 2001, Linking the Wasatchian/Bridgerian boundary to the Cenozoic global climate optimum: New magnetostratigraphic and isotopic results from South Pass, Wyoming: *Palaeogeography, Palaeoclimatology, Palaeoecology*, v. 167, p. 175–199, doi: 10.1016/S0031-0182(00)00238-8.
- Clyde, W.C., Bartels, W.S., Gunnell, G.F., and Zonneveld, J.-P., 2004, ⁴⁰Ar/³⁹Ar geochronology of the Eocene Green River Formation, Wyoming: Discussion: *Geological Society of America Bulletin*, v. 116, p. 251–252, doi: 10.1130/B25398.1.
- Cole, R.D., 1985, Depositional environments of oil shale in the Green River Formation, Douglas Creek arch, Colorado and Utah, in Picard, M.D., ed., *Geology and energy resources, Uinta Basin of Utah*: Utah Geological Association Publication 12, p. 211–224.
- Constenius, K.N., 1996, Late Paleogene extensional collapse of the Cordilleran foreland fold and thrust belt: *Geological Society of America Bulletin*, v. 108, p. 20–39, doi: 10.1130/0016-7606(1996)108<0020:LPECOT>2.3.CO;2.
- Covert, H.H., Robinson, P., and Harris, J.R., 1998, Evidence for two lineages of *Notharctus* during the Bridger C and D: *Journal of Vertebrate Paleontology*, v. 18, no. 3, supplement, p. 36.
- Crews, S.G., and Ethridge, F.G., 1993, Laramide tectonics and humid alluvial fan sedimentation, NE Uinta uplift, Utah and Wyoming: *Journal of Sedimentary Petrology*, v. 63, p. 420–436.
- Crowley, K.D., Duchon, C.E., and Rhi, J., 1986, Climate record in varved sediments of the Green River Formation: *Journal of Geophysical Research*, v. 91, p. 8637–8647.
- Culbertson, W.C., 1966, Trona in the Wilkins Peak Member of the Green River Formation, southwestern Wyoming, in *Geological research 1966*: U.S. Geological Survey Professional Paper 550-B, p. 159–164.
- Dane, C.H., 1955, Stratigraphic and facies relationships of the upper part of the Green River Formation and the lower part of the Uinta Formation in Duchesne, Uintah, and Wasatch Counties, Utah: U.S. Geological Survey Oil and Gas Investigations Chart OC-52, 2 p.
- DeCelles, P.G., and Currie, B.S., 1996, Long-term sediment accumulation in the Middle Jurassic–early Eocene Cordilleran retroarc foreland-basin system: *Geology*, v. 24, p. 591–594, doi: 10.1130/0091-7613(1996)024<0591:LTSAIT>2.3.CO;2.
- Deino, A., and Potts, R., 1990, Single-crystal ⁴⁰Ar/³⁹Ar dating of the Ologesailie Formation, Southern Kenya Rift: *Journal of Geophysical Research*, v. 95, p. 8453–8470.
- Desborough, G.A., Pitman, J.K., and Donnell, J.R., 1973, Microprobe analysis of biotites—A method of correlating tuff beds in the Green River Formation, Colorado and Utah: U.S. Geological Society [London] *Journal of Research*, v. 1, p. 39–44.
- Dickinson, W.R., Lawton, T.F., and Inman, K.F., 1986, Sandstone detrital modes, central Utah foreland region: Stratigraphic record of Cretaceous–Paleogene tectonic evolution: *Journal of Sedimentary Petrology*, v. 56, p. 276–293.
- Dickinson, W.R., Klute, M.A., Hayes, M.J., Janecke, S.U., Lundin, E.R., McKittrick, M.A., and Olivares, M.D., 1988, Paleogeographic and paleotectonic setting of Laramide sedimentary basins in the central Rocky Mountain region: *Geological Society of America Bulletin*, v. 100, p. 1023–1039, doi: 10.1130/0016-7606(1988)100<1023:PAPSOL>2.3.CO;2.
- Doelling, H.H., 1972, Tertiary strata, Sevier-Sanpete region, in Baer, J.L., and Callaghan, E., eds., *Plateau–Basin and Range transition zone, central Utah, 1972*: Utah Geological Association Publication 2, p. 41–54.
- Doi, K., 1990, Geology and paleontology of two primate families of the Raven Ridge, northwestern Colorado and northeastern Utah [M.S. thesis]: Boulder, University of Colorado, 215 p.
- Donnell, J.R., 1961a, Tertiary geology and oil-shale resources of the Piceance Creek Basin between the Colorado and White Rivers, northwestern Colorado: U.S. Geological Survey Bulletin 1082-L, p. 835–891.
- Donnell, J.R., 1961b, Tripartition of the Wasatch Formation near De Beque in northwestern Colorado, in *Geological Survey research 1961*: U.S. Geological Survey Professional Paper 424-B, p. 147–148.
- Dorr, J.A., Jr., Spearing, D.R., and Steidtmann, J.R., 1977, Deformation and deposition between a foreland uplift and an impinging thrust belt: Hoback Basin, Wyoming: *Geological Society of America Special Paper* 177, 82 p.
- Douglass, E., 1914, Geology of the Uinta Formation: *Geological Society of America Bulletin*, v. 25, p. 417–420.
- Dyni, J.R., 1969, Structure of the Green River Formation, northern part of the Piceance Creek Basin, Colorado: *Mountain Geologist*, v. 6, p. 57–66.
- Dyni, J.R., 1974, Stratigraphy and nacholite resources of the saline facies of the Green River Formation in northwest Colorado, in Murray, D.K., ed., *Guidebook to the energy resources of the Piceance Creek Basin, Colorado*: Denver, Colorado, Rocky Mountain Association of Geologists, 25th Annual Field Conference, p. 111–122.
- Dyni, J.R., 1981, Geology of the nacholite deposits and associated oil shales of the Green River Formation in the Piceance Creek Basin, Colorado [Ph.D. thesis]: Boulder, University of Colorado, 144 p.
- Dyni, J.R., 1996, Sodium carbonate resources of the Green River Formation in Utah, Colorado, and Wyoming: U.S. Geological Survey Open-File Report 96–729, 39 p.
- Dyni, J.R., Milton, C., and Cashion, W.B., 1985, The saline facies of the upper part of the Green River Formation near Duchesne, Utah, in Picard, M.D., ed., *Geology and energy resources, Uinta Basin of Utah*: Utah Geological Association Publication 12, p. 51–60.
- Eaton, J.G., 1980, Preliminary report on paleontological exploration of the southeastern Absaroka Range, Wyoming, in Gingerich, P.D., ed., *Early Cenozoic paleontology and stratigraphy of the Bighorn Basin, Wyoming*: University of Michigan Museum of Paleontology Papers on Paleontology 24, p. 139–142.
- Eaton, J.G., 1982, Paleontology and correlation of Eocene volcanic rocks in the Carter Mountain area, Park County, southeastern Absaroka Range, Wyoming: University of Wyoming Contributions to Geology, v. 21, p. 153–194.
- Eaton, J.G., 1985, Paleontology and correlation of the Eocene Tepee Trail and Wiggins Formations in the north fork of Owl Creek area, southeastern Absaroka Range, Hot Springs County, Wyoming: *Journal of Vertebrate Paleontology*, v. 5, p. 345–370.
- Elston, D.P., Lantos, M., and Hamor, T., 1994, High resolution polarity records and the stratigraphic and magnetostratigraphic correlation of late Miocene and Pliocene (Pannonian, s.l.) deposits of Hungary, in Teleki, P.G., et al., eds., *Basin analysis and petroleum exploration: Dordrecht, Kluwer Academic Publishers*, p. 111–142.
- Emry, R.J., 1975, Revised Tertiary stratigraphy and paleontology of the western Beaver Divide, Fremont County, Wyoming: *Smithsonian Contributions to Paleobiology* 25, 20 p.
- Eugster, H.P., and Hardie, L.A., 1978, Saline lakes, in Lerman, A., ed., *Lakes—Chemistry, geology, physics*: New York, Springer-Verlag, p. 237–293.
- Eugster, H.P., and Surdam, R.C., 1973, Depositional environment of the Green River Formation of Wyoming: A preliminary report: *Geological Society of America Bulletin*, v. 84, p. 1115–1120, doi: 10.1130/0016-7606(1973)84<1115:DEOTGR>2.0.CO;2.
- Evanoff, E., Robinson, P., Murphey, P.C., Kron, D.G., Engard, D., and Monaco, P., 1994, An Early Uintan fauna from Bridger E: *Journal of Vertebrate Paleontology*, v. 14, no. 3, supplement, p. 24.
- Evanoff, E., Brand, L.R., and Murphey, P.C., 1998, Bridger Formation (middle Eocene) of southwest Wyoming: Widespread marker units and subdivisions of Bridger B through D: *Dakoterra*, v. 5, p. 115–122.
- Evernden, J.F., Savage, D.E., Curtis, G.H., and James, G.T., 1964, Potassium-argon dates and the Cenozoic mammalian chronology of North America: *American Journal of Science*, v. 262, p. 145–198.
- Fahey, J.J., 1962, Saline minerals of the Green River Formation: U.S. Geological Survey Professional Paper 405, 50 p.
- Feeley, T.C., and Cosca, M.A., 2003, Time vs. composition trends of magmatism at Sunlight volcano, Absaroka Volcanic Province, Wyoming: *Geological Society of America Bulletin*, v. 115, p. 714–728, doi: 10.1130/0016-7606(2003)115<0714:TVCTOM>2.0.CO;2.
- Feeley, T.C., Cosca, M.A., and Lindsay, C.R., 2002, Petrogenesis and implications of calc-alkaline cryptic hybrid magmas from Washburn Volcano, Absaroka Volcanic Province, USA: *Journal of Petrology*, v. 43, p. 663–703, doi: 10.1093/ptrology/43.4.663.
- Flynn, J.J., 1986, Correlation and geochronology of middle Eocene strata from the western United States: *Palaeogeography, Palaeoclimatology, Palaeoecology*, v. 55, p. 335–406, doi: 10.1016/0031-0182(86)90155-0.
- Fouch, T.D., 1981, Distribution of rock types, lithologic groups, and interpreted depositional environments for some lower Tertiary and Upper Cretaceous rocks from outcrops at Willow Creek–Indian Canyon through the subsurface of Duchesne and Altamont oil fields, southwest to north central parts of the Uinta Basin, Utah: U.S. Geological Survey Oil and Gas Investigations Chart OC-81, 2 p.
- Franczyk, K.J., Pitman, J.K., Cashion, W.B., Dyni, J.R., Fouch, T.D., Johnson, R.C., Chan, M.A., Donnell, J.R., Lawton, T.F., and Remy, R.R., 1989, Evolution of resource-rich foreland and intermontane basins in eastern Utah and western Colorado, in Hanshaw, P.M., ed., *28th International Geological Congress Field Trip Guidebook*: Washington, D.C., American Geophysical Union, 53 p.

- Fricke, H.C., 2003, Investigation of early Eocene water-vapor transport and paleoelevation using oxygen isotope data from geographically widespread mammal remains: *Geological Society of America Bulletin*, v. 115, no. 9, p. 1088-1096.
- Fritz, W.J., and Harrison, S., 1985, Early Tertiary volcaniclastic deposits of the northern Rocky Mountains, in Flores, R.M., and Kaplan, S.S., eds., *Cenozoic paleogeography of the west central United States: Rocky Mountain Section, Society of Economic Paleontologists and Mineralogists, Rocky Mountain Paleogeography Symposium 3*, p. 383-402.
- Froehlich, D.J., and Breithaupt, B.H., 1998, Mammals from the Eocene epoch Fossil Butte Member of the Green River Formation, Fossil Basin, Wyoming: *Journal of Vertebrate Paleontology*, v. 18, no. 3, supplement, p. 43-44.
- Froehlich, J.F., and Froehlich, D.J., 2002, Using mammal fossils to locate the edge of the Green River Lake in the Piceance Creek Basin during the late-early Eocene: *Geological Society of America Abstracts with Programs*, v. 34, no. 6, p. 480-481.
- Gazin, C.L., 1959, Paleontological exploration and dating of the early Tertiary deposits in basins adjacent to the Uinta Mountains, in Williams, N.C., ed., *Guidebook to the geology of the Wasatch and Uinta Mountains, Transition Area: Salt Lake City, Intermountain Association of Petroleum Geologists, 10th Annual Field Conference*, p. 139-149.
- Gazin, C.L., 1962, A further study of lower Eocene mammalian faunas of southwestern Wyoming: *Smithsonian Miscellaneous Collections*, v. 144, no. 1, 98 p.
- Gazin, C.L., 1965, Early Eocene mammalian faunas and their environment in the vicinity of the Rock Springs Uplift, Wyoming, in De Voto, R.H., and Bitter, R.K., eds., *Sedimentation of Late Cretaceous and Tertiary outcrops, Rock Springs Uplift: Casper, Wyoming Geological Association, 19th Annual Field Conference, Guidebook*, p. 171-180.
- Gazin, C.L., 1976, Mammalian faunal zones of the Bridger Middle Eocene: *Smithsonian Contributions to Paleobiology* 26, 25 p.
- Gingerich, P.D., and Clyde, W.C., 2001, Overview of mammalian biostratigraphy in the Paleocene-Eocene Fort Union and Willwood Formations of the Bighorn and Clarks Fork Basins, in Gingerich, P.D., ed., *Paleocene-Eocene stratigraphy and biotic change in the Bighorn and Clarks Fork Basins, Wyoming: University of Michigan Museum of Paleontology Papers on Paleontology* 33, p. 1-14.
- Goldstrand, P.M., 1994, Tectonic development of Upper Cretaceous to Eocene strata of southwestern Utah: *Geological Society of America Bulletin*, v. 106, p. 145-154, doi: 10.1130/0016-7606(1994)106<0145:TDOUCT>2.3.CO;2.
- Grande, L., 1984, Paleontology of the Green River Formation, with a review of the fish fauna (second edition): *Geological Survey of Wyoming Bulletin* 63, 333 p.
- Grant, G.E., Jefferson, A.J., O'Connor, J.E., Tague, C., Lewis, S.L., and Haluska, T.L., 2003, Drainage network evolution in volcanic landscapes: how much time does it take to get the river flowing?: *Geological Society of America Abstracts with Programs*, v. 35, no. 6, p. 23.
- Groll, P.E., and Steidtmann, J.R., 1987, Fluvial response to Eocene tectonism, the Bridger Formation, southern Wind River Range, Wyoming, in Ethridge, F.G., et al., eds., *Recent developments in fluvial sedimentology: Society of Economic Paleontologists and Mineralogists Special Publication* 39, p. 263-268.
- Grose, L.T., 1972, Tectonics, in Mallory, W.W., ed., *Geologic atlas of the Rocky Mountain region: Denver, Colorado, Rocky Mountain Association of Geologists*, p. 35-44.
- Gunnell, G.F., and Bartels, W.S., 1994, Early Bridgerian (middle Eocene) vertebrate paleontology and paleogeology of the southern Green River Basin, Wyoming: *University of Wyoming Contributions to Geology*, v. 30, p. 57-70.
- Gunnell, G.F., and Bartels, W.S., 1999, Middle Eocene vertebrates from the Uinta Basin, Utah, and their relationship with faunas from the southern Green River Basin, Wyoming, in Gillette, D.D., ed., *Vertebrate paleontology of Utah: Utah Geological Survey Miscellaneous Publication* 99-1, p. 429-442.
- Gunnell, G.F., and Bartels, W.S., 2001, Basin margins, biodiversity, evolutionary innovation, and the origin of new taxa: *Topics in Geobiology*, v. 18, p. 403-432.
- Gunnell, G.F., and Yarborough, V.L., 2000, Brontotheriidae (Perissodactyla) from the late early and middle Eocene (Bridgerian), Wasatch and Bridger Formations, southern Green River Basin, southwestern Wyoming: *Journal of Vertebrate Paleontology*, v. 20, p. 349-368, doi: 10.1671/0272-4634(2000)020[0349:BPFTLE]2.0.CO;2.
- Gunnell, G.F., Bartels, W.S., Gingerich, P.D., and Torres, V., 1992, Wapiti Valley faunas: Early and middle Eocene vertebrates from the North Fork of the Shoshone River, Park County, Wyoming: *University of Michigan Contributions from the Museum of Paleontology*, v. 28, p. 247-287.
- Gunnell, G.F., Bartels, W.S., and Zonneveld, J.-P., 2004, A late Wasatchian (late early Eocene) vertebrate assemblage preserved in meandering stream channel deposits, northern Red Desert, Wyoming: *Geological Society of America Abstracts with Programs*, v. 36, no. 5, p. 92.
- Hail, W.J., Jr., 1987, Chart showing intertongued units of the Eocene Green River and Uinta Formations, northwestern Piceance Creek Basin, northwestern Colorado: U.S. Geological Survey Miscellaneous Investigations Series Map I-1797, 1 p.
- Hail, W.J., Jr., 1992, Geology of the central Roan Plateau area, northwestern Colorado: U.S. Geological Survey Bulletin 1787-R, 26 p.
- Hamblin, W.K., 1994, Late Cenozoic lava dams in the western Grand Canyon: *Geological Society of America Memoir* 183, 139 p.
- Harlan, S.S., Snee, L.W., and Geissman, J.W., 1996, ⁴⁰Ar/³⁹Ar geochronology and paleomagnetism of Independence volcano, Absaroka Volcanic Supergroup, Beartooth Mountains, Montana: *Canadian Journal of Earth Sciences*, v. 33, p. 1648-1654.
- Hayden, F.V., 1869, Preliminary field report of the United States Geological Survey of Colorado and New Mexico: U.S. Geological Survey of the Territories, Third Annual Report, 155 p.
- Herdendorf, C.E., 1984, Inventory of the morphometric and limnologic characteristics of the large lakes of the world: Ohio State University Sea Grant Program Technical Bulletin OHSU-TB-17, 78 p.
- Hickenlooper, J.W., and Guttman, J.T., Jr., 1982, Geology of the Slough Creek tuff, northern Absaroka Volcanic Field, Park County, Montana, in Reid, S.G., and Foote, D.J., eds., *Geology of Yellowstone Park area: Casper, Wyoming Geological Association, 33rd Annual Field Conference, Guidebook*, p. 55-63.
- Hiza, M.M., 1999, The geochemistry and geochronology of the Eocene Absaroka volcanic province, northern Wyoming and southern Montana, USA [Ph.D. thesis]: Corvallis, Oregon State University, 243 p.
- Holroyd, P.A., and Smith, K.T., 2000, Preliminary biostratigraphic evidence for age of the Wasatch and Green River Formations, Washakie Basin, Southwestern Wyoming: *Geological Society of America Abstracts with Programs*, v. 32, no. 7, p. 498.
- Honey, J.G., 1988, A mammalian fauna from the base of the Eocene Cathedral Bluffs Tongue of the Wasatch Formation, Cottonwood Creek area, southeast Washakie Basin, Wyoming: U.S. Geological Survey Bulletin 1669-C, 14 p.
- Honey, J.G., 1990, New Washakiin primates (Omomyidae) from the Eocene of Wyoming and Colorado, and comments on the evolution of the Washakiini: *Journal of Vertebrate Paleontology*, v. 10, p. 206-221.
- Horsfield, B., Curry, D.J., Bohacs, K.M., Littke, R., Rullkötter, J., Schenk, H.J., Radke, M., Schaefer, R.G., Carroll, A.R., Isaksen, G., and Witte, E.G., 1994, Organic geochemistry of freshwater and alkaline lacustrine sediments in the Green River Formation of the Washakie Basin, Wyoming, U.S.A: *Organic Geochemistry*, v. 22, p. 415-440, doi: 10.1016/0146-6380(94)90117-1.
- House, M.A., Bowring, S.A., and Hodges, K.V., 2002, Implications of middle Eocene epizonal plutonism for the unroofing history of the Bitterroot metamorphic core complex, Idaho-Montana: *Geological Society of America Bulletin*, v. 114, p. 448-461, doi: 10.1130/0016-7606(2002)114<0448:IOMEEP>2.0.CO;2.
- Ispolatov, V.O., 1997, ⁴⁰Ar/³⁹Ar geochronology of the Lowland Creek Volcanic Field and its temporal relations with other Eocene volcanic areas [M.S. thesis]: Norfolk, Virginia, Old Dominion University, 106 p.
- Izett, G.A., Honey, J.G., and Brownfield, M.E., 1985, Geology of the Citadel Plateau quadrangle, Moffat County, Colorado: U.S. Geological Survey Miscellaneous Investigations Series Map I-1532, scale 1:48,000.
- Janecke, S.U., and Snee, L.W., 1993, Timing and episodicity of middle Eocene volcanism and onset of conglomerate deposition, Idaho: *Journal of Geology*, v. 101, p. 603-621.
- Janecke, S.U., Hammond, B.F., Snee, L.W., and Geissman, J.W., 1997, Rapid extension in an Eocene volcanic arc: Structure and paleogeography of an intra-arc half graben in central Idaho: *Geological Society of America Bulletin*, v. 109, p. 253-267, doi: 10.1130/0016-7606(1997)109<0253:REIAEV>2.3.CO;2.
- Janecke, S., McIntosh, W., and Good, S., 1999, Testing models of rift basins: Structure and stratigraphy of an Eocene-Oligocene supradetachment basin, Muddy Creek half graben, south-west Montana: *Basin Research*, v. 11, p. 143-165, doi: 10.1046/j.1365-2117.1999.00092.x.
- Janecke, S.U., VanDenburg, C.J., Blankenau, J.J., and M'Gonigle, J.W., 2000, Long-distance longitudinal migration of gravel across the Cordilleran thrust belt of Montana and Idaho: *Geology*, v. 28, p. 439-442, doi: 10.1130/0091-7613(2000)28<439:LLTOGA>2.0.CO;2.
- Jersky, R.G., 1981, A paleomagnetic study of the Bridger Formation, southern Green River Basin, Wyoming [M.S. thesis]: Milwaukee, University of Wisconsin, 113 p.
- Johnson, R.C., 1984, New names for units in the lower part of the Green River Formation, Piceance Creek Basin, Colorado: U.S. Geological Survey Bulletin 1529-I, 20 p.
- Johnson, R.C., 1985, Early Cenozoic history of the Uinta and Piceance Creek basins, Utah and Colorado, with special reference to the development of Eocene Lake Uinta, in Flores, R.M., and Kaplan, S.S., eds., *Cenozoic paleogeography of the west central United States: Rocky Mountain Section, Society of Economic Paleontologists and Mineralogists, Rocky Mountain Paleogeography Symposium 3*, p. 247-276.
- Johnson, R.C., Nichols, D.J., and Hanley, J.H., 1988, Stratigraphic sections of lower Tertiary strata and charts showing polymorph and mollusc assemblages, Douglas Creek Arch area, Colorado and Utah: U.S. Geological Survey Miscellaneous Field Studies Map MF-1997, 2 p.
- Karner, D.B., and Renne, P.R., 1998, ⁴⁰Ar/³⁹Ar geochronology of Roman province tephra in the Tiber River valley: Age calibration of middle Pleistocene sea level changes: *Geological Society of America Bulletin*, v. 110, p. 740-747, doi: 10.1130/0016-7606(1998)110<0740:AAGORV>2.3.CO;2.
- Kay, J.L., 1934, The Tertiary formations of the Uinta Basin, Utah: *Carnegie Museum Annals*, v. 23, p. 357-371.
- Kay, J.L., 1957, The Eocene vertebrates of the Uinta Basin, Utah, in Seal, O.G., ed., *Guidebook to the geology of the Uinta Basin: Salt Lake City, Utah, Intermountain Association of Petroleum Geologists, 8th Annual Field Conference*, p. 110-114.
- Keighley, D., Flint, S., Howell, J., and Moscarillo, A., 2003, Sequence stratigraphy in lacustrine basins: A model for part of the Green River Formation (Eocene), southwest Uinta Basin, Utah, U.S.A: *Journal of Sedimentary Research*, v. 73, p. 987-1006.
- Kelts, K.R., 1988, Environments of deposition of lacustrine petroleum source rocks: An introduction, in Fleet, A.J., et al., eds., *Lacustrine petroleum source rocks: Geological Society [London] Special Publication* 40, p. 3-26.
- Kihm, A.J., 1984, Early Eocene mammalian faunas of the Piceance Creek basin, northwestern Colorado [Ph.D. thesis]: Boulder, University of Colorado, 407 p.
- King, C., 1878, Systematic geology: U.S. Geological Exploration of the Fortieth Parallel Report, v. 1, 803 p.
- Kistner, F.B., 1973, Stratigraphy of the Bridger Formation in the Big Island-Blue Rim area, Sweetwater County, Wyoming [M.S. thesis]: Laramie, University of Wyoming, 174 p.
- Koppers, A.A.P., 2002, ArArCALC-software for ⁴⁰Ar/³⁹Ar age calculations: *Computers & Geosciences*, v. 28, p. 605-619, doi: 10.1016/S0098-3004(01)00095-4.
- Krause, M.J., 1985, Early Tertiary quartzite conglomerates of the Bighorn Basin and their significance for paleo-

- geographic reconstruction of northwest Wyoming, in Flores, R.M., and Kaplan, S.S., eds., Cenozoic paleogeography of the west central United States: Rocky Mountain Section, Society of Economic Paleontologists and Mineralogists, Rocky Mountain Paleogeography Symposium 3, p. 71–91.
- Krishtalka, L., and Stucky, R.K., 1986, Early Eocene artiodactyls from the San Juan Basin, New Mexico, and the Piceance Creek Basin, Colorado, in Flanagan, K.M., and Lillegraven, J.A., eds., Vertebrates, phylogeny, and philosophy: University of Wyoming Contributions to Geology, Special Paper 3, p. 183–196.
- Krishtalka, L., West, R.M., Black, C.C., Dawson, M.R., Flynn, J.J., Turnbull, W.D., Stucky, R.K., McKenna, M.C., Bown, T.M., Golz, D.J., and Lillegraven, J.A., 1987, Eocene (Wasatchian through Duchesnean) biochronology of North America, in Woodburne, M.O., ed., Cenozoic mammals of North America, geochronology and biostratigraphy: Berkeley, University of California Press, p. 77–117.
- Ku, T.-L., Luo, S., Lowenstein, T.K., Li, J., and Spencer, R.J., 1998, U-series chronology of lacustrine deposits in Death Valley, California: Quaternary Research, v. 50, p. 261–275, doi: 10.1006/qres.1998.1995.
- Lageson, D.R., 1987, Laramide uplift of the Gros Ventre Range and implications for the origin of the Teton Fault, Wyoming, in Miller, W.R., ed., The thrust belt revisited: Wyoming Geological Association, 38th Annual Field Conference, Guidebook, p. 79–89.
- Lamerson, P.R., 1982, The Fossil Basin and its relationship to the Absaroka Thrust system, Wyoming and Utah, in Powers, R.B., ed., Geologic studies of the Cordilleran Thrust Belt: Denver, Colorado, Rocky Mountain Association of Geologists, 33rd Annual Field Conference, v. 1, p. 279–340.
- Langereis, C.G., Dekkers, M.J., de Lange, G.J., Paternite, M., and van Santvoort, P.J.M., 1997, Magnetostratigraphy and astronomical calibration of the last 1.1 Myr from an eastern Mediterranean piston core and dating of short events in the Brunhes: Geophysical Journal International, v. 129, p. 75–94, doi: 10.1111/j.1365-246X.1997.tb00938.x.
- Lee, T.-Q., and Shive, P.N., 1983, Paleomagnetic study of the volcanic and volcanoclastic rocks from the southeastern Absaroka, Wyoming: Bulletin of the Institute of Earth Sciences Academia Sinica, v. 3, p. 155–172.
- Leopold, E.B., and MacGinitie, H.D., 1972, Development and affinities of Tertiary flora in the Rocky Mountains, in Graham, A., ed., Floristics and paleofloristics of Asia and eastern North America: Amsterdam, Elsevier Publishing Company, p. 147–200.
- Lillegraven, J.A., 1993, Correlation of Paleogene strata across Wyoming—A users' guide, in Snoke, A.W., et al., eds., Geology of Wyoming: Geological Survey of Wyoming Memoir 5, p. 414–477.
- Lillegraven, J.A., and Ostresh, L.M., Jr., 1988, Evolution of Wyoming's early Cenozoic topography and drainage patterns: National Geographic Research, v. 4, p. 303–327.
- Love, J.D., 1960, Cenozoic sedimentation and crustal movement in Wyoming: American Journal of Science, v. 258-A, p. 204–214.
- Love, J.D., 1964, Uraniferous phosphatic lake beds of Eocene age in intermontane basins of Wyoming and Utah: U.S. Geological Survey Professional Paper 474-E, 66 p.
- Love, J.D., 1970, Cenozoic geology of the Granite Mountains area, central Wyoming: U.S. Geological Survey Professional Paper 495-C, 154 p.
- Love, J.D., and Christiansen, A.C., compilers, 1985, Geologic map of Wyoming: U.S. Geological Survey, 3 sheets, scale 1:500,000.
- Love, J.D., McGrew, P.O., and Thomas, H.D., 1961, Relationship of latest Cretaceous and Tertiary deposition and deformation to oil and gas in Wyoming: American Association of Petroleum Geologists Bulletin, v. 45, p. 197–208.
- Ludwig, K.R., 2003, User's manual for Isoplot 3.00: A geochronological toolkit for Microsoft Excel: Berkeley Geochronology Center Special Publication 4, 70 p.
- MacGinitie, H.D., 1969, The Eocene Green River Flora of northwestern Colorado and northeastern Utah: University of California Publications in the Geological Sciences, v. 83, 203 p.
- MacGinitie, H.D., 1974, An early middle Eocene flora from the Yellowstone-Absaroka Volcanic Province, northwestern Wind River Basin, Wyoming: University of California Publications in Geological Sciences, v. 108, 103 p.
- Machlus, M., Hemming, S.R., Olsen, P.E., and Christie-Blick, N., 2004, Eocene calibration of geomagnetic polarity time scale reevaluated: Evidence from the Green River Formation of Wyoming: Geology, v. 32, p. 137–140, doi: 10.1130/G20091.1.
- Malone, D.H., 1995, Very large debris-avalanche deposit within the Eocene volcanic succession of the northeastern Absaroka Range, Wyoming: Geology, v. 23, p. 661–664, doi: 10.1130/0091-7613(1995)023<0661:VLDADW>2.3.CO;2.
- Marsh, O.C., 1871, On the geology of the eastern Uinta Mountains: American Journal of Science, v. 1, p. 191–198.
- Mason, G.M., 1983, Mineralogy of the Mahogany Marker tuff of the Green River Formation, Piceance Creek Basin, Colorado, in Gary, J.H., ed., Sixteenth Oil Shale Symposium Proceedings: Golden, Colorado School of Mines Press, p. 124–131.
- Matthew, W.D., 1909, The carnivora and insectivora of the Bridger Basin, middle Eocene: American Museum of Natural History Memoir 9, p. 289–576.
- Mauger, R.L., 1977, K-Ar ages of biotites from tuffs in Eocene rocks of the Green River, Washakie, and Uinta basins, Utah, Wyoming, and Colorado: University of Wyoming Contributions to Geology, v. 15, p. 17–41.
- McCarroll, S.M., Flynn, J.J., and Turnbull, W.D., 1996a, Biostratigraphy and magnetostratigraphy of the Bridgerian-Uintan Washakie Formation, Washakie Basin, Wyoming, in Prothero, D.R., and Emry, R.J., eds., The terrestrial Eocene-Oligocene transition in North America: Cambridge, UK, Cambridge University Press, p. 25–39.
- McCarroll, S.M., Flynn, J.J., and Turnbull, W.D., 1996b, The mammalian faunas of the Washakie Formation, Eocene age, of southern Wyoming. Part III: The perissodactyls: Fieldiana Geology, new series, no. 33, 38 p.
- McGookey, D.P., 1960, Early Tertiary stratigraphy of part of central Utah: American Association of Petroleum Geologists Bulletin, v. 44, p. 589–615.
- McGrew, P.O., 1959, The geology and paleontology of the Elk Mountain and Tabernacle Butte area, Wyoming: American Museum of Natural History Bulletin, v. 117, p. 117–176.
- McGrew, P.O., and Roehler, H.W., 1960, Correlation of Tertiary units in southwestern Wyoming, in McGookey, D.P., and Miller, D.N., Jr., eds., Overthrust Belt of southwestern Wyoming and adjacent areas: Wyoming Geological Association, 15th Annual Field Conference, Guidebook, p. 157–158.
- M'Gonigle, J.W., and Dalrymple, G.B., 1996, ⁴⁰Ar/³⁹Ar ages of some Challis Volcanic Group rocks and the initiation of Tertiary sedimentary basins in southwestern Montana: U.S. Geological Survey Bulletin 2132, 17 p.
- Min, K., Mundil, R., Renne, P.R., and Ludwig, K.R., 2000, A test for systematic errors in ⁴⁰Ar/³⁹Ar geochronology through comparison with U-Pb analysis of a 1.1 Ga rhyolite: Geochimica et Cosmochimica Acta, v. 64, p. 73–98, doi: 10.1016/S0016-7037(99)00204-5.
- Mitchell, V.E., compiler, 1998, Geologic map of Idaho: Moscow, Idaho Geological Survey.
- Moncure, G., and Surdam, R.C., 1980, Depositional environment of the Green River Formation in the vicinity of the Douglas Creek Arch, Colorado and Utah: University of Wyoming Contributions to Geology, v. 19, p. 9–24.
- Morris, W.J., 1954, An Eocene fauna from the Cathedral Bluffs Tongue of the Washakie Basin, Wyoming: Journal of Paleontology, v. 28, p. 195–203.
- Moye, F.J., Hackett, W.R., Blakley, J.D., and Snider, L.G., 1988, Regional geologic setting and volcanic stratigraphy of the Challis Volcanic Field, central Idaho, in Link, P.K., and Hackett, W.R., eds., Guidebook to the geology of central and southern Idaho: Idaho Geological Survey Bulletin 27, p. 87–97.
- Muessig, S., 1951, Eocene volcanism in central Utah: Science, v. 114, p. 234, doi: 10.1126/science.114.2957.234.
- Murphey, P.C., 2001, Stratigraphy, fossil distribution, and depositional environments of the upper Bridger Formation (middle Eocene) of southwestern Wyoming, and the taphonomy of an unusual Bridger microfossil assemblage [Ph.D. thesis]: Boulder, University of Colorado, 345 p.
- Nelson, M.E., 1973, Age and stratigraphic relations of the Fowkes Formation, Eocene, of southwestern Wyoming and northeastern Utah: University of Wyoming Contributions to Geology, v. 12, p. 27–31.
- Nelson, W.H., and Pierce, W.G., 1968, Wapiti Formation and Trout Peak Trachyandesite northwest Wyoming: U.S. Geological Survey Bulletin 1254-H, 11 p.
- Ogg, J.G., and Smith, A.G., 2004, The geomagnetic polarity time scale, in Gradstein, F.M., et al., eds., A geologic time scale: Cambridge, UK, Cambridge University Press, p. 63–86.
- O'Neill, J.M., Lonn, J.D., Lageson, D.R., and Kunk, M.J., 2004, Early Tertiary Anaconda metamorphic core complex, southwest Montana: Canadian Journal of Earth Sciences, v. 41, p. 63–72, doi: 10.1139/e03-086.
- O'Neill, W.A., 1980, ⁴⁰Ar/³⁹Ar ages of selected tuff of the Green River Formation: Wyoming, Colorado, and Utah [M.S. thesis]: Columbus, Ohio State University, 142 p.
- Oriel, S.S., and Tracey, J.I., Jr., 1970, Uppermost Cretaceous and Tertiary stratigraphy of Fossil Basin, southwestern Wyoming: U.S. Geological Survey Professional Paper 635, 53 p.
- Osborn, H.F., 1895, Fossil mammals of the Uinta Basin. Expedition of 1894: American Museum of Natural History Bulletin, v. 7, p. 71–105.
- Pekarek, A.H., Marvin, R.F., and Menhert, H.H., 1974, K-Ar ages of the volcanics in the Rattlesnake Hills, central Wyoming: Geology, v. 2, p. 283–285, doi: 10.1130/0091-7613(1974)2<283:KAOTVI>2.0.CO;2.
- Pierce, K.L., and Morgan, L.A., 1992, The track of the Yellowstone hot spot: Volcanism, faulting and uplift, in Link, P.K., et al., eds., Regional geology of eastern Idaho and western Wyoming: Geological Society of America Memoir 179, p. 1–53.
- Pietras, J.T., Carroll, A.R., and Rhodes, M.K., 2003a, Lake basin response to tectonic drainage diversion: Eocene Green River Formation, Wyoming: Journal of Paleolimnology, v. 30, p. 115–125, doi: 10.1023/A:1025518015341.
- Pietras, J.T., Carroll, A.R., Singer, B.S., and Smith, M.E., 2003b, 10 k.y. depositional cyclicity in the early Eocene: Stratigraphic and ⁴⁰Ar/³⁹Ar evidence from the lacustrine Green River Formation: Geology, v. 31, p. 593–597, doi: 10.1130/0091-7613(2003)031<0593:KDCITE>2.0.CO;2.
- Powell, J.W., 1876, Report of the geology of the eastern portion of the Uinta Mountains and region of country adjacent thereto: U.S. Geological and Geographical Survey of the Territories Second Division, 218 p.
- Prothero, D.R., 1996, Magnetic stratigraphy and biostratigraphy of the middle Eocene Uinta Formation, Uinta Basin, Utah, in Prothero, D.R., and Emry, R.J., eds., The terrestrial Eocene-Oligocene transition in North America: Cambridge, UK, Cambridge University Press, p. 25–39.
- Prothero, D.R., and Emry, R.J., 1996, Summary, in Prothero, D.R., and Emry, R.J., eds., The terrestrial Eocene-Oligocene transition in North America: Cambridge, UK, Cambridge University Press, p. 664–683.
- Prothero, D.R., and Swisher, C.C., III, 1992, Magnetostratigraphy and geochronology of the terrestrial Eocene-Oligocene transition in North America, in Prothero, D.R., and Berggren, W.A., eds., Eocene-Oligocene climatic and biotic evolution: Princeton, New Jersey, Princeton University Press, p. 47–73.
- Pusca, V.A., 2003, Wet/dry, terminal fan-dominated sequence architecture: A new, outcrop-based model for the lower Green River Formation, Utah [Ph.D. thesis]: Laramie, University of Wyoming, 175 p.
- Rasmussen, D.T., Conroy, G.C., Friscia, A.R., Townsend, K.E., and Kinkel, M.D., 1999, Mammals of the middle Eocene Uinta Formation, in Gillette, D.D., ed., Vertebrate paleontology of Utah: Utah Geological Survey Miscellaneous Publication 99–1, p. 401–420.
- Remy, R.R., 1992, Stratigraphy of the Eocene part of the Green River Formation in the south-central part of the Uinta Basin, Utah: U.S. Geological Survey Bulletin 1787-BB, 79 p.
- Renaut, R.W., and Tiercelin, J.-J., 1994, Lake Bogoria, Kenya rift valley—A sedimentological overview, in Renaut, R.W., and Last, W.M., eds., Sedimentology and geochemistry of modern and ancient saline lakes:

- SEPM (Society for Sedimentary Geology) Special Publication 50, p. 101–123.
- Renne, P.R., 2000, K-Ar and $^{40}\text{Ar}/^{39}\text{Ar}$ dating, in Noller, J.S., et al., eds., Quaternary geochronology: Methods and applications: American Geophysical Union Reference Shelf 4, p. 77–100.
- Renne, P.R., Swisher, C.C., Deino, A.L., Karner, D.B., Owens, T.L., and DePaolo, D.J., 1998, Intercalibration of standards, absolute ages and uncertainties in $^{40}\text{Ar}/^{39}\text{Ar}$ dating: *Chemical Geology*, v. 145, p. 117–152, doi: 10.1016/S0009-2541(97)00159-9.
- Ripepe, M., Roberts, L.T., and Fischer, A.G., 1991, ENSO and sunspot cycles in varved Eocene oil shales from image analysis: *Journal of Sedimentary Petrology*, v. 61, p. 1155–1163.
- Robinson, P., 1972, Tertiary history, in Mallory, W.W., ed., *Geologic atlas of the Rocky Mountain region*: Denver, Colorado, Rocky Mountain Association of Geologists, p. 233–242.
- Robinson, P., Gunnell, G.F., Walsh, S.L., Clyde, W.C., Storer, J.E., Stucky, R.K., Froehlich, D.J., Ferrusquia-Villafranca, I., and McKenna, M.C., 2004, Wasatchian through Duchesnean biochronology, in Woodburne, M.O., ed., *Late Cretaceous and Cenozoic mammals of North America*: New York, Columbia University Press, p. 106–155.
- Roehler, H.W., 1973, Stratigraphy of the Washakie Formation in the Washakie Basin, Wyoming: *U.S. Geological Survey Bulletin* 1369, 40 p.
- Roehler, H.W., 1974, Depositional environments of rocks in the Piceance Creek Basin, Colorado, in Murray, D.K., ed., *Guidebook to the energy resources of the Piceance Creek Basin, Colorado*: Denver, Colorado, Rocky Mountain Association of Geologists, 25th Annual Field Conference, p. 57–64.
- Roehler, H.W., 1992a, Correlation, composition, areal distribution, and thickness of Eocene stratigraphic units, greater Green River basin, Wyoming, Utah, and Colorado: *U.S. Geological Survey Professional Paper* 1506-E, 49 p.
- Roehler, H.W., 1992b, Description and correlation of Eocene rocks in stratigraphic reference sections for the Green River and Washakie Basins, southwest Wyoming: *U.S. Geological Survey Professional Paper* 1506-D, 83 p.
- Roehler, H.W., 1993, Eocene climates, depositional environments, and geography, greater Green River basin, Wyoming, Utah, and Colorado: *U.S. Geological Survey Professional Paper* 1506-F, 74 p.
- Rohrer, W.L., and Gazin, C.L., 1965, Gray Bull and Lysite faunal zone of the Willwood Formation in the Tatman Mountain area, Bighorn Basin, Wyoming: *U.S. Geological Survey Professional Paper* 525-D, p. 133–138.
- Rohrer, W.L., and Smith, J.W., 1969, Tatman Formation, in Barlow, J.A., ed., *Symposium on Tertiary rocks of Wyoming*: Casper, Wyoming Geological Association, 21st Annual Field Conference, Guidebook, p. 49–54.
- Ross, C.P., Andrews, D.A., and Witkind, I.J., compilers, 1955, *Geologic map of Montana*: U.S. Geologic Survey, Scale 1:500 000, 2 Sheets.
- Ryder, R.T., Fouch, T.D., and Elison, J.H., 1976, Early Tertiary sedimentation in the western Uinta Basin, Utah: *Geological Society of America Bulletin*, v. 87, p. 496–592, doi: 10.1130/0016-7606(1976)87<496:ETSITW>2.0.CO;2.
- Saula, E., Mato, E.E., and Puigdefabregas, C., 2002, Catastrophic debris-flow deposits from an inferred landslide-dam failure, Eocene Berga Formation, eastern Pyrenees, Spain, in Martini, I.P., et al., eds., *Flood and megaflood processes and deposits: recent and ancient examples*: International Association of Sedimentologists Special Publication 32, p. 195–209.
- Savage, D.E., Waters, B.T., and Hutchison, J.H., 1972, Northwestern border of the Washakie Basin, in West, R.M., ed., *Field conference on Tertiary biostratigraphy of southern and western Wyoming*: Garden City, New York, Adelphi University, p. 32–50.
- Schneider, J.-L., Pollet, N., Chapron, E., Wessels, M., and Wassmer, P., 2004, Signature of Rhine Valley struzstrom dam failures in Holocene sediments of Lake Constance, Germany: *Sedimentary Geology*, v. 169, p. 75–91, doi: 10.1016/j.sedgeo.2004.04.007.
- Seeland, D.A., 1978, Eocene fluvial drainage patterns and their implications for uranium and hydrocarbon exploration in the Wind River Basin, Wyoming: *U.S. Geological Survey Bulletin* 1446, 21 p.
- Seeland, D., 1992, Depositional systems of a synorogenic continental deposit—The upper Paleocene and lower Eocene Wasatch Formation of the Powder River Basin: *U.S. Geological Survey Bulletin* 1917-H, 20 p.
- Seeland, D.A., 1998, Late Cretaceous, Paleocene, and early Eocene paleogeography of the Bighorn Basin and northwestern Wyoming, in Keefer, W.R., and Goolsby, J.E., eds., *Cretaceous and lower Tertiary rocks of the Bighorn Basin, Wyoming and Montana*: Wyoming Geological Association, 49th Annual Field Conference, Guidebook, p. 137–165.
- Sewall, J.O., and Sloan, L.C., 2006, Come a little bit closer: A high-resolution climate study of the early Paleogene Laramide foreland: *Geology*, v. 34, p. 81–84, doi: 10.1130/G22177.1.
- Sheliga, C.M., 1980, Sedimentation of the Eocene Green River Formation in Sevier and Sanpete Counties, Utah [M.S. thesis]: Columbus, Ohio State University, 166 p.
- Shive, P.N., and Pruss, E.F., 1977, A paleomagnetic study of basalt flows from the Absaroka Mountains, Wyoming: *Journal of Geophysical Research*, v. 82, p. 3039–3048.
- Simmacher, F., 1970, Stratigraphy, depositional environments, and paleontology of the Cathedral Bluffs tongue of the Wasatch Formation, Parnelle Creek area Sweetwater County, Wyoming [M.S. thesis]: Laramie, University of Wyoming, 101 p.
- Sinclair, W.J., and Granger, W., 1911, Eocene and Oligocene of the Wind River and Bighorn Basins: *American Museum of Natural History Bulletin*, v. 30, p. 83–117.
- Singer, B.S., Brown, L.L., Rabassa, J.O., and Guillou, H., 2004, $^{40}\text{Ar}/^{39}\text{Ar}$ chronology of late Pliocene and early Pleistocene geomagnetic and glacial events in southern Argentina, in Channell, J.E.T., et al., eds., *Timescales of the paleomagnetic field*: American Geophysical Union Geophysical Monograph 145, p. 175–190.
- Sklenar, S.E., and Anderson, D.W., 1985, Origin and early evolution of an Eocene lake system within the Washakie Basin of southwestern Wyoming, in Flores, R.M., and Kaplan, S.S., eds., *Cenozoic paleogeography of the west central United States*: Rocky Mountain Section, Society of Economic Paleontologists and Mineralogists, Rocky Mountain Paleogeography Symposium 3, p. 231–245.
- Smedes, H.W., and Prostka, H.J., 1972, Stratigraphic framework of the Absaroka Volcanic Supergroup in the Yellowstone National Park region: *U.S. Geological Survey Professional Paper* 729-C, 33 p.
- Smith, K.T., and Holroyd, P.A., 2003, Rare taxa, biostratigraphy, and the Wasatchian-Bridgerian boundary in North America, in Wing, S.R., et al., eds., *Causes and consequences of globally warm climates in the early Paleogene*: Geological Society of America Special Paper 369, p. 501–511.
- Smith, M.E., 2007, Stratigraphy, geochronology, and paleogeography of the Green River Formation, Wyoming, Colorado, and Utah [Ph.D. thesis]: Madison, University of Wisconsin, 318 p.
- Smith, M.E., Singer, B., and Carroll, A.R., 2003, $^{40}\text{Ar}/^{39}\text{Ar}$ geochronology of the Eocene Green River Formation, Wyoming: *Geological Society of America Bulletin*, v. 115, p. 549–565, doi: 10.1130/0016-7606(2003)115<0549:AGOTEG>2.0.CO;2.
- Smith, M.E., Singer, B., and Carroll, A.R., 2004, $^{40}\text{Ar}/^{39}\text{Ar}$ geochronology of the Eocene Green River Formation, Wyoming: Reply: *Geological Society of America Bulletin*, v. 116, p. 253–256, doi: 10.1130/B25491R.1.
- Smith, M.E., Singer, B.S., Carroll, A.R., and Fournelle, J.H., 2006, High-resolution calibration of Eocene strata: $^{40}\text{Ar}/^{39}\text{Ar}$ geochronology of biotite in the Green River Formation: *Geology*, v. 34, p. 393–396, doi: 10.1130/G22265.1.
- Smoot, J.P., 1983, Depositional subenvironments in an arid closed basin, the Wilkins Peak Member of the Green River Formation (Eocene), Wyoming, U.S.A.: *Sedimentology*, v. 30, p. 801–827, doi: 10.1111/j.1365-3091.1983.tb00712.x.
- Snider, L.G., 1995, Stratigraphic framework, geochemistry, geochronology, and eruptive styles of Eocene volcanic rocks in the White Knob Mountains area, southeastern Challis Volcanic Field, central Idaho [M.S. thesis]: Pocatello, Idaho State University, 212 p.
- Snider, L.G., and Moyer, F.J., 1989, Regional stratigraphy, physical volcanology, and geochemistry of the southeastern Challis Volcanic Field: *U.S. Geological Survey Open-File Report* 89–639, p. 122–127.
- Solomon, B.J., McKee, E.H., and Anderson, D.W., 1979, Stratigraphy and depositional environments of Paleogene rocks near Elko, Nevada, in Armentrout, J.M., et al., eds., *Cenozoic paleogeography of the western United States*: Pacific Section, Society of Economic Paleontologists and Mineralogists, Pacific Coast Paleogeography Symposium 3, p. 75–88.
- Spieker, E.M., 1946, Late Mesozoic and early Cenozoic history of central Utah: *U.S. Geological Survey Professional Paper* 205-D, p. 117–161.
- Spieker, E.M., 1949, The transition between the Colorado Plateaus and the Great Basin in central Utah: Salt Lake City, Utah Geological Society, 106 p.
- Stanley, K.O., and Surdam, R.C., 1978, Sedimentation on the front of Eocene Gilbert-type deltas, Washakie Basin, Wyoming: *Journal of Sedimentary Petrology*, v. 48, p. 557–573.
- Steidtmann, J.R., and Middleton, L.T., 1991, Fault chronology and uplift history of the southern Wind River Range, Wyoming: Implications for Laramide and post-Laramide deformation in the Rocky Mountain foreland: *Geological Society of America Bulletin*, v. 103, p. 472–485, doi: 10.1130/0016-7606(1991)103<0472:FCAUHO>2.3.CO;2.
- Stewart, J.H., and Carlson, J.E., compilers, 1978, *Geologic map of Nevada*: U.S. Geological Survey State Geologic Map, scale 1:500,000.
- Stucky, R.K., 1982, Mammalian fauna and biostratigraphy of the upper part of the Wind River Formation (early to middle Eocene), Natrona County, Wyoming, and the Wasatchian-Bridgerian boundary [Ph.D. thesis]: Boulder, University of Colorado, 285 p.
- Stucky, R.K., 1984, The Wasatchian-Bridgerian land mammal age boundary (early to middle Eocene) in Western North America: *Carnegie Museum Annals*, v. 53, p. 347–382.
- Stucky, R.K., Prothero, D.R., Lohr, W.G., and Snyder, J.R., 1996, Magnetic stratigraphy, sedimentology, and mammalian faunas of the early Uintan Washakie Formation, Sand Wash Basin, northwestern Colorado, in Prothero, D.R., and Emry, R.J., eds., *The terrestrial Eocene-Oligocene transition in North America*: Cambridge, Cambridge University Press, p. 40–51.
- Sullivan, R., 1985, Origin of lacustrine rocks of the Wilkins Peak Member, Wyoming: *American Association of Petroleum Geologists Bulletin*, v. 69, p. 913–922.
- Sundell, K.A., 1993, A geologic overview of the Absaroka Volcanic Province, in Snoke, A.W., Steidtmann, J.R., and Roberts, S.M., eds., *Geology of Wyoming*: Geological Survey of Wyoming Memoir 5, p. 480–506.
- Sundell, K.A., Shive, P.N., and Eaton, J.G., 1984, Measured sections, magnetic polarity and biostratigraphy of the Eocene Wiggins, Tepee Trail and Aycross Formations within the southeastern Absaroka Range, Wyoming: *Wyoming Geological Association Earth Science Bulletin*, v. 17, p. 1–48.
- Surdam, R.C., and Parker, R.D., 1972, Authigenic aluminosilicate minerals in the tuffaceous rocks of the Green River Formation, Wyoming: *Geological Society of America Bulletin*, v. 83, p. 689–700, doi: 10.1130/0016-7606(1972)83(689:AAMITT)2.0.CO;2.
- Surdam, R.C., and Stanley, K.O., 1979, Lacustrine sedimentation during the culminating phase of Eocene Lake Gosiute, Wyoming (Green River Formation): *Geological Society of America Bulletin*, v. 90, p. 93–110, doi: 10.1130/0016-7606(1979)90<93:LSDTCP>2.0.CO;2.
- Surdam, R.C., and Stanley, K.O., 1980, Effects of changes in drainage-basin boundaries on sedimentation in Eocene Lakes Gosiute and Uinta of Wyoming, Utah, and Colorado: *Geology*, v. 8, p. 135–139, doi: 10.1130/0091-7613(1980)8<135:EOCIDB>2.0.CO;2.
- Tauxe, L., Gee, J., Gallet, Y., Pick, T., and Bown, T., 1994, Magnetostratigraphy of the Willwood Formation, Bighorn Basin, Wyoming: New constraints on the location of Paleocene/Eocene boundary: *Earth and Planetary Science Letters*, v. 125, p. 159–172, doi: 10.1016/0012-821X(94)90213-5.
- Taylor, J.R., 1982, *An introduction to error analysis*: Mill Valley, California, University Science Books, 270 p.
- Torres, V., 1985, Stratigraphy of the Eocene Willwood, Aycross, and Wapiti Formations along the North Fork

- of the Shoshone River, north-central Wyoming: University of Wyoming Contributions to Geology, v. 23, p. 83–97.
- Torres, V., and Gingerich, P.D., 1983, Summary of Eocene stratigraphy at the base of the Jim Mountain, North Fork of the Shoshone River, northwestern Wyoming, in Boberg, W.W., ed., *Geology of the Bighorn Basin: Wyoming Geological Association, 34th Annual Field Conference, Guidebook*, p. 205–208.
- Trudell, L.G., Beard, T.N., and Smith, J.W., 1970, Green River Formation lithology and oil-shale correlations in the Piceance Creek Basin, Colorado: U.S. Bureau of Mines Report of Investigations 7357, 226 p.
- Trudell, L.G., Roehler, H.W., and Smith, J.W., 1973, Geology of Eocene rocks and oil yields of Green River oil shales on part of Kinney Rim, Washakie Basin, Wyoming: U.S. Bureau of Mines Report of Investigations 7775, 151 p.
- Trudell, L.G., Beard, T.N., and Smith, J.W., 1974, Stratigraphic framework of Green River Formation oil shales in the Piceance Creek Basin, Colorado, in Murray, D.K., ed., *Guidebook to the energy resources of the Piceance Creek Basin, Colorado: Denver, Colorado, Rocky Mountain Association of Geologists, 25th Annual Field Conference*, p. 65–69.
- Turnbull, W.D., 1978, The mammalian faunas of the Washakie Formation, Eocene age, of southern Wyoming: *Fieldiana Geology*, v. 33, p. 569–601.
- Tweto, O., compiler, 1979, *Geologic map of Colorado: U.S. Geological Survey, scale 1:500 000*.
- Vandenberg, C.J., Janecke, S.U., and McIntosh, W.C., 1998, Three-dimensional strain produced by >50My of episodic extension, Horse Prairie Basin area, SW Montana, U.S.A: *Journal of Structural Geology*, v. 20, p. 1747–1767, doi: 10.1016/S0191-8141(98)00084-4.
- Van Houten, F.B., 1964, Tertiary geology of the Beaver Rim area Fremont and Natrona counties, Wyoming: U.S. Geological Survey Bulletin 1164, 99 p.
- Wallace, C.A., Lidke, D.J., Elliott, J.E., Desmarais, N.R., Obradovich, J.D., Lopez, D.A., Zarske, S.E., Heise, B.A., Blackowski, M.J., and Loen, J.S., 1992, Geologic map of the Anaconda-Pintlar Wilderness and contiguous roadless area, Granite, Deer Lodge, and Ravalli Counties, western Montana: U.S. Geological Survey Miscellaneous Field Studies Map MF-1633-C, scale 1:50,000, 36 p.
- Walsh, S.L., Prothero, D.R., and Lundquist, D.J., 1996, Stratigraphy and paleomagnetism of the middle Eocene Friars Formation and Poway Group, southwestern San Diego County, California, in Prothero, D.R., and Emry, R.J., eds., *The terrestrial Eocene-Oligocene transition in North America: Cambridge, UK, Cambridge University Press*, p. 120–154.
- Walton, A.H., 1992, Magnetostratigraphy of the lower and middle members of the Devil's Graveyard Formation (Middle Eocene), Trans-Pecos Texas, in Prothero, D.R., and Berggren, W.A., eds., *Eocene-Oligocene climatic and biotic evolution: Princeton, New Jersey, Princeton University Press*, p. 74–87.
- Weiss, M.P., and Warner, K.N., 2001, The Crazy Hollow Formation (Eocene) of Central Utah: *Brigham Young University Geology Studies*, v. 46, p. 143–161.
- Weiss, M.P., Witkind, I.J., and Cashion, W.B., 1990, Geologic map of the Price 30' x 60' quadrangle, Carbon, Duchesne, Uintah, Utah, and Wasatch Counties, Utah: U.S. Geological Survey Miscellaneous Investigations Series Map I-1981, scale 1:100,000.
- West, R.M., 1970, Sequence of mammalian faunas of Eocene age in the northern Green River Basin, Wyoming: *Journal of Paleontology*, v. 44, p. 142–147.
- West, R.M., 1973, Geology and mammalian paleontology of the New Fork-Big Sandy area, Sublette County, Wyoming: *Fieldiana Geology*, v. 29, 193 p.
- West, R.M., 1976, Paleontology and geology of the Bridger Formation, southern Green River Basin, southwestern Wyoming: *Milwaukee Public Museum Contributions in Biology and Geology*, no. 7, 10 p.
- West, R.M., and Atkins, E.G., 1975, Additional middle Eocene (Bridgerian) mammals from Tabernacle Butte, Sublette County, Wyoming: *American Museum Novitates*, no. 2404, 26 p.
- West, R.M., and Dawson, M.R., 1973, Fossil mammals from the upper part of the Cathedral Bluffs Tongue of the Wasatch Formation (Early Bridgerian), northern Green River Basin, Wyoming: *University of Wyoming Contributions to Geology*, v. 12, p. 33–41.
- West, R.M., and Dawson, M.R., 1975, Eocene fossil mammalia from the Sand Wash Basin, northwest Moffat County, Colorado: *Carnegie Museum Annals*, v. 45, p. 231–253.
- West, R.M., and Huchison, J.H., 1981, Geology and paleontology of the Bridger Formation, southern Green River Basin, southwestern Wyoming, Part 6: The fauna and correlation of Bridger E: *Milwaukee Public Museum Contributions in Biology and Geology*, no. 46, 8 p.
- Wilf, P., 2000, Late Paleocene–early Eocene climate changes in southwestern Wyoming: Paleobotanical analysis: *Geological Society of America Bulletin*, v. 112, p. 292–307, doi: 10.1130/0016-7606(2000)112<0292:LPEECC>2.3.CO;2.
- Wilf, P., Labandeira, C.C., Johnson, K.R., Coley, P.D., and Cutter, A.D., 2001, Insect herbivory, plant defense, and early Cenozoic climate change: *National Academy of Sciences Proceedings*, v. 98, p. 6221–6226, doi: 10.1073/pnas.111069498.
- Wilson, A.B., and Elliott, J.E., 1997, Geologic maps of western and northern parts of Gallatin National Forest, south-central Montana: U.S. Geological Survey Geological Investigations Series Map I-2584, scale 1:126,720.
- Winfrey, M.W., Jr., 1960, Stratigraphy, correlation, and oil potential of the Sheep Pass Formation, east-central Nevada, in Boettcher, J.W., and Sloan, W.W., Jr., eds., *Guidebook to the geology of east central Nevada: Salt Lake City, Utah, Intermountain Association of Petroleum Geologists, 11th Annual Field Conference*, p. 126–133.
- Wing, S.L., Bown, T.M., and Obradovich, J.D., 1991, Early Eocene biotic and climatic change in interior western North America: *Geology*, v. 19, p. 1189–1192, doi: 10.1130/0091-7613(1991)019<1189:EEBACC>2.3.CO;2.
- Wing, S.L., Bao, H., and Koch, P.L., 2000, An early Eocene cool period? Evidence for continental cooling during the warmest part of the Cenozoic, in Huber, B.T., et al., eds., *Warm climates in Earth history: Cambridge, UK, Cambridge University Press*, p. 197–237.
- Witkind, I.J., and Grose, L.T., 1972, Areal geologic map of the Rocky Mountain region and environs, in Malloy, W.W., ed., *Geologic atlas of the Rocky Mountain region: Denver, Colorado, Rocky Mountain Association of Geologists*, p. 34.
- Wolfe, J.A., Forest, C.E., and Molnar, P., 1998, Paleobotanical evidence of Eocene and Oligocene paleoaltitudes in midlatitude western North America: *Geological Society of America Bulletin*, v. 110, no. 5, p. 664–678.
- Wood, H.E., II, Chaney, R.W., Clark, J., Colbert, E.H., Jepson, G.L., Reedsides, J.B., and Stock, C., 1941, Nomenclature and correlation of the North American continental Tertiary: *Geological Society of America Bulletin*, v. 52, p. 1–48.
- Wotling, G., Bouvier, C., Danloux, J., and Fritsch, J.M., 2000, Regionalization of extreme precipitation distribution using the principal components of the topographical environment: *Journal of Hydrology*, v. 233, p. 86–101, doi: 10.1016/S0022-1694(00)00232-8.
- Yen, F., and Goodwin, J.H., 1976, Correlation of tuff layers in the Green River Formation, Utah using biotite compositions: *Journal of Sedimentary Petrology*, v. 46, p. 345–354.
- York, D., 1969, Least squares fitting of a straight line with correlated errors: *Earth and Planetary Science Letters*, v. 5, p. 320–324, doi: 10.1016/S0012-821X(68)80059-7.
- Zachos, J., Pagani, M., Sloan, L., Thomas, E., and Billups, K., 2001, Trends, rhythms, and aberrations in global climate 65 Ma to present: *Science*, v. 292, p. 685–693.
- Zonneveld, J.-P., Gunnell, G.F., and Bartels, W.S., 2000, Early Eocene fossil vertebrates from the southwestern Green River Basin, Lincoln and Uinta Counties, Wyoming: *Journal of Vertebrate Paleontology*, v. 20, p. 369–386, doi: 10.1671/0272-4634(2000)020[0369:EEFVFT]2.0.CO;2.
- Zonneveld, J.-P., Bartels, W.S., and Clyde, W.C., 2003, Stratal architecture of an early Eocene fluvial-lacustrine depositional system, Little Muddy Creek area, southwestern Green River Basin, Wyoming, in Reynolds, R.G., and Flores, R.M., eds., *Cenozoic systems of the Rocky Mountain region: Rocky Mountain Section, SEPM (Society for Sedimentary Geology)*, p. 253–287.

MANUSCRIPT RECEIVED 13 JULY 2006

REVISED MANUSCRIPT RECEIVED 7 APRIL 2007

MANUSCRIPT ACCEPTED 28 MAY 2007

Printed in the USA